National Library of Canada
Bibliothèque nationale du Canada

Acquisitions and Bibliographic Services Branch
Direction des acquisitions et des services bibliographiques

395 Wellington Street
Ottawa, Ontario
K1A 0N4

395, rue Wellington
Ottawa (Ontario)
K1A 0N4

Your file Votre référence

Our file Notre référence

NOTICE

The quality of this microform is heavily dependent upon the quality of the original thesis submitted for microfilming. Every effort has been made to ensure the highest quality of reproduction possible.

If pages are missing, contact the university which granted the degree.

Some pages may have indistinct print especially if the original pages were typed with a poor typewriter ribbon or if the university sent us an inferior photocopy.

Reproduction in full or in part of this microform is governed by the Canadian Copyright Act, R.S.C. 1970, c. C-30, and subsequent amendments.

AVIS

La qualité de cette microforme dépend grandement de la qualité de la thèse soumise au microfilmage. Nous avons tout fait pour assurer une qualité supérieure de reproduction.

S'il manque des pages, veuillez communiquer avec l'université qui a conféré le grade.

La qualité d'impression de certaines pages peut laisser à désirer, surtout si les pages originales ont été dactylographiées à l'aide d'un ruban usé ou si l'université nous a fait parvenir une photocopie de qualité inférieure.

La reproduction, même partielle, de cette microforme est soumise à la Loi canadienne sur le droit d'auteur, SRC 1970, c. C-30, et ses amendements subséquents.

Canada

University of Alberta

Functional Characterization of a Recombinant Sodium-dependent Nucleoside Transporter ($cNT1_{rat}$) in Cultured Mammalian Cells

By

Xiao Fang ©

A thesis submitted to the Faculty of Graduate Studies and Research in partial fulfillment of the requirements for a degree of Master of Science

Department of Biochemistry

Edmonton, Alberta
Spring, 1996

National Library
of Canada

Acquisitions and
Bibliographic Services Branch

395 Wellington Street
Ottawa, Ontario
K1A 0N4

Bibliothèque nationale
du Canada

Direction des acquisitions et
des services bibliographiques

395, rue Wellington
Ottawa (Ontario)
K1A 0N4

Your file Votre référence

Our file Notre référence

The author has granted an irrevocable non-exclusive licence allowing the National Library of Canada to reproduce, loan, distribute or sell copies of his/her thesis by any means and in any form or format, making this thesis available to interested persons.

L'auteur a accordé une licence irrévocable et non exclusive permettant à la Bibliothèque nationale du Canada de reproduire, prêter, distribuer ou vendre des copies de sa thèse de quelque manière et sous quelque forme que ce soit pour mettre des exemplaires de cette thèse à la disposition des personnes intéressées.

The author retains ownership of the copyright in his/her thesis. Neither the thesis nor substantial extracts from it may be printed or otherwise reproduced without his/her permission.

L'auteur conserve la propriété du droit d'auteur qui protège sa thèse. Ni la thèse ni des extraits substantiels de celle-ci ne doivent être imprimés ou autrement reproduits sans son autorisation.

ISBN 0-612-10704-3

Canada

University of Alberta

Library Release Form

Name of Author: Xiao Fang

Title of Thesis: Functional Characterization of a Recombinant Sodium-dependent Nucleoside Transporter ($cNT1_{rat}$) in Cultured Mammalian Cells

Degree: Master of Science

Year this Degree Granted: 1996

Permission is hereby granted to the University of Alberta Library to reproduce single copies of this thesis and to lend or sell such copies for private, scholarly, or scientific research purposes only.

The author reserves all other publication and other rights in association with the copyright in the thesis, and except as hereinbefore provided, neither the thesis nor any substantial portion thereof may be printed or otherwise reproduced in any material form whatever without the author's prior written permission.

3B-9007-112st
Edmonton, Alberta
T6G 2C5, Canada

Jan, 17 / 1996

University of Alberta

Faculty of Graduate Studies and Research

The undersigned certify that they have read, and recommend to the Faculty of Graduate Studies and Research for acceptance, a thesis entitled **Functional characterization of a recombinant sodium-dependent nucleoside transporter (cNT1$_{rat}$) in cultured mammalian cells** submitted by **Xiao Fang** in partial fulfillment of the requirements for the degree of Master of Science.

Carol Cass

C. Cass (Supervisor)

Bernard Lemire

B. Lemire

J. Young

L. Agellon

C. Cheeseman

Jan 5, 1996

ABSTRACT

Nucleoside transporters are required for cellular uptake of nucleosides and many nucleoside drugs. $cNT1_{rat}$ is a sodium-dependent concentrative nucleoside transporter of rat intestine that was identified by molecular cloning and functional expression of its cDNA. This thesis describes the transient expression of $cNT1_{rat}$ cDNA in monkey kidney (COS-1) cells, whose endogenous nucleoside transport process could be selectively blocked by inhibitors of equilibrative nucleoside transport. The production of $cNT1_{rat}$ was examined by analysis of ^{3}H-labeled nucleoside uptake in transfected COS-1 cells. Kinetic studies showed that $cNT1_{rat}$ was sodium-dependent and selective for pyrimidine nucleosides, including uridine, thymidine and cytidine. Although adenosine exhibited high affinity for $cNT1_{rat}$, its V_{max} was low. Several antiviral and anticancer nucleoside drugs inhibited $cNT1_{rat}$-mediated uptake of uridine, suggesting that concentrative pyrimidine-selective nucleoside transporters may play a role in cellular uptake of these drugs. The $cNT1_{rat}$ mammalian expression system is a useful tool for analysis of $cNT1_{rat}$-mediated transport processes.

ACKNOWLEDGMENTS

I would like to thank my supervisor, Dr. C.E. Cass for her supervision, encouragement, patience and help. Also, I would like to thank my committee members, Dr, B. Lemire, Dr. J.Young, Dr. L. Agellon and Dr. C.Cheeseman for their constructive suggestions and discussions.

My gratitude goes to my lab fellows, Delores, Mark, Fiona, Doug, Imogen, Milada, Miguel, Karen, Lily, John and Christine for their help and friendship. Thanks to many people in other labs for their invaluable help. The name list is just too long.

In addition, I wish to thank Department of Biochemistry for providing me an opportunity to pursue my graduate study in an excellent academic environment.

Finally, this thesis is dedicated to my parents and my beloved ones. Their encouragement and support made my study possible.

TABLE OF CONTENTS

CHAPTER PAGE

I. INTRODUCTION 1

1.1 Overview 2

1.2 Nucleoside and nucleoside analogues 2

1.2a Natural nucleosides 4

1.2b Nucleoside analogs 5

(i) Antiviral nucleoside drugs 6

(ii) Anticancer drugs 7

1.3 Nucleoside transporters 9

1.3a Equilibrative nucleoside transporters of mammalian cells 9

1.3b Concentrative nucleoside transporters of mammalian cells 10

1.4 Expression DNA in mammalian cells 14

1.4a Transient expression 15

1.4b Stable transfection 15

1.4c Host cell lines 16

1.4d Expression vectors 17

1.4e Transfection techniques 17

1.5 Objective of Research 19

II. MATERIALS AND METHODS 31

2.1 Materials 32

2.2 Mammalian cell lines 32

2.3 E *coli* 33

2.4 Transient transfection of COS-1 cells 34

2.5 Stable transfection of CHO-K1 cells 35

2.6 Transformation of plasmid DNA into bacteria 36

2.7 Isolation of DNA from bacteria 36

2.8 Enzymatic manipulation of DNA 37

2.9 Polymerase chain reaction 38

2.10 Western blotting 39

2.11 Determination of protein concentrations 40

2.12 Uptake assays 40

2.13 NBMPR binding assay 44

III. CHARACTERIZATION OF NUCLEOSIDE TRANSPORT PROCESSES OF COS-1 CELLS 45

3.1 Overview 46

3.2 Nucleoside transport activity in COS-1 cells 46

3.3 Nucleoside transport activity in COS-1 cells was sodium-independent 48

3.4 Kinetic parameters 49

3.5 Summary 49

IV. TRANSIENT EXPRESSION OF cNT1$_{rat}$ IN COS-1 CELLS 66

4.1 Overview 67

4.2 Construction of pCDNAI/Amp/cNT1$_{rat}$ 68

4.3 Transient expression of cNT1$_{rat}$ in COS-1 cells 70

4.4 Construction of c-*myc* tagged cNT1$_{rat}$ 72

4.5 Functional analysis of recombinant c-*myc* tagged cNT1$_{rat}$

proteins in COS-1 cells 73

4.6 Identification of recombinant c-*myc* tagged $cNT1_{rat}$ in COS-1 cells 74

4.7 Inhibition of $cNT1_{rat}$-mediated transport of uridine by physiological nucleosides 74

4.8 Kinetic studies 75

4.9 Inhibition studies of nucleoside drugs 78

4.10 Summary 78

IV. **DISCUSSION** 129

5.1 Discussion 130

5.2 Future work 135

APPENDIX 138

BIBLIOGRAPHY 153

LIST OF TABLES

TABLE PAGE

3.1 Effect of excess nonradioactive nucleoside on rate of uptake of tracer nucleoside 51

3.2 NBMPR-binding sites in some cell types 52

3.3 Uptake rates of uridine, thymidine and adenosine in sodium-containing and sodium-free buffer 53

4.1 Optimization of the DEAE-dextran concentration used in trnasfection of COS-1 cells 81

4.2 Kinetic parameters of uridine, thymidine, cytidine adenosine in $cNT1_{rat}$ in COS-1 cells and *Xenopus* ooctes 82

FIGURE LIST

FIGURE PAGE

1.1 Metabolic pathways of adenosine 22

1.2 Structures of purine nucleosides used in this study 23

1.3 Structures of pyrimidine nucleosides used in this study 24

1.4 Structures of antiviral nucleoside drugs used in this study 25

1.5 Structures of anticancer nucleoside drugs used in this study 26

1.6 Structures of the two enantiomers of 3TC 27

1.7 Metabolism and mechanism of araC 28

1.8 Alignment of cNT1_{rat}, NUPC and SPNT amino acid sequences 30

3.1 Time course of uptake of uridine, thymidine and adenosine in COS-1 cells 55

3.2 The effect of NBMPR on initial rates of uptake of uridine and thymidine by COS-1 cells 57

3.3 Effects of NBMPR, dilazep and dipyridamole on uridine and thymidine uptake in COS-1 cells 59

3.4 Scatchard analysis of NBMPR binding by COS-1 cells 61

3.5 Transport of nucleosides by COS-1 cells in sodium-containing and sodium-free buffer 63

3.6 Uridine uptake kinetics in COS-1 cells 65

4.1.a Structure of pCDNAI/Amp vector 84

4.2.b Construction of pCDNAI/Amp-cNT1_{rat} 86

4.3.c pCDNAI/Amp-cNT1_{rat} expression construct 88

4.3.d Restriction mapping of pCDNAI/Amp-cNT1$_{rat}$ 90

4.2 Uridine uptake by COS-1 cells transfected with cNT1$_{rat}$ cDNA 92

4.3 ^{3}H-Uridine uptake by cNT1$_{rat}$ cDNA-transfected COS-1 cells in the presence of 1 mM nonradioactive uridine 94

4.4 Construction of c-*myc* tagged cNT1$_{rat}$ 96

4.5 Uridine uptake by recombinant cNT1$_{rat}$ and c-*myc* tagged cNT1$_{rat}$ 98

4.6 Western blotting of c-*myc* tagged cNT1$_{rat}$ 100

4.7 Inhibition of uridine uptake by physiological nucleosides in cNT1$_{rat}$ cDNA-transfected COS-1 cells 102

4.8 Uptake of ^{3}H-guanosine in cNT1$_{rat}$ cDNA-transfected COS-1 cells 104

4.9 Concentration-effect relationships for inhibition by cytidine and deoxycytidine of recombinant cNT1$_{rat}$-mediated uridine transport 106

4.10 Time courses of uridine uptake in cNT1$_{rat}$ cDNA-transfected COS-1 cells 108

4.11 Kinetics of uridine uptake in cNT1$_{rat}$ cDNA-transfected COS-1 cells 110

4.12 Time courses of thymidine uptake in cNT1$_{rat}$ cDNA-transfected COS-1 cells 112

4.13 Kinetics of thymidine uptake in cNT1$_{rat}$ cDNA-transfected COS-1 cells 114

4.14 Time courses of cytidine uptake in cNT1$_{rat}$ cDNA-transfected COS-1 cells 116

4.15 Kinetics of cytidine uptake in cNT1$_{rat}$ cDNA-transfected COS-1 cells 118

4.16 Time courses of adenosine uptake in cNT1$_{rat}$ cDNA-transfected COS-1 cells 120

4.17 Kinetics of adenosine uptake in cNT1$_{rat}$ cDNA-transfected

COS-1 cells 122

4.18 Comparison ^{3}H-adenosine and ^{3}H-uridine uptake in in $\mathrm{cNT1}_{rat}$ cDNA-transfected COS-1 cells 124

4.19 Inhibiton OF $\mathrm{cNT1}_{rat}$-mediated uridine uptake in COS-1 cells by nucleoside drugs 126

4.20 Concentration-effect relationships for inhibition by IUdR and FUdR of recombinant $\mathrm{cNT1}_{rat}$-mediated uridine transport 128

A.1 Inhibition of endogenous uridine transport in CHO-K1 cells by NBMPR and dilazep 146

A.2 Nucleoside uptake by geneticin-resistant stable transfectants 148

A.3 Demonstration of integration of $\mathrm{cNT1}_{rat}$ cDNA into genomic DNA of CHO-K1/$\mathrm{cNT1}_{rat}$ by PCR amplification 150

A.4 Uridine uptake by nontransfected CHO-K1 cells and CHO-K1/ $\mathrm{cNT1}_{rat}$ cells in sodium-containing or sodium-free buffer 152

ABBREVIATIONS

3TC	2'-Deoxy-3-thiacytidine
Ado	Adenosine
AIDS	Acquired immunodeficiency syndrome
araC	1-β-D-arabinofuranosylcytosine
ATCC	American Type Cuture Collection
AZT	3'-Azido 3'-deoxythymidine
BES	N, N'-bis-(2-hydroxyethyl)-2-aminoethanesulfonic acid
Bmax	Maximum number of ligand binding sites per cell
bp	Nucleotide basepair
BSA	Bovine serum albumin
cDNA	Complementary DNA
CHO-K1	Chinese hamster ovary cell line
cNT	Concentrative nucleoside transporter
COS-1	African green monkey kidney cell line
Cyd	Cytidine
dCyd	Deoxycytidine
ddC	2', 3'-Dideoxycytidine
DEAE	Diethylaminoethyl
dFdC	Gemcitabine; 2', 2'-difluorodeoxycytidine
dH_2O	Distilled H_2O
DMEM	Dulbecco's modified Eagle medium
DMSO	Dimethylsulfoxide
DNA	Deoxynucleic acid

dNTP	Deoxyribonucleoside triphosphate
dThd	Thymidine
ECL	Enhanced chemiluminescence
EDTA	Ethylenediaminetetraacetic acid
FUdR	2'-Deoxy-5-fluorouridine
Guo	Guanosine
h	Hour
HEPES	N-2-Hydroxyethylpiperazine-N'-2-ethanesulfonic acid
HIV	Human immuno-deficiency virus
HPLC	High performance liquid chromatography
HRP	Horse-horse radish peroxidase
IC_{50}	Concentration at which 50 percent inhibition was achieved
IUdR	2'-Deoxy-5-iodouridine
Kd	Dissociation constant
kDa	Kilodaltons
Km	Concentration at which half-maximal flux occurred
min	Minute
NBMPR	Nitrobenzylthioinosine
NMDG	N-Methyl-D-glucammonium
NT	Nucleoside transporter
PBS	Phosphate-buffered saline
PCR	Polymerase chain reaction
PMSF	Phenylmethylsulfonyl fluoride
RNA	Ribonucleic acid
RT	Room temperature

SD	Standard deviation
SDS-PAGE	Sodium dodecylsulphate-polyacrylamide gel electrophoresis
SDS	Sodium dodecylsulphate
sec	Second
SPNT	Sodium-dependent purine nucleoside transporter
Tris	Tris-(hydroxymethyl) aminomethane
Urd	Uridine
UV	Ultraviolet
v/v	Volume per unit volume
w/v	Weight per unit volume
w/w	Weight per unit weight
X-Gal	5-Bromo-4-chloro-3-indoyl-β-D-galacopyranoside

CHAPTER I

INTRODUCTION

1.1 Overview

Many nucleosides and nucleoside analogues play important physiologic and pharmacologic roles. However, most of them are highly hydrophilic and require functional nucleoside transport processes to cross the lipid bilayer of biological membranes. Cells lacking nucleoside transporters by mutations (1-5) or treatment with nucleoside transporter (NT) inhibitors (6-8) have low levels of uptake of physiologic nucleosides and no response to a variety of nucleoside drugs. Thus, the presence of functional NT proteins in plasma membranes is an important prerequisite for physiologic and pharmacologic activities. The knowledge of substrate selectivities and distribution of NT proteins should be informative for the design and use of nucleoside drugs.

Today, seven functionally distinct nucleoside transport processes have been described. However, purification of nucleoside transport proteins is very difficult because they are minor components of plasma membranes. Efforts in molecular cloning of nucleoside transport proteins have resulted in the recent isolation of a sodium-dependent NT cDNA from rat intestine, named $cNT1_{rat}$ (9). The objectives of this study were to express $cNT1_{rat}$ cDNA in mammalian cell lines, using transfection techniques, and to functionally characterize recombinant $cNT1_{rat}$ by analysis of inward fluxes of ^{3}H-labeled nucleosides.

1.2 Nucleosides and Nucleoside Analogues

The addition of a pentose sugar (β-D-ribofuranose or β-D-deoxyribofuranose) to a nucleobase generates a nucleoside. If the sugar is ribose, the nucleoside is a ribonucleoside; if the sugar is 2'-deoxyribose, the nucleoside is a deoxyribonucleoside. Esterification of the 5'-hydroxyl group of the sugar with phosphoric acid produces a mononucleotide (nucleoside monophosphate), and the subsequent addition of two more phosphoryl groups produces a nucleoside triphosphate. Nucleoside triphosphates are the building blocks of DNA and RNA. Nucleotides also play many key roles in cellular metabolism. For example, ATP, an adenine nucleotide, is a major energy carrier in biosynthetic reactions. Adenine nucleotides are also structural components of some important coenzymes, such as Coenzyme A. Therefore, nucleotides are essential for cell survival.

Nucleotides are produced biosynthetically by *de novo* pathways. Although most mammalian cells have the capacity to synthesize purine and pyrimidine nucleotides by *de novo* pathways, nucleotides are also formed directly from preformed bases and nucleosides. The latter processes, which are commonly called "salvage pathways", are bioenergetically less costly than the *de novo* pathways. The salvage pathways are essential for cells lacking *de novo* pathways, such as bone marrow, leukocytes, blood platelets and erythrocytes (10).

Permeation across the plasma membrane is the first step in the nucleoside salvage pathway. Nucleosides enter cells only slowly by passive diffusion. In addition, transporter systems are present in cell membranes for the efficient uptake from the extracellular space of nucleosides, derived from nutrients or degraded nucleic acids. Nucleosides, once inside cells, are phosphorylated by various nucleoside kinases, which transfer the γ phosphate from ATP to the 5'-hydroxyl group of the pentose sugar to produce a mononucleotide.

Nucleoside transporters are believed to have relatively broad substrate specificities, whereas the nucleoside kinases, which catalyze the second step in the salvage pathways, have narrow substrate specificities. For example, thymidine kinase 1 accepts thymidine and deoxyuridine but not uridine as substrates. For some nucleosides, beside phosphorylation, other reactions (e.g., deamination) are also involved in intracellular metabolism. For example, adenosine is subject to deamination to inosine, which, in turn, is degraded by nucleoside phosphorylase to hypoxanthine and ribose-1-P (Figure 1.1).

Nucleoside kinases play an important role in the intracellular activation of many nucleoside analogues with antiviral or anticancer activities. For example, deoxycytidine kinase is the enzyme primarily responsible for phosphorylation of the antiviral drug 2', 3'-dideoxycytidine (ddC) and the anticancer drug 1-β-D-arabinofuranosylcytosine (araC). Cell mutants lacking deoxycytidine kinase are resistant to the cytotoxicity of ddC and araC (11).

Generally, nucleoside transport and nucleoside intracellular metabolism are believed to be independent events. However, it is possible that there may be relationships between nucleoside metabolism and transport activities. For example, mitogenic stimulation of lymphocytes leads to simultaneous increases in thymidine uptake and thymidine kinase activity (12). The precise relationship remains to be determined.

1.2a Natural Nucleosides

The natural nucleosides used in this study were adenosine, guanosine, thymidine, uridine, cytidine and deoxycytidine (Figure 1.2 and 1.3).

Adenosine, once it enters the cell, can follow two distinct pathways (13): it can be phosphorylated by adenosine kinase or be deaminated by adenosine deaminase. These two enzymes influence the intracellular concentration of adenosine.

Adenosine and adenine nucleotides are involved in the regulation of cellular function, such as platelet aggregation, coronary vasodilation, cardiac contractility, and renal vasoconstriction by the interaction with cell surface purinergic receptors, P1 and P2 (14, 15). P1 purinergic receptors prefer adenosine to adenine nucleotides, and act basically through G-protein coupled proteins and the adenylate cyclase pathway. P2 purinoceptors prefer adenine nucleotides to adenosine, and act either through G-protein coupled cascades or ligand-gated ion fluxes.

A rapid increase in concentration of adenosine is required to activate the receptor and a rapid decrease is required to deactivate the receptor. Nucleoside transporters may be involved in these processes, although less is known about the mechanisms of release than of uptake. The deactivation of purinoceptors may be achieved by cellular reuptake of adenosine by nucleoside transporters.

Another important natural nucleoside is thymidine. By the salvage enzyme thymidine kinase, provision of exogenous thymidine can elevate intracellular dTTP levels. The major effect of elevated dTTP is the inhibition of ribonucleotide reductase, which leads to depletion of dCTP (16, 17). Enhanced sensitivity to DNA-damaging agents (18, 19) and enhanced mutagenesis (20) have been observed when dTTP levels are increased, suggesting an additional action of dTTP on preformed DNA or its normal repair. The regulation by dTTP of key enzymes of the pyrimidine-synthetic pathways also has important implications for the therapeutic use of thymidine in combination with other antimetabolites such as araC, 5-azacytidine and FUra (21). Therefore, thymidine may have a role in clinical therapy as a modulator of other anticancer drugs.

Uridine is the only nucleoside that has been directly shown to be transported by all major NT subtypes (22). The "universality" of this natural nucleoside has allowed researchers to compare the transporter characteristics among various NT subtypes. Moreover, uridine monophosphate is a precursor of other pyrimidine nucleotides. Thus, uridine and uridine phosphates play an important role in the cellular metabolism of pyrimidine nucleotides.

1.2b Nucleoside Analogues

Because of the essential role of nucleotides in cellular life, it is not surprising that their analogues would be particularly toxic to cells with rapid proliferation and would inhibit the multiplication of viruses. Many nucleosides and their analogues interfere with or block DNA synthesis after conversion to nucleotides by intracellular phosphorylation. Some nucleoside analogues have been widely used in antiviral and anticancer chemotherapies (Figure 1.4, 1.5).

(i) Antiviral nucleoside drugs

Acquired immunodeficiency syndrome (AIDS) is caused by human immunodeficiency virus (HIV). HIV is an RNA virus. It contains an RNA-directed DNA polymerase that reverse transcribes its RNA genome into DNA as the first step of viral replication. Over the past almost ten years, a large number of drugs have been designed and tested for their effects on different steps of HIV replication. Among them, the only drugs that have been proved to be effective clinically are the nucleoside analogues that terminate DNA chain elongation (23). Three of the nucleoside drugs used in this study exhibit activity against HIV. They are 3'-azido 3'-deoxythymidine (AZT), ddC and 2'-deoxy-3-thiacytidine (3TC) (Figure 1.4).

AZT has received much attention because it is currently the drug of choice in patients with AIDS (24). It is a thymidine analogue with an azido group in place of the hydroxyl group on the ribose. AZT is converted to its monophosphate (AZTMP) by thymidine kinase; thymidylate kinase then converts AZTMP to the triphosphate (AZTTP). AZTTP is incorporated into the growing DNA chain and blocks chain elongation because there is no 3'-OH group on the AZT residue for attachment of the next nucleotide unit (25). The effect of AZT is increased by the accumulation of AZTMP in cells because AZTMP inhibits thymidylate kinase and subsequently decreases the dTTP level in the cell (26-29). With less competition of dTTP, there is more efficient incorporation of AZTTP into viral DNA synthesis. However, strains of HIV resistant to AZT have been isolated from patients on long-term AZT therapy (30, 31).

2',3'-Dideoxycytidine (ddC) is an analogue of deoxycytidine that is missing the hydroxyl group on the ribose. The mechanism of action of ddC is quite similar to that of

AZT in that it is phosphorylated to the triphosphate form which subsequently terminates DNA chain elongation (32). ddC is used to treat patients with AIDS who are intolerant of or are resistant to AZT (24). Recently, it has been found that combination therapy with ddC and AZT is more effective than therapy with either drug alone (24).

3TC is a new anti-HIV drug and is currently being investigated in clinical trials. It is a cytidine analogue, with more diverse modifications than previous compounds, particularly to the sugar. Its L-sugar configuration, or (-) enantiomer, is the most potent form for antiviral effect (Figure 1.6) (33, 34). Moreover, studies have shown that the intracellular concentrations of the (-) form and its metabolites were approximately 5-fold higher than those of the (+) form metabolites (35, 36). Like AZT and ddC, 3TC is phosphorylated to the triphosphate form, which inhibits HIV replication.

Another antiviral nucleoside drug used in my work was 2'-deoxy-5-iodouridine (IUdR) (Figure 1.4). IUdR was the first clinically effective antiviral nucleoside analogue (23). It has been found effective in the treatment of herpetic keratitis and ocular herpes virus infections (37, 38). IUdR is a nucleoside analogue in which the methyl group of thymidine is replaced by an iodine atom. The drug is phosphorylated by cellular thymidine kinase and then to the triphosphate form, which is incorporated into viral DNA.

(ii) Anticancer Drugs

Three anticancer nucleoside drugs were used in this study. They were araC, difluorodeoxycytidine (gemcitabine or dFdC) and 2'-deoxy-5-fluorouridine (FUdR) (Figure 1.5).

AraC is a cytidine analogue that is effective in the treatment of some forms of leukemia (39). AraC is taken up by cells and first converted to its monophosphate (araCMP) by deoxycytidine kinase and araCMP is then metabolized to araCDP and araCTP by dCMP kinase and nucleoside diphosphate kinase, respectively (40, 41). Incorporation of araCTP into elongating DNA chains results in the termination of DNA synthesis (42-

44). araCTP is a competitor of dCTP, and its efficacy increases with the reduction of intracellular dCTP levels (45). Production of dCTP requires ribonucleotide reductase, because dCTP is phosphorylated from dCDP, and dCDP is converted from CDP by ribonucleotide reductase. Ribonucleotide reductase is inhibited by high levels of dTTP, for example, when cells are exposed to high concentrations of thymidine. Therefore, araC cytotoxicity can be enhanced by use in combination with thymidine, which leads to reduced dCTP levels (46, 47) (Figure 1.7).

Gemcitabine is a relatively new deoxycytidine analogue, which has promising activity against solid tumors. Activity has been observed in non-small cell lung cancer and ovarian cancer patients. Gemcitabine differs from deoxycyticine, the endogenous nucleoside, by two fluorine atoms at C-2'. Like araC, gemcitabine is phosphorylated by deoxycytidine kinase (48). dFdCTP can be incorporated into DNA, which is postulated to be the main target for the drug (48). In spite of the close structural relationship between gemcitabine and araC, the cellular accumulation of active metabolites and the antineoplastic effects of gemcitabine are much greater than those of araC (49).

FUdR is an important anticancer drug. It is a fluorinated pyrimidine, and used widely for the treatment of breast cancer and other solid tumors. FUdR is converted to 5'-fluoro-2'-deoxyuridine 5'-monophosphate (FdUMP), which is a potent inhibitor of thymidylate synthetase (50).

1.3 Nucleoside Transporters

NT-mediated processes in mammalian cells can be divided into two classes, depending on whether they are equilibrative or concentrative (22). The equilibrative NTs are driven by the concentration gradient of nucleoside permeants, whereas the concentrative NTs are driven by the transmembrane sodium gradient.

1.3a Equilibrative Nucleoside Transporters of Mammalian Cells

The equilibrative NTs are widely distributed in mammalian cells and tissues, including many neoplastic cell types (51-54) and appear to be able to transport purine as well as pyrimidine nucleosides. Equilibrative NT-mediated processes can be further classified into two subtypes based on their sensitivity to inhibition by nitrobenzylthioinosine (NBMPR). One subtype is named *es* (equilibrative sensitive), and the other is named *ei* (equilibrative insensitive). The *es* processes are inhibited by low concentrations ($\leq$ 1 nM) of NBMPR, whereas the *ei* processes are unaffected by NBMPR, or are inhibited only by high concentrations ($\geq$ 10 μM) (22). A 10^4-fold difference in NBMPR sensitivity exists between *es* and *ei* transporters (55-61). Both transporter subtypes are inhibited by low concentrations (0.1 - 100 nM) of dipyridamole and dilazep (62-70).

The NBMPR transport inhibitory sites are believed to be associated specifically with the *es* transporters. The extent of NBMPR inhibition is directly correlated with the presence of NBMPR binding sites in plasma membranes (2, 71, 72). NBMPR-binding sites, determined by Scatchard analysis, have been identified in isolated membrane preparations (73) and intact cells (55, 71, 72, 74, 75), which exhibit *es* nucleoside transport activity. The number of NBMPR-binding sites varies considerably among different types of cells, from relatively low numbers of 10^4/cell reported for erythrocytes (74) and lymphocytes (76) to 10^7/cell for cultured human choriocarcinoma (BeWo) cells (77).

The primary structure of the equilibrative NTs has not been determined and the relationship between *es* and *ei* processes is still controversial. They could be mediated by different, but structurally related, proteins, or by alternate forms of the same protein. While nothing is known about the protein(s) associated with *ei* processes, some major features of *es* proteins have been determined. The *es* transporter of human erythrocytes has been identified (78-80) and is believed to be structurally similar to the erythrocyte glucose transporter (GLUT1). The two polypeptides co-migrate in the "band 4.5" region (45-65 kDa) of electrophoretograms when detergent-solubilized erythrocyte membranes are subjected to SDS-PAGE. Although the two polypeptides are co-purified by DEAE-cellulose chromatography, subsequent passage through affinity columns with specific antibodies for GLUT1 resulted in purification of *es* transporter polypeptides of human erythrocytes (81).

Es transporters may have multiple isoforms (22). Polyclonal antibodies against the human erythrocyte *es* transporter recognized polypeptides in immunoblots prepared from brush-border membranes of human placenta but not from basal membranes, although both brush-border and basal membrane exhibited *es* NT activity and similar numbers of NBMPR sites (82). A similar conclusion was reached from immunohistochemical studies. The antibodies against the human erythrocyte *es* transporter bound to brush-border surfaces, but not to basolateral surfaces, of synctiotrophoblasts (82). These observations have suggested that multiple *es* transporter isoforms may exist in a single species and tissue.

1.3b Concentrative Nucleoside Transport Processes

Concentrative nucleoside transport processes can be classified into five functional subtypes. N1/*cif* processes exhibit selectivity for purine nucleosides and uridine and have been found in many different cell types (66, 83-88), for example, IEC6 rat intestinal cells (87). N2/*cit* processes are selective for pyrimidine nucleosides and adenosine and have been observed in freshly isolated enterocytes, in brush border vesicles from renal epithelial cells of bovine, rat and rabbit, and in *Xenopus* oocytes injected with rat and rabbit intestinal mRNA (84, 89-93). N3/*cib* processes have broad specificity for both purine and pyrimidine nucleosides and have been observed in cultured colorectal (CACO-2) cells (51) and differentiated human promyelocytic (HL-60) leukemia cells (94, 95). The N4/*cit* process resembles N2/*cit* processes in that it is selective for pyrimidine nucleosides and adenosine, but it also transports guanosine. N4/*cit* has been found only in brush border vesicles from human kidney (96). Coupling stoichiometries for sodium and nucleoside have been reported to be 1:1 for N1/*cif* and N2 or N4/*cit* (85, 86, 90-92, 96, 97) but 2:1 for N3/*cib* (98). None of these NTs are affected by high concentrations (> 10 μM) of the classic inhibitors of equilibrative NT-mediated processes (NBMPR, dilazep and dipyridamole). A fifth subtype of concentrative NT designated as N5/*cs* has been found to be highly sensitive to inhibition by low (<10 nM) concentrations of NBMPR and dipyridamole (99). N5/*cs* activity has been observed only in freshly isolated human leukemic cells. Its substrate selectivity and coupling stoichiometry have not yet been established.

From the functional studies conducted thus far (84, 89-93), N2/*cit* activity seems to be limited to intestinal and kidney epithelia. This NT subtype has been shown to be driven by sodium gradient. It is not inhibited by NBMPR or dilazep or dipyridamole. Direct measurements of radiolabed nucleosides indicate that this NT subtype transports pyrimidine nucleosides, such as uridine and thymidine. Kinetic studies (84, 90-92) showed that it has high affinity for uridine and thymidine (K_m values, < 50 μM). Inhibition studies (84, 89-93) showed that it is inhibited by pyrimidine nucleosides, adenosine and analogues of adenosine, but not by other purine nucleosides. No direct measurements of ^{3}H-adenosine transport in N2/*cit* systems have been reported.

Although concentrative NT proteins have not yet been physically purified, several cDNAs encoding proteins with concentrative nucleoside transport activities (9, 100, 101) have recently been cloned. Thus, the information about concentrative NT proteins has greatly increased.

cNT1$_{rat}$ is a newly identified transporter protein with sodium-dependent nucleoside transport activity (9). It is encoded by a cDNA that was isolated from a rat intestine cDNA library by expression selection in *Xenopus* oocytes (9). A rat jejunum mRNA size-fraction (about 2.3 kb), which exhibited high levels of sodium-dependent nucleoside transport activity in microinjected oocytes, was used to construct a directional cDNA library in the vector pGEM-3Z. Subsequent expression screening of this library in *Xenopus* oocytes resulted in the isolation of the cNT1$_{rat}$ cDNA. cNT1$_{rat}$ is predicted to be a 71 kDa protein with 648 amino acids, 14 transmembrane domains, three possible N-linked and four O-linked glycosylation sites, and four consensus sites for protein kinase C phosphorylation. When produced in the *Xenopus* oocytes expression system, recombinant cNT1$_{rat}$ exhibits high levels of nucleoside transport activity and shows N2/*cit*-like characteristics (9). Northern blot analysis showed that cNT1$_{rat}$ mRNA is present in rat kidney and intestine.

SPNT is encoded by a cDNA that was isolated from a rat liver cDNA library by functional expression selection in *Xenopus* oocytes (100). SPNT is predicted to be a 72 kDa protein with 659 amino acids, 14 transmembrane domains, and five possible N-linked glycosylation sites. It has three consensus sites for protein kinase A and six consensus sites for protein kinase C. When produced in the *Xenopus* oocyte expression system, recombinant SPNT exhibits substrate selectivity characteristic of an N1/*cif* transport process. mRNA for SPNT was detected in rat liver, jejunum, spleen, and heart.

SNST1 is encoded by a cDNA that was isolated from a rabbit kidney library by low stringency hybridization with a DNA probe that was derived from the Na$^+$/glucose cotransporter (SGLT1) of rabbit intestine (101). SNST1 is believed to be a member of the SGLT family, with 61% identity and 80% similarity in amino acid sequence to rabbit

SGLT1. SNST1 is predicted to have twelve hydrophobic transmembrane domains. When produced in the *Xenopus* oocyte expression system, recombinant SNST1 exhibits weak (1.7 fold over background) sodium-dependent nucleoside transport activity with N3/*cib*-like substrate selectivity. Higher levels of SNST1 activity have not yet been achieved in various expression systems. On Northern blots, SNST1 mRNA was not observed in rabbit intestine but in heart, which has not been found to have sodium-dependent nucleoside transport activity. The physiologic significance of SNST1 is uncertain.

Two nucleoside transport systems, NUPG and NUPC, have been reported in the inner membrane of *E. coli*. Transport studies have provided abundant evidence that these two systems are driven by proton motive force (102-105). NUPC and NUPG can be distinguished by their substrate selectivity. NUPC has a poor ability to transport guanosine and inosine, but is selective for pyrimidine nucleosides (106, 107). NUPG has broad permeant selectivity, and transports both purine and pyrimidine nucleosides. Genes encoding these two proteins have been identified (108, 109). Their predicted structures are unrelated. NUPC is predicted to be a 43 kDa protein with 401 amino acids, while NUPG is a 45 kDa protein with 418 amino acids.

Database searching has revealed similarities among $cNT1_{rat}$, SPNT and NUPC. $cNT1_{rat}$ is 27% identical to NUPC, and the most similar region is in the carboxyl-terminus (Figure 1.8). SPNT shows 64% identity at the amino acid level to $cNT1_{rat}$. The N- and C-terminal regions show more differences. Some short distinct stretches of similar amino acid sequence are present in the transmembrane regions. SPNT also shows similarities to NUPC. Thus, two rat Na^+-dependent nucleoside transport proteins ($cNT1_{rat}$, SPNT) and one bacterial H^+-dependent nucleoside transport protein (NUPC) appear to be structurally related. The similarities in amino acid sequence among the three proteins are about 30% to 60%, especially in the C-terminal half. $cNT1_{rat}$ and SPNT are both predicted to have 14 transmembrane segments whereas NUPC is predicted to have 10 transmembrane segments. Segments 3-10 of NUPC correspond to segments 7-14 of $cNT1_{rat}$ and SPNT. There are conserved amino acid residues and stretches found throughout all three proteins. $cNT1_{rat}$ and SPNT select pyrimidine and purine nucleosides, respectively, but are driven by the same cation. By contrast, $cNT1_{rat}$ and NUPC share the same nucleoside specificity, but are driven by different cations. Thus, these three transporter proteins appear to be members of a cation-dependent family of NTs. The structural differences and similarities of these members may provide clues for mechanisms of transport function and ion-dependence. The conserved motifs may lead to the discovery of other important members of this family.

1.4 Expression of DNA in Mammalian Cells

After a cDNA has been cloned, it is usually expressed in various cell types to characterize the function of the protein. Ideally, cDNAs encoding proteins of higher eukaryotes are expressed in mammalian cells because the signals for synthesis, processing, and secretion are likely to be recognized. DNA expression systems are often classified into two categories, transient and stable transfection, depending on the fate of the introduced DNA.

1.4a Transient Expression

After transfection, some of the introduced DNA is transcribed in the cell nucleus, and the resulting mRNA is exported to the cytoplasm and translated to protein (110). However, the transfected DNA is expressed for only a limited period of time. In some instances, the transfected DNA gradually disappears, by degradation by nucleases (110) or dilution by cell division (110); sometimes the transfected DNA is replicated to high copy numbers ultimately leading to death of the host cells (111). By transient transfection, one can conveniently and rapidly verify that the protein of interest is functional before initiating the more laborious procedure of isolation and characterization of stably transfected cell lines. The major limitation of transient expression is that it has to be repeated for each experiment.

1.4b Stable Transfection

Stable transfectants are produced when the transfected DNA is incorporated into the host cell's genome by recombination (110). Cells that have stably integrated the foreign DNA into their genome can often be isolated by a selection procedure. For example, stable transfectants can be selected by their ability to survive when treated with cytotoxic drugs. Selectable marker genes are often derived from bacterial genes for which there is no mammalian counterpart. For example, the neomycin phosphotransferase gene encoding resistance to the antibiotic geneticin (G418) has been engineered into many mammalian expression vectors for use as a selection marker (112).

Stable transfection yields permanent cell lines that can be used repeatedly for similar experiments. However, the selection procedure for stable transfectants is time consuming, usually requiring months to perform and verify.

1.4c Host Cell Lines

To select a cell line to be used as the host for transfection studies, it is most important to consider the following three questions: (i) is the cell line transfectable? (ii) is the endogenous protein activity of the cell line absent, or can it be blocked? (iii) what are the goals of the expression work?

To demonstrate the functional activity of a recombinant mammalian protein, transient expression in COS cells is often the most convenient approach (111). COS cells were derived from African green monkey kidney cells (113) by transformation with an origin-defective simian virus 40 (SV40). COS cells express high levels of SV40 large tumor (T) antigen which is required to initiate viral DNA replication at the origin of SV40 (114). T antigen-mediated replication can amplify the copy number of plasmids containing the SV40 origin to >100,000 copies per cell (110), which leads to high expression levels of the transfected DNA. COS cells were first used to express mutant glycoproteins of vesicular stomatitis virus by Rose and Bergmann (115). COS cells have also been used to study recombinant acetylcholine receptors (116), insulin (117), somatostatin (118), and some transporters, such as the dopamine transporter (119). These experiments demonstrated that COS cells could be used to express functional secreted and cell-surface proteins, including many transporter proteins.

To generate a stable expression system, cell lines that allow transfected DNA to be integrated into their chromosomes relatively easily, such as CHO cells, are frequently selected. For example, it has been used successfully to stably express many proteins, such as S-adenosylmethionine decarboxylase (120), H1-histamine-receptor (121) and glucose transporters (122).

1.4d Expression Vectors

Most mammalian cell expression vectors contain multiple elements. Many have an SV40 origin for high copy number replication in cells with large T antigen, such as COS cells. There is usually an efficient promoter element for high-level transcription initiation. Many of the promoters used in mammalian expression vectors have been derived from viruses; the SV40 promoter, Rous sarcoma virus long terminal repeat and the cytomegalovirus (CMV) promoter are active in a variety of mammalian cell types. The CMV promoter has been found to be effective when transfected into a variety of cell types (123). Expression vectors also contain (i) mRNA processing signals, including GU- or U-rich sequences and a conserved AAUAAA sequence for posttranscriptional cleavage and polyadenylation; (ii) polylinkers for insertion of transfected DNA; (v) selection markers that can be used to identify cells that have stably integrated the plasmid DNA, and (vi) sequences to permit propagation in bacterial cells.

1.4e Transfection Techniques

Over the past three decades, many biochemical and physical transfection methods have been developed. Among them, four techniques are commonly used today. They are electroporation (124), liposome-mediated transfection (125), calcium phosphate transfection (126,127) and DEAE-dextran transfection (128-131). The first three can be used for both transient and stable transfection, whereas the last one is only effective for transient transfection.

(i) Electroporation:

Subjecting cells to a high-voltage electric field results in a potential difference across the membrane, and this potential difference induces temporary breakdown and the formation of pores in the membrane that allow DNA to enter cells (124, 132). The two parameters that are critical for successful electroporation are the maximum voltage of the shock and the duration of the current pulse, because excessive field strength and duration of the electrical pulse can damage the cells (133, 134). Electroporation can be easily carried out and can be used for both adherent and suspension cells. Its drawback is that almost five-fold more cells and DNA are needed than with other transfection methods (the reason is not clear), and that a special electroporation apparatus is required.

(ii) Liposome-mediated transfection

The mechanism of this method is based on an ionic interaction between the DNA and the cationic liposome (125). Since the liposomal surfaces are positively charged, they are easily attracted to the phosphate backbone of DNA and the negatively charged surfaces of cells (125). This method can yield high transfection efficiencies in a wide variety of mammalian cells (111).

(iii) Calcium phosphate transfection

The mechanism of this method is that the mixture of calcium chloride, DNA plasmid and phosphate buffer leads to the formation of calcium phosphate precipitates, which contain condensed DNA (126, 127, 135). These calcium phosphate/DNA particles adhere to cell membranes and enter cells by phagocytosis (136). The optimum pH range of the phosphate buffer is narrow and critical for successful transfections (127, 135). A useful feature of calcium phosphate transfection is that one can prepare a certain molar ratio of two plasmids and expect that the plasmids will be present in that ratio in the transfected cells (111). The calcium phosphate method was used in this study for stable cotransfection of two plasmids under conditions where the molar ratio of the two transfecting plasmids were different.

(iv) DEAE-dextran transfection

DEAE-dextran/DNA complexes stick to cell surfaces and are thought to be taken up by endocytosis (137). The DEAE-dextran concentration is an important parameter for transfection efficiency (111). This is a highly reproducible, convenient and inexpensive means to study gene expression in a variety of cell types, including COS cells. However, it is only used for transient transfection in adherent cells (111). The DEAE-dextran method was used in this study for transient transfection of COS-1 cells.

1.5 Objectives of Research

Many cell types simultaneously exhibit two or three NT-mediated processes and it is often difficult to study the characteristics of a particular process in the presence of others with overlapping substrate selectivities. Although a few cell types that naturally express a single transporter subtype have been used profitably for structure-activity studies, such a cell type has not been identified for the concentrative pyrimidine-selective NTs. Prior to the cloning of cNT1$_{rat}$ cDAN, N2/*cit* and N4/*cit* activities had been studied only in freshly isolated mouse intestinal epithelial cells, brush border membrane vesicles from human, bovine, rat and rabbit kidney and oocytes of *Xenopus* laevis injected with mRNA from rabbit intestine. Most, and possibly all, of these preparations contain more than one NT-mediated process. A system that exhibits a single transporter subtype would provide a more convenient and specific approach for analysis of functional characteristics. The transfection technology and the availability of cloned cNT1$_{rat}$ cDNA made it possible to attempt to develop an N2/*cit* mammalian cell expression system that would allow study of the N2/cit transporter in the absence of other NT subtype activities. The goals of my work were (i) to transiently express the cNT1$_{rat}$ cDNA in a mammalian cell line at levels that allowed kinetic characterization of the transport of radioactive nucleosides; (ii) to investigate if the characteristics of recombinant cNT1$_{rat}$ in a mammalian expression system were similar to those determined previously (9, 138) in the *Xenopus* oocyte expression system during the cloning of the cDNA; (iii) to further characterize the function (kinetics, nucleoside selectivities and nucleoside drugs transportabilities) of recombinant cNT1$_{rat}$ when expressed in a mammalian physiological environment; (iv) to determine if $cNT1_{rat}$ stable transfectants could be produced in mammalian cells.

1. Figure 1.1 Metabolic pathways of adenosine

Ado : adenosine

Ino : inosine

Hyp : hypoxanthine

AMP : adenosine monophosphate

ADP : adenosine diphosphate

ATP : adenosine triphosphate

IMP : inosine monophosphate

PRPP : phosphoribosyl pyrophosphate

NT : nucleoside transporter

(1) : adenosine kinase

(2) : adenylate kinase

(3) : nucleotide kinases

(4) : adenosine deaminase

(5) : purine nucleoside phosphorylase

(6) : adenylate deaminase

(7) : adenylosuccinate synthetase

(8) : adenylosuccinate lyase

(9) : hypoxanthine-guanine phosphoribosyltransferase

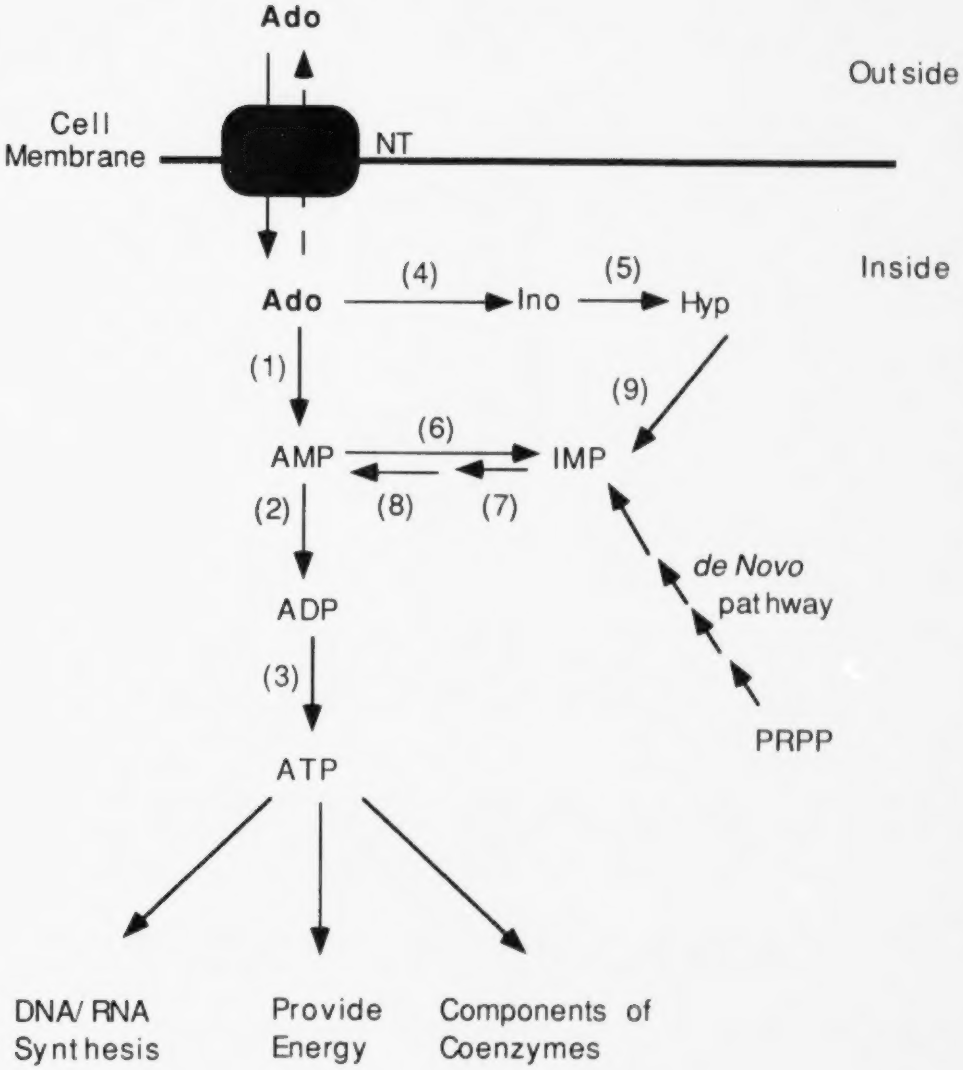
Ado
Outside
Cell Membrane
NT
Inside
Ado
(4)
Ino
(5)
Hyp
(1)
(9)
AMP
(6)
IMP
(2)
(8)
(7)
de Novo pathway
ADP
(3)
PRPP
ATP
DNA/ RNA Synthesis
Provide Energy
Components of Coenzymes

Figure 1.2 Structures of the purine nucleosides used in this study

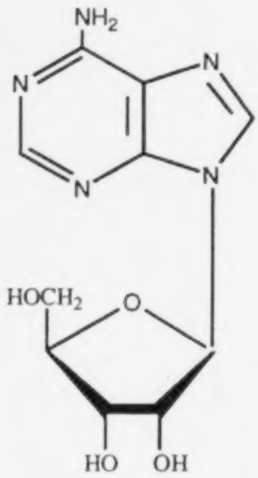
NH2
N
N
N
N
HOCH2
O
HO
OH

Adenosine
(Ado)

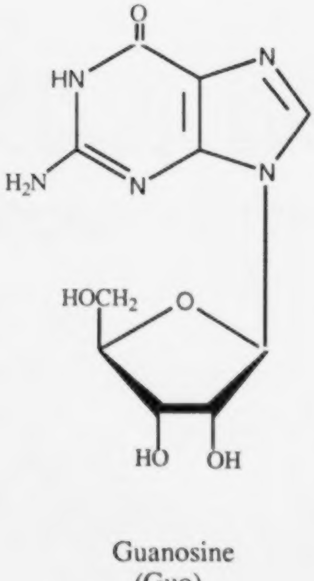
O
HN
N
N
H2N
N
HOCH2
O
HO
OH

Guanosine
(Guo)

Figure 1.3 Structures of the pyrimidine nucleosides used in this study

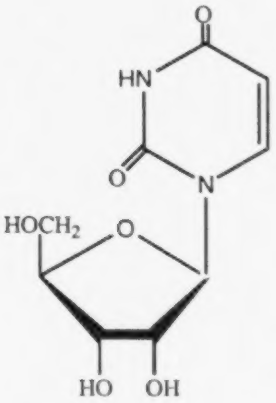
O
HN
O
N
HOCH$_2$
O
HO
OH

Uridine
(Urd)

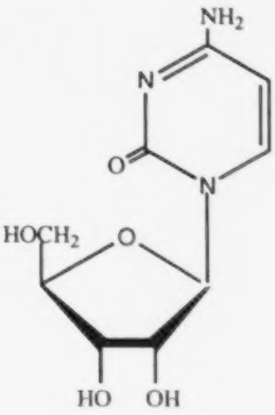
NH$_2$
N
O
N
HOCH$_2$
O
HO
OH

Cytidine
(Cyd)

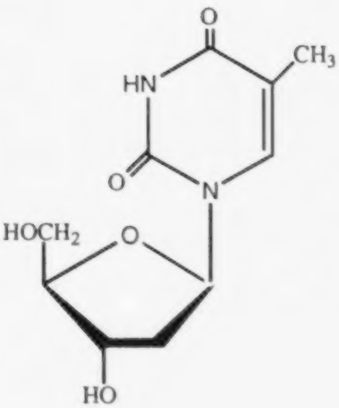
O
CH$_3$
HN
O
N
HOCH$_2$
O
HO

Thymidine
(dThd)

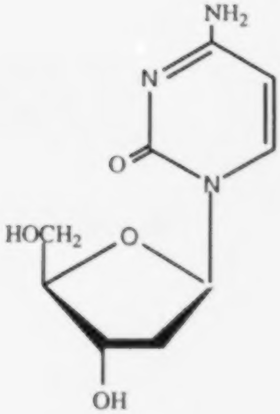
NH$_2$
N
O
N
HOCH$_2$
O
OH

Deoxycytidine
(dCyd)

Figure 1.4 Structures of the antiviral nucleoside drugs used in this study

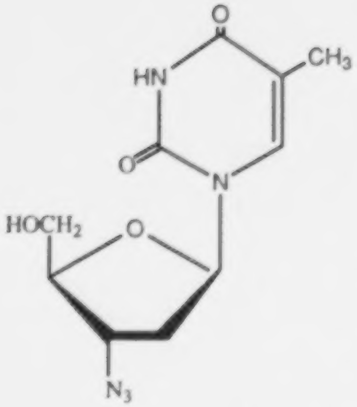
O
HN
CH3
O
N
HOCH2
O
N3

3'-Azido 3'-deoxythymidine
(AZT), Zidovudine

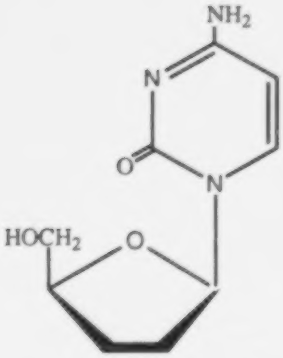
NH2
N
O
N
HOCH2
O

2',3'-Dideoxycytidine
(ddC), Zalcitibine

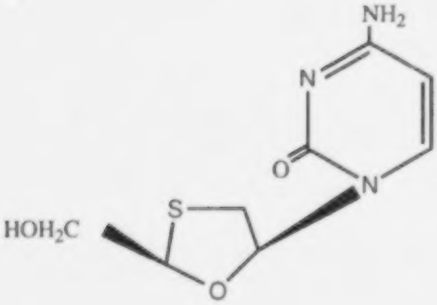
NH2
N
O
N
S
HOH2C
O

2'-deoxy-3'-thiacytidine
(3TC)

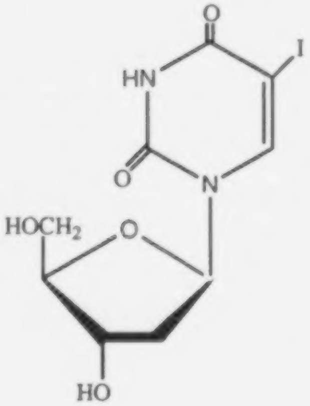
O
I
HN
O
N
HOCH2
O
HO

2'-deoxy-5-iodouridine
(IUdR), Idoxuridine

Figure 1.5 Structures of the anti-cancer nucleoside drugs used in this study

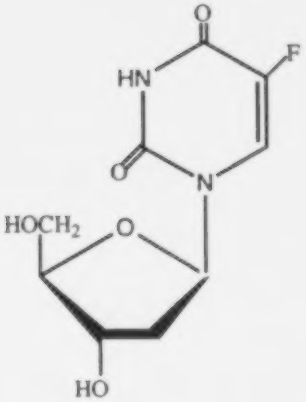
O
F
HN
O
N
HOCH2
O
HO

2'-deoxy-5-fluorouridine
(FUdR), Floxidine

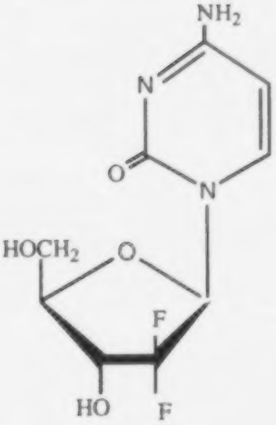
NH2
N
O
N
HOCH2
O
F
HO
F

2', 2'-difluorodeoxycytidine
(dFdC), Gemcitabine

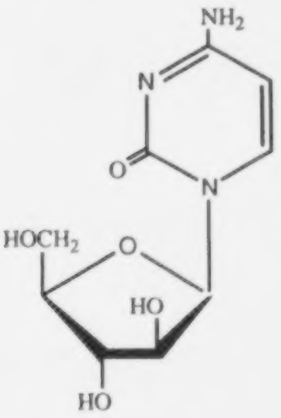
NH2
N
O
N
HOCH2
O
HO
HO

1-ß-D-arabinofuranosylcytosine
(araC), Cytarabine

Figure 1.6 Structures of the two enantiomers of 3TC

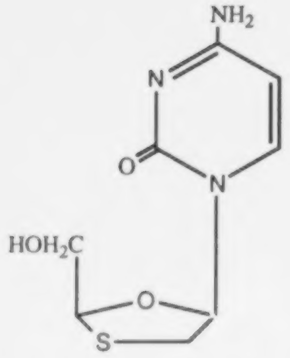
NH2
N
O
N
HOH2C
O
S

(+) 2'-deoxy-3'-thiacytidine

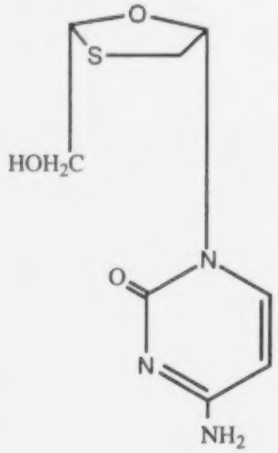
O
S
HOH2C
N
O
N
NH2

(-) 2'-deoxy-3'-thiacytidine

Figure 1.7 Metabolism and Mechanism of AraC

araC	Cytarabine
araCMP	Cytarabine monophosphate
araCDP	Cytarabine diphosphate
araCTP	Cytarabine triphosphate
1	deoxycytidine kinase
2	nucleoside monophosphate kinase
3	nucleoside diphosphate kinase
CDP	cytidine diphosphate
dCDP	deoxycytidine diphosphate
dCTP	deoxycytidine triphosphate
dTTP	thymidine triphosphate

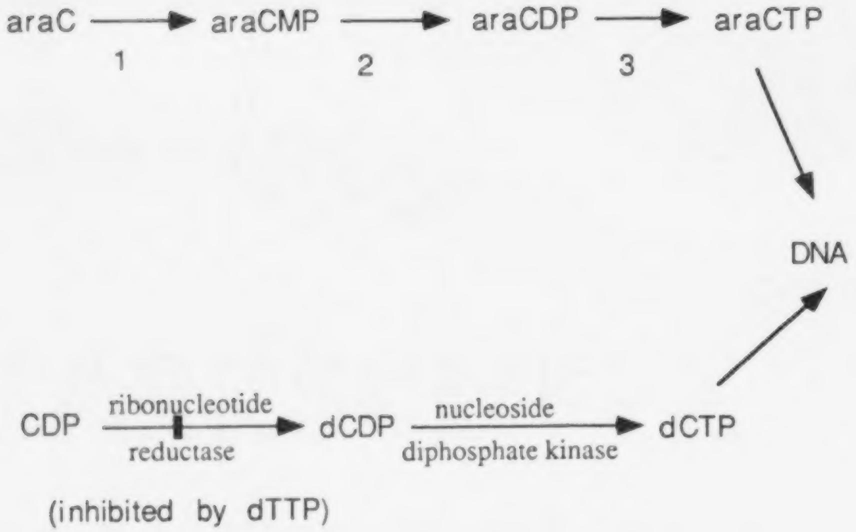
araC
1
araCMP
2
araCDP
3
araCTP
DNA
CDP
ribonucleotide
reductase
dCDP
nucleoside
diphosphate kinase
dCTP
(inhibited by dTTP)

Figure 1.8 Alignment of cNT1$_{rat}$, NUPC and SPNT amino acid sequences

```
      1                                                  50
cNT1  MADNTQRQRE SISLTPMAHG LENMGAEFLE ..SMEEGRLP HSHSSLPEGE
SPNT  MAKSEGRK.. SASQDTSENG MENPGLELME VGNLEQGK.. ....TLEEVT
NUPC  .......... .......... .......... .......... ..........

      51                                                100
cNT1  GGLNKAERKA FS..RWRSLQ PTVQARSFCR EHRQLFGWIC KGLLSTACLG
SPNT  QGHSLKDGLG HSSLWRRILQ PFTKARSFYQ RHAGLFKKIL LGLLCLAYAA
NUPC  .......... .......... .......... .......... ..........

      101                                               150
cNT1  FLMVACLLDL QRALALLIIT CVVLVFLAYD LLKRLLGSKL RRCVKFQGHS
SPNT  YLLAACILNF RRALALFVIT CLVIFILACH FLKKFFAKKS IRCLKPLKNT
NUPC  .......... .......... .......... .......... ..........

      151                                               200
cNT1  CLSLWLKRGL ALAAGVGLIL WLSLDTAQRP EQLVSFAGIC VFLVLLFAGS
SPNT  RLRLWLKRVF MGAAVVGLIL WLALDTAQRP EQLISFAGIC MFILILFACS
NUPC  .......... .....MDRVL HF........ ..VLALAVVA ILALLV...S

      201                                               250
cNT1  KHHRAVSWRA VSWGLGLQFV LGLFVIRTEP GFIAFQWLGD QIQVFLSYTE
SPNT  KHHSAVSWRT VFWGLGLQFV FGILVIRTEP GFNAFQWLGD QIQIFLAYTV
NUPC  SDRKKIRIRY VIQLLVIEVL LAWFFLNSDV GLGFVKGFSE MFEKLLGFAN

      251                                               300
cNT1  AGSSFVFG.. EALVKDVFAF QVLPIIIFFS CVMSVLYYLG LMQWVILKIA
SPNT  EGSSFVFG.. DTLVQSVFAF QSLPIIIFFG CVMSILYYLG LVQWVIQKIA
NUPC  EGTNFVFGSN DQGLAEFFFL KVLCPIVFIS ALIGILQHIR VLPVIIRAIG

      301                                               350
cNT1  WLMQVTMGTS ATETLSVAGN IFVSQTEAPL LIRPYLADMT LSEVHVVMTG
SPNT  WFLQITMGTT AAETLAVAGN IFVGMTEAPL LIRPYLADMT LSEIHAVMTG
NUPC  FLLSKVNGMG KLESFNAVSS LILGQSENFI AYKDILGKIS RNRMYTMAAT

      351                                               400
cNT1  GYATIAGSLL GAYISFGIDA ASLIAASVMA APCALALSKL VYPEVEESKF
SPNT  GFATIAGTVL GAFISFGIDA SSLISASVMA APCALALSKL VYPEVEESKF
NUPC  AMSTVSMSIV GAYMTM.LEP KYVVAALVLN MFSTFIVLSL INPYRVDA..

      401                                               450
cNT1  RSENGVKLTY .GDAQNLLEA ASAGAAISVK VVANIAANLI AFLAVLAFVN
SPNT  KSKEGVKLPR .GEERNILEA ASNGATDAIA LVANVAANLI AFLAVLAFIN
NUPC  .SEENIQMSN LHEGQSFFEM LGEYILAGFK VAIIVAAMLI GFIALIAALN

      451                                               500
cNT1  AALSWLGDMV DIQGLSFQLI CSYVLRPVAF LMGVAWEDCP VVAELLGIKF
SPNT  STLSWLGEMV DIHGLTFQVI CSYVLRPMVF MMGVQWADCP LVAEIVGVKF
NUPC  ALFATVTGWF GY.SISFQGI LGYIFYPIAW VMGVPSSEAL QVGSIMATKL

      501                                               550

cNT1  FLNEFVAYQE LSQYKQRRLA GAEEWLGDKK QWISVRAEIL TTYALCGFAN
SPNT  FINEFVAYQQ LSQYKNKRLS GVEEWINGEK QWISVKAEII ATFSLCGFAN
NUPC  VSNEFVAMMD L.....QKIA ST........ ..LSPRAEGI ISVFLVSFAN

      551                                               600
cNT1  FSSIGIMLGG LTSLVPQRRS DFSQIVLRAL ITGAFVSLLN ACVAGILYVP
SPNT  LTSIGITLGG LTSMVPQRKS DLCKLVVRAL FTGACVSFIS ACMAGILYVP
NUPC  FSSIGIIAGA VKGLNEEQGN VVSRFGLKLV YGSTLVSVLS ASIAALVL..

      601                                               650
cNT1  RGVEVDCVSL LNQTVSSSSF EVYLCCRQVF QST....... ........SS
SPNT  RGAETDCVSF LNTNFTNRTY ETYVCCRELF QSTLLNGTNM PSFSGPWQDK
NUPC  .......... .......... .......... .......... ..........

      651                  670
cNT1  EFSQVALDNC CRFYNHTVCT
SPNT  ESSLRNLAKC CDLYTSTVCA
NUPC  .......... ..........
```

CHAPTER II

MATERIALS AND METHODS

2.1 Materials

Dulbecco's modified Eagle medium (DMEM), Ham's F-12 medium and calf serum were from Gibco/BRL; Nu-serum culture I supplement was from Collaborative Biomedical.; restriction enzymes and DNA modification enzymes were from either Gibco/BRL or New England Biolabs; pcDNA1-AMP vector was from Invitrogen Corp.; nitrobenzylthioinosine (NBMPR), dipyridamole, dimethyl sulfoxide (DMSO), 3'-azido-3'deoxythymidine (AZT), 2', 3'-dideoxycytidine (ddC), 2'-deoxy-5-fluorouridine (FUdR) and 2'-deoxy-5-iodouridine (IUdR) were from Sigma Chemical Company; DEAE-dextran and deoxyribonucleoside triphosphates (dNTPs) solutions were from Pharmacia; 5-bromo-4-chloro-3-indoyl-β-D-galacopyranoside (X-gal) was from Boehringer Mannheim Biochemical; D-[5,6-^{3}H]uridine, D-[methyl-^{3}H]thymidine, D-[3, 8-^{3}H]adenosine, N, N'-bis-(2-hydroxyethyl)-2-aminoethanesulfonic acid (BES) and EcoLite scintillant were from ICN Biomedicals Inc.; [5-^{3}H(N)]cytidine was from Moravek Biochemicals Inc.; pCMVβGal and pSV2neo were from Clontech; anti-c-*myc* monoclonal antibody was from Berkeley Antibody Company; goat anti-mouse IgG horseradish peroxidase conjugate was from BIO-RAD; Dilazep was a gift from F.Hoffman-La Roche and Co. (Basel, Switzerland); 3'-thiacytidine (3TC) was a gift from Dr. Lorne Tyrrell (University of Alberta); 2', 2'-difluorodeoxycytidine (gemcitabine) was a gift from Eli Lilly Inc; and other materials were obtained from standard commercial sources.

2.2 Mammalian Cell Lines

(i) COS-1 cells

Monkey kidney COS-1 cells from the American Type Culture Collection (ATCC) were grown as adherent cultures in DMEM containing 5% calf serum and 5% NuSerum.

Stock cultures were maintained in the latter medium without antibiotics at 37°C in 95% air and 5% CO_2 with 95% humidity. Cell concentrations were determined using a Coulter Counter Model ZF electronic particle counter (Counter Electronics Inc.). Cultures were trypsinized with trypsin-EDTA (0.05% trypsin, 0.02% EDTA in 0.15 M NaCl) and subcultured to 0.2×10^5cells/T-25 flask every 3-4 days. Cells proliferated with a mean doubling time of approximately 17.5 hr. Cultures were reinitiated at about 3-month intervals from frozen cells. The frozen stocks were shown to be free of mycoplasma by a rapid detection kit from Gen-Probe Inc., according to the manufacturer's instructions.

(ii) CHO-K1 cells

Chinese hamster ovary CHO-K1 cells from ATCC were grown as adherent cultures in Ham's F-12 medium containing 10% calf serum without antibiotics. Stock cultures were maintained in the latter medium without antibiotics at 37°C in 95% air and 5% CO_2 with 95% humidity. Cultures were trypsinized with trypsin-EDTA and subcultured to 0.2×10^5 cells/T-25 flask every 3-4 days. Cell numbers were determined as described for COS-1 cells. Cells proliferated with a mean doubling time of approximately 12 hr. Cultures were reinitiated at about 3-month intervals from frozen cells. The frozen stocks were shown to be free of mycoplasma by a rapid detection kit from Gen-Probe Inc., according to the manufacturer's instructions.

2.3 *E coli*

The DH5α strain of *E. coli* was used to carry out plasmid propagation. *E. coli* were grown in Luria Broth (LB; 10 g/l Bacto-Tryptone, 5 g/l Yeast Extract, 5 g/l NaCl) or on LB plates (LB contained 2% Bacto-agar (w/v)) at 37°C. Ampicillin (0.1 mg/ml) was added to LB or LB plates for selection and maintenance of ampicillin-resistant plasmids.

2.4 Transient Transfection of COS-1 Cells

Plasmid DNA (pCDNAI/AMP with or without various cNT1_{rat}-derived inserts) was transiently transfected in COS-1 cells using the procedure described by Ausubel *et al.* (111). Actively proliferating cells (1×10^6 cells per dish) were plated and grown (usually 24 hr) to an estimated 70% confluence in 100-mm dishes (the number of dishes varied between experiments). The cultures were washed once with sterile phosphate-buffered saline (PBS: 137 mM NaCl, 2.7 mM KCl, 8.1 mM Na_2HPO_4, 1.5 mM KH_2PO_4 pH 7.4). Thereafter, 5 ml of fresh prewarmed DMEM medium that contained 10% NuSerum and 100 µM chloroquine was added to each dish. Transfected DNA (5 µg) was diluted to 0.1 ml in PBS and mixed with 0.1 ml DEAE-dextran (10 mg/ml). This 0.2-ml portion of DNA/dextran mixture was then added dropwise to each dish which contained 5 ml medium. The cultures were incubated at 37°C for 4 hr, after which the cells were treated with 2 ml PBS containing 10% (v/v) dimethylsulfoxide (DMSO) for 2 min at room temperature (RT), washed three times with PBS, and, after addition of growth medium (DMEM containing 5% calf serum and 5% NuSerum), allowed to recover for 24 hr at 37°C in 95% air and 5% CO_2 with 95% humidity. The cultures were then trypsinized, pooled together and subjected to centrifugation (100 x g, 5 min, RT). The cell pellet was suspended in growth medium, plated into 60-mm dishes at 5×10^5 cells/dish and incubated at 37°C in 95% air and 5% CO_2 with 95% humidity. Transport studies utilizing transfected cells were conducted 72 hr after transfection.

The efficiency of transfection was estimated using a β-galactosidase staining procedure (139). pCMVßGal DNA (5 µg) was transiently transfected in COS-1 cells.

The procedure was exactly as described above for cultures transfected with pCDNAI/Amp-cNT1$_{rat}$. pCMVβGal transfected COS-1 cells were incubated with fixative solution (0.5% glutaraldehyde in PBS) for 15 min at RT and then washed three times with PBS. The cells were then incubated overnight in a staining mixture (1 mg/ml 5-bromo-4-chloro-3-indoyl-β-D-galacopyranoside (X-Gal), 20 mM potassium ferricyanide, 20 mM potassium ferrocyanide, and 2 mM $MgCl_2$ in PBS). Cells expressing β-galactosidase stained an aqua-blue color and the transfection efficiency was estimated by counting stained and unstained cells in several microscopic fields. The transfection efficiency varied between experiments (20-30%).

2.5 Stable Transfection of CHO-K1 Cells

Stable transfection of wild-type CHO-K1 cells was carried out using a modified calcium phosphate protocol (127). Cells were cotransfected with plasmids that contained either the cNT1$_{rat}$ sequence (pCDNAI/Amp-cNT1$_{rat}$) or the neomycin (geneticin) resistant gene (pSV2neo) (112). Actively proliferating cells were plated and grown to an estimated 15-20% confluence in a T75 flask. pCDNAI/Amp-cNT1 (10 μg) and pSV2neo (0.3 μg) in 100 μl dH_2O were mixed with 500 μl N, N'-bis-(2-hydroxyethyl)-2-aminoethanesulfonic acid (BES)-buffered saline (50 mM BES at pH 6.95, 280 mM NaCl, 1.5 mM Na_2HPO_4). A 400-μl portion of 25 mM $CaCl_2$ was added dropwise to the DNA/BES mixture while vortexing. The resulting solution was incubated at RT for 20-30 min, vortexed vigorously for 30 sec and added dropwise into the growth medium already present in the T75 flask of cells. The culture was then incubated at 37°C for 4 hr, the DNA-containing medium was removed and a 3-ml portion of 15% (v/v) glycerol in PBS was added. After 2 min at RT, the glycerol-containing PBS was removed, and the cells were washed twice with PBS. Fresh growth medium was added, and the culture was incubated at 37°C. After 48 hr, the culture was trypsinized and the cells were plated in two 100-mm dishes, each of which contained 10 ml growth medium with 400 μg/ml geneticin. The medium was changed at 3- or 4-day intervals. Geneticin-resistant colonies were evident after 14-21 days.

Colonies were isolated when they were about 1 mm in diameter. A cloning cylinder was gently placed around the colony to be picked and drops of trypsin/EDTA solution (prewarmed to 37°C) were added to the cloning cylinder. After 1 min, the trypsinized cells were removed from the dish with a Pasteur pipet and plated in a 35-mm dish in growth media that contained 400 μg/ml geneticin. Geneticin-resistant colonies were isolated and expanded for analysis of cNT1_{rat} expression and for preparation of frozen stocks. cNT1_{rat} expression was tested by analysis of uridine transport activity as described below.

Frozen stock cultures were prepared as follows. Actively proliferating cultures were subjected to centrifugation (100 x g, 5 min, RT). The pellet was resuspended in freezing medium (80% growth medium, 10% fetal bovine serum, 10% DMSO) at a concentration of about 1×10^7 cells/ml. The resulting cell suspensions were frozen at -70°C overnight, and transferred to liquid nitrogen the next day.

2.6 Transformation of Plasmid DNA into Bacteria

Plasmid DNA was mixed with 100 μl of competent *E. coli* DH5α cell suspension and the mixture was incubated on ice for 30 min and then heat shocked by exposure to 42°C for 45 sec. The mixture was placed again on ice for 20 sec and the bacteria were then plated onto LB plates with ampicillin (0.1 mg/ml). LB plates were incubated at 37°C overnight. Plates were stored at 4°C.

2.7 Isolation of DNA from Bacteria

Plasmid DNA was isolated using a modification of the alkaline lysis mini-prep procedure (140). A single bacterial colony from LB plates (see the above section) was inoculated into 3 ml LB with 0.1 mg/ml ampicillin. The culture was grown to saturation (12-16 hr) and harvested by centrifugation (9000 x g, 20 sec). The pellet was resuspended in 0.1 ml solution I (50 mM glucose, 10 mM EDTA, 25 mM Tris-HCl pH 8.0), mixed gently with 0.2 ml solution II (0.2 M NaOH, 1% SDS) and incubated at RT for 5 min, after which 0.15 ml solution III (1:1.72 (v/v) of 5 M CH_3COOK/5 M CH_3COOH) was added. The mixture was incubated on ice for 15 min and centrifuged (9000 x g, 5 min, 4°C). The supernatant was mixed with 3 volumes of ice-cold 95% ethanol, incubated on ice for 5 min and centrifuged again (9000 x g, 5 min, 4°C). The supernatant was removed. The pellet was dissolved in Tris-EDTA buffer (TE; 10 mM Tris-Cl, 1 mM EDTA, pH 8.0) and stored at -20°C. Plasmid DNA prepared in this manner was used for all DNA manipulations except for sequencing and transfection.

For DNA sequencing and transfection, a Qiagen-tip 100 Plasmid Preparation kit (Qiagen Corp.) was used to purify plasmid DNA. Bacteria in 100 ml LB medium were harvested by centrifugation (6000 x g, 15 min, 4°C) and used to prepare plasmid DNA according to the manufacturer's instructions.

2.8 Enzymatic Manipulation of DNA

Restriction enzyme digestion of DNA was accomplished by incubating enzyme(s) with the DNA in appropriate reaction conditions as recommended by the manufacturers. The reactions were stopped by adding 0.5 M EDTA (pH 8.0) to a final concentration of 10 mM, or by adding a 0.17 volume of 6X DNA loading buffer (0.25% bromophenol blue (w/v), 40% sucrose (w/v)). DNA fragments were separated by gel electrophoresis

(0.8% agarose (w/v), 0.05 μg/ml ethidium bromide, 2 mM EDTA, 40 mM tris-acetate pH 8.5) in Tris-acetate-EDTA buffer (TAE; 2 mM EDTA, 40 mM Tris-acetate pH 8.5). DNA products were visualized with a UV light box.

Purification of DNA fragments from the agarose gel was performed using the Geneclean II Kit (Bio 101 Inc.) according to the manufacturer's instructions.

E. coli DNA polymerase I (Klenow fragment) was used to convert 5' overhangs to blunt ends. After the restriction digestion of 4 μg DNA that generated the 5' overhangs, 1 U Klenow fragment and 1 μl 0.5 mM 4dNTP (dATP, dGTP, dCTP, dTTP; 0.5 mM each) were added to the 20-μl reaction mixture. The mixture was incubated at 37° C for 15 min and the reaction was stopped by adding 0.5 M EDTA (pH 8.0) to a final concentration of 10 mM.

DNA fragments were ligated by combining the vector DNA and the insert DNA (molar ratio 1:3), 2 μl of T4 DNA ligase (Gibco/BRL), 4 μl of ligase buffer (5X concentration, Gibco/BRL), and sterile dH_2O which gave a final mixture volume of 20 μl. The ligation mixture was incubated at 15°C overnight, then transformed into bacteria, as described above.

2.9 Polymerase Chain Reaction (PCR)

Amplification of DNA by the PCR method (141) was performed as follows. In a 0.5-ml tube at 4°C, the following ingredients were combined: 55 μl dH_2O, 10 μl 10 x PCR buffer (200 mM Tris-HCl, pH 8.4; 500 mM KCl), 3 μl 50 mM $MgCl_2$, 1 μl 5'-primer (50 pmol), 1 μl 3'-primer (50 pmol), 10 μl template (10 ng plasmid DNA, 1 μg genomic DNA), 10 μl dNTPs (dATP, dGTP, dCTP, dTTP; 2 mM each), 1 μl Taq DNA polymerase (5 U/μl). A 50-μl portion of mineral oil was layered over the mixtures before the thermal cycling.

The tube containing the reaction mixtures was placed into the thermal block of a thermal cycling instrument (Robocycler 40; Stratagene). The thermal cycling program was as follows: denaturing at 94°C (45 sec), annealing at 45°C (2 min), and extension at 72°C (2 min). The cycle was repeated 25-35 times. A 10-μl portion of PCR product was analyzed by agarose gel electrophoresis as describe above. Whenever stated, the remaining PCR product was purified with Geneclean II Kit, then subjected to restriction digestion. The DNA fragment was subcloned into pBluescript for sequencing. DNA template was submitted to the DNA Sequencing Laboratory, Department of Biochemistry, University of Alberta. This sequencing lab used an applied Biosystems Model 373A DNA Sequencer with a Taq Dye Deoxy Terminator Cycle Sequencing Kit (Applied Biosystems).

2.10 Protein Immunoblotting

Crude cell membranes were prepared using an established method (111) as follows : Cells grown in 100-mm dishes were washed once with PBS and harvested in 1 ml ice-cold preparation buffer (0.25 M sucrose, 1 mM phenylmethylsulfonyl fluoride (PMSF) and 10 mM N-2-hydroxyethylpiperazine-N'-2-ethanesulfonic acid (HEPES)) by scraping with a rubber scraper. The cell suspension was disrupted on ice with a Teflon homogenizer (35 strokes) and centrifuged (900 x g, 10 min, 4°C) to sediment the nuclei. The resulting supernatant was further centrifuged (30,000 x g, 15 min, 4°C), and the pellet was resuspended in ice-cold preparation buffer and stored at -70°C.

Membrane protein samples were combined with equal volumes of sample buffer (4% (w/v) sodium dodecylsulphate (SDS), 20% (v/v) glycerol, 2% (v/v) β-mercaptoethanol, 0.01% (w/v) bromophenol blue, 20 mM Tris-HCl pH 6.8) and boiled for 5 min. Proteins (25 μg) were separated by SDS polyacrylamide gel electrophoresis

(SDS/PAGE; 12% gel) and transferred to polyvinylidene difluoride (PVDF) membranes (Immobilon-P; Millipore) by semi-dry electrophoretic transfer using an ET-20 Transfer Module (Tyler Research Instruments). Transfers were performed at 400 mA for 60 min in transfer buffer (180 mM glycine, 20% (v/v) methanol, 0.02% (w/v) SDS, 25 mM Tris-HCl pH 8.3).

Membrane blots were immunostained by the following method. All the washes and incubations were performed at 4°C and on a shaking platform. Each wash took at least 15 min, unless otherwise indicated. Blots were first washed for 30 min in TTBS (0.2% (v/v) Tween-20, 0.5 M NaCl, 20 mM Tris-HCl, pH 7.5), then blocked by incubating overnight in TTBS containing 5% (w/v) skim milk powder. The blots were then washed twice with TTBS and incubated in TTBS that contained 1% skim milk powder and anti-c-*myc* monoclonal antibody (1:2000 dilution (v/v)) for at least 6 hr. Thereafter, blots were washed three times with TTBS and incubated for at least 3 hr in TTBS that contained 1% skim milk power (w/v) and secondary antibodies (goat anti-mouse horseradish peroxidase (HRP) conjugate; 1:3000 (v/v) dilution). Blots were then washed twice with TTBS and once with TBS (0.5 M NaCl, 20 mM Tris-HCl, pH 7.5). Thereafter, blots were detected with the enhanced chemiluminescence (ECL) kit (Amersham Life Sciences), according to the manufacturer's instructions, and exposed to Kodak XAR-5 film.

2.11 Determination of Protein Concentrations

Protein quantitation was performed by bicinchoninic acid (BCA) assay (142). Briefly, 100-µl portions of standard proteins (bovine serum albumin) or unknown samples were mixed with 200-µl portions of working solution in the wells of a microtiter plate. Working solution was a mixture (1:20, v/v) of reagent A (sodium carbonate, sodium bicarbonate, BCA detection reagent and sodium tartrate in 0.1 M NaOH) and reagent B (4% $CuSO_4 \cdot 5H_2O$). The microtiter plate was incubated at 37°C for 30 min. The absorbance of each well was measured at near 562 nm using a UVmax microtiter plate reader (Molecular Devices Corp.). The protein concentration of the unknown sample was determined from the standard curve constructed with bovine serum albumin.

2.12 Uptake Assays

2.12a Buffers and Solutions

(i) Nucleoside and NT Inhibitor Solutions

Stock solutions of nonradioactive nucleosides and NT inhibitors were prepared in dH_2O. The concentration of stock solutions was determined by measuring UV absorbance at a wavelength of maximum absorption, as listed below (solution concentration (mM) = UV absorbance / molar extinction coefficient). Radiolabeled nucleosides were purified with a Varian 5000 high-pressure liquid chromatography instrument using water-methanol gradients on a C18 reverse phase column (143) by Ms. Delores Mowles.

Compound	wavelength(nm)	extinction coefficient ($mM^{-1}cm^{-1}$)
Uridine	262	10.1
Thymidine	267	9.7
NBMPR	290	25.1
Dilazep	266	18.4
Adenosine	260	15.1
Cytidine	271	9.1
Guanosine	252	13.7

(ii) Transport Buffers

These buffers were adjusted to pH 7.4. N-Methyl-D-Glucamine (NMDG)-Cl was used in sodium-free medium as a substitute for NaCl and was prepared by combining equimolar quantities of NMDG and HCl (144). The osmolalities (300 ± 15 mOsm) of these buffers were checked using a osmometer (Multi-Osmette computerized micro-osmometer, Precision Systems Inc.).

Sodium-Containing Buffer		Sodium -Free Buffer	
20 mM	Tris·Cl	20 mM	Tris·Cl
3 mM	K_2HPO_4	3 mM	K_2HPO_4
1 mM	$MgCl_2 \cdot 6H_2O$	1 mM	$MgCl_2 \cdot 6H_2O$
2 mM	$CaCl_2$	2 mM	$CaCl_2$
5 mM	glucose	5 mM	glucose
130 mM	NaCl	130 mM	NMDG-Cl

2.12b Uptake Assay

Nucleoside uptake assays (three or two cultures/condition) were conducted at RT in transport buffer. Cells were washed once with transport buffer and were (i) processed immediately, or (ii) in some experiments, incubated with NBMPR or dilazep at RT for 30 min before the uptake assay. Each culture was measured individually. Uptake intervals were started by adding 1.5 ml of transport buffer containing ^{3}H-labeled nucleoside and in some experiments with inhibitors. Uptake intervals were ended by rapidly aspirating the solution (2 sec before the end point) and immersing the culture dishes (at the end point) in 1.5 liter of ice-cold transport buffer. The dishes were drained, and the cells were solubilized in 1 ml of 5% (v/v) Triton X-100 and combined with 5.0 ml of EcoLite scintillint for radioactivity measurement.

Uptake at time zero was determined by incubating cells for 10 min at 4°C with transport buffer that contained NBMPR or dilazep and, immediately thereafter, for ≤ 3 sec with ice-cold transport buffer that contained the appropriate concentration of ^{3}H-labeled nucleoside and in some experiments with inhibitor. For inhibition experiments, cells were exposed to nonradioactive nucleosides at the same time as ^{3}H-labeled nucleoside.

2.12c Calculation of Kinetic Parameters

The relationship between uptake velocity (V) and substrate concentration (S) can be described by the Michaelis-Menten equation (70) in which $V=(S \cdot V_{max})/(K_m+S)$, where V_{max} represents the maximal limiting uptake and K_m represents the substrate concentration at the half maximal uptake. In this study, the methods used to calculate kinetic parameters were:

(a) Woolf plot of s/v versus s

$S/V=(S/V_{max})+(K_m/V_{max})$, where the slope is equal to $1/V_{max}$ (145)

(b) Eadie-Hofstee plot of v versus v/s

$V=(-VK_m/S)+V_{max}$, where the slope is equal to $-K_m$ (146, 147)

(c) Lineweaver-Burke plot of 1/v versus 1/s

$1/V=(1/V_{max})+K_m/(SV_{max})$, where the slope is equal to K_m/V_{max} (148)

2.12d Calculation of Transport Rates

Transport rates were derived by analysis of time courses of initial uptake of radioactive nucleosides by linear regression.

2.13 NBMPR Binding Assay

NBMPR binding by COS-1 cells was determined under equilibrium conditions. Cells were preincubated in sodium buffer in the presence and absence of 10 µM nonradioactive NBMPR at RT for 15 min. A 1-ml portion of binding medium (sodium buffer that contained one of several graded concentrations of ^{3}H-NBMPR) was then added. Cultures were incubated at RT for 30 min and the binding assays were ended by aspiration of the binding medium. The cells were air dried and solubilized with 5% Triton X-100. Cell-associated radioactivities were determined by liquid scintillation counting. Free NBMPR concentrations were determined from the radioactive content of the binding medium at the end of the assay. Specific NBMPR binding was defined as the difference between cell-associated radioactivity in the presence and the absence of 10 µM nonradioactive NBMPR. NBMPR binding parameters were determined from Scatchard plots of bound/free versus bound NBMPR (77). Linear K_d and B_{max} values were obtained from the slope and abscissa intercepts.

CHAPTER III

CHARACTERIZATION OF NUCLEOSIDE TRANSPORT PROCESSES OF COS-1 CELLS[1]

---

[1] The transport and binding assays described in this chapter were conducted by Delores Mowles.

3.1 Overview

The aim of the work described in this chapter was to characterize the nucleoside transport processes of COS-1 cells. COS cells have been widely used for transient expression of foreign DNA by transfection techniques, and the studies described below were to ascertain the usefulness of this cell type for expression and study of transfected recombinant nucleoside transport proteins. In general, functional analysis of recombinant nucleoside transport proteins should be conducted in cells that either (i) lack endogenous activity or (ii) possess a nucleoside transport process that can be inhibited pharmacologically. When this study was initiated, little was known about NT activities in COS-1 cells.

In the work described this chapter, a rapid-assay technique that allowed measurements of the initial rate of uptake of radiolabeled permeant (149) was used to determine nucleoside transport activity in COS-1 cells. The effects of three NT inhibitors (NBMPR, dilazep and dipyridamole) were then examined to establish the nature of the nucleoside transport activity in COS-1 cells --that is, to determine if uptake occurred by equilibrative or concentrative NT-mediated processes. NBMPR is a diagnostic tool for identifying *es* NTs, whose activity can be inhibited by nanomolar concentration of NBMPR. The other major types of nucleoside transport processes are insensitive to NBMPR (22). Dilazep and dipyridamole are two other NT inhibitors, that inhibit both equilibrative NT subtypes (*es* and *ei*) at nanomolar concentrations. Finally, NBMPR-binding assays, which have been found to be associated with *es* nucleoside transport process (2, 71, 72), were conducted to quantitate the number of high affinity NBMPR-binding sites in COS-1 cells.

3.2 Nucleoside Transport Activity in COS-1 Cells

To investigate nucleoside transport activity in COS-1 cells, the uptake of several radioactive labeled tracer nucleosides was examined. Figure 3.1 shows time courses of uptake of 1 μM ^{3}H-uridine, ^{3}H-thymidine or ^{3}H-adenosine in sodium-containing buffer in the absence or presence of a large excess (1 mM) of the nonradioactive form of the same nucleoside. In each these experiments, substantially reduced uptake was observed in the presence of the high concentration of nonradioactive nucleoside (Table 3.1). These results indicated that the transport of uridine, thymidine and adenosine in COS-1 cells was transporter mediated, because the competition of radioactive and nonradioactive nucleosides for transporter sites resulted in reduced tracer flux.

Figure 3.2 shows the transport of 10 μM ^{3}H-uridine or ^{3}H-thymidine in a 10 sec-interval, with or without NBMPR. The initial rates of transport were reduced from 2.27 to 0.1 pmol/10^6/sec cells (uridine) and from 1.97 to 0.2 pmol/10^6/sec cells (thymidine) by 10 nM NBMPR. The consistent and virtually complete inhibition of uridine and thymidine uptake by nanomolar concentrations of NBMPR provided a further indication that nucleoside uptake in COS-1 cells was transporter-mediated. In addition, it established that the transport process of COS-1 cells belonged to the NBMPR-sensitive NT subtype.

Figure 3.3 shows the inhibition of uridine transport as a function of the concentration of NBMPR and of two other potent nucleoside transport inhibitors. Transport of 100 μM uridine was measured in the absence or in the presence of graded concentrations of each of the inhibitors. The resulting concentration-effect curves established the concentrations at which 50 percent inhibition was achieved (IC_{50}). The IC_{50} values for NBMPR, dilazep and dipyridamole were 1, 4 and 28 nM, respectively. Moreover, each of the dose response curves was monophasic, suggesting that there was probably only one type of nucleoside transport process in COS-1 cells.

Concentration-effect curves were also determined in experiments carried out with 100 µM thymidine (Figure 3.3). The IC_{50} values for NBMPR, dilazep and dipyridamole inhibition of thymidine transport were 0.7 nM, 6 nM and 27 nM, respectively. The thymidine concentration-effect curves were also monophasic. These results confirmed that COS-1 cells possess only one nucleoside transport process, which was highly sensitive to known inhibitors of equilibrative nucleoside transport process.

It has been found that inhibition of nucleoside transport by NBMPR is associated wtih high-affinity binding of the inhibitor to the cell membrane (2, 71, 72). Thus, a complementary approach to investigate the NBMPR-sensitive nucleoside transport process of COS-1 cells was to conduct NBMPR-binding assays. Figure 3.4 shows a plot of the ratio of cell-associated to free NBMPR as a function of the amount of cell-associated NBMPR in COS-1 cells. The plot was linear, suggesting that COS-1 cells had only one population of NBMPR binding sites. Scatchard analysis of NBMPR binding by COS-1 cells yielded a K_d value of 0.8 nM and a B_{max} value of 1.2 pmol/10^6 cells. When the B_{max} value was converted to the number of NBMPR-binding sites per cell, a value of 0.5 x 10^6 sites was obtained. This number was close to that previously observed in HeLa cells (77). These values, together with those of several other cultured cell types, are shown in Table 3.1. Thus, the inhibition of nucleoside transport by NBMPR in COS-1 cells evidently resulted from the occupancy by NBMPR of high affinity binding sites thought to be physically associated with the equilibrative transporter.

3.3 Nucleoside Transport Activity in COS-1 Cells Was Sodium-independent

Among the seven subtypes of NT-mediated processes, one subtype (*cs*/N5) has been found to be sensitive to NBMPR and be sodium-dependent (93). To determine if the nucleoside transport process of COS-1 cells, which was found to be sensitive to NBMPR, was also sodium dependent, transport of nucleosides (1 µM) into COS-1 cells was measured in sodium-containing buffer or in sodium-free buffer. In Figure 3.5, it is evident that uridine transport was not substantially different in cells assayed in sodium-containing buffer or in sodium-free buffer. Similar results were observed with thymidine and adenosine. It appeared that the nucleoside transport process of COS-1 cells was sodium-independent.

3.4 Kinetic Parameters

The kinetic parameters of uridine transport by COS-1 cells were estimated by determining the concentration dependence of initial rates of uptake of ^{3}H-uridine. Velocities of transport determined at various concentrations gave rise to the Lineweaver-Burke, Woolf and Eadie-Hofstee plots as shown in Figure 3.6. The Woolf and Eadie-Hofstee plots emphasize data obtained at relatively high and low concentrations, respectively. Lineweaver-Burke plot is the most commonly used plot for determination of apparent K_m and V_{max} values. The three plots were all linear and fit to a single-transporter kinetic model. The kinetic parameters obtained from these plots were similar. The K_m and V_{max} values (average of values of the three plots) were 176 µM and 43 pmol/10^6 cells/sec, respectively. This was consistent with the presence of a single type of nucleoside transport process of COS-1 cells, as suggested by the results of the NBMPR inhibition and NBMPR binding experiments.

3.5 Summary

This study showed that COS-1 cells had only one type of nucleoside transport process, which was equilibrative, NBMPR-sensitive and sodium-independent. The IC_{50} values for inhibition by the three NT inhibitors were at nanomolar levels. The number of high affinity NBMPR-binding sites was 0.7 x 10^6 sites per cell, which was close to that of some other cell lines exibiting *es* transport activities. Detailed kinetic studies, which were conducted with only one ^{3}H-labeled permeant (uridine), yielded K_m and V_{max} values, respectively, of 176 μM and 43 pmol/10^6 cells/sec.

Thus, endogenous NT activity in COS-1 cells could be inhibited by NBMPR, dilazep or dipyridamole, making it feasible to use COS-1 cells for functional studies of recombinant NT proteins that are insensitive to these inhibitors. For example, COS-1 cells would be an ideal host for expression of cDNAs encoding $cNT1_{rat}$, which is not inhibited by micromolar concentrations of either NBMPR or dilazep (9, 84).

Table 3.1 Effect of excess nonradioactive nucleoside on rate of uptake of tracer nucleoside

	Rate	(pmol/10^6 cells/min)	Remaining activity (%)
	tracer nucleoside only	with nonradioactive nucleoside	
uridine	14.4	0.12	0.8
thymidine	5.8	0.38	6.6
adenosine	14.8	0.4	2.7

The uptake rates are from the experiments of Figure 3.1. The uptake activity remaining in the presence of nonradioactive nucleoside was calculated as the percentage of the rate in the absence of nonradioactive nucleoside.

Table 3.2 NBMPR-binding sites in some cell types

Cell Type	NBMPR-binding sites per cell	Source
COS-1	0.5×10^6	Fig.3.4
HeLa	0.45×10^6	Ref. 77
S49	0.07×10^6	Ref. 2
CHO	0.06×10^6	Ref. 179, 180
BeWo	27.5×10^6	Ref. 77

The number of NBMPR-binding sites in COS-1 cells was derived from the data obtained from Figure 3.4.

Table 3.3 Uptake rates of uridine, thymidine and adenosine in sodium-containing and sodium-free buffer

	Rate sodium-containing buffer	(pmol/10^6 cells/sec) sodium-free buffer
uridine	0.17	0.16
thymidine	0.17	0.14
adenosine	0.36	0.33

Uptake rates are from the experiments of Figure 3.5.

Figure 3.1 Time courses of uptake of uridine, thymidine and adenosine in COS-1 cells

Actively proliferating COS-1 cells were grown on 60-mm dishes. Uptake of 1 μM ^{3}H-uridine, ^{3}H-thymidine or ^{3}H-adenosine by COS-1 cells was measured in sodium-containing buffer in the absence (□, ○, △) or in the presence (■, ●, ▲) of 1 mM nonradioactive uridine, thymidine or adenosine, respectively. Uptake assays were started by adding 1.5 ml of transport buffer containing ^{3}H-nucleoside, ended by aspirating the permeant solution and immediately washing the dishes by immersion in 1.5 liter of ice-cold transport buffer. Uptake at time zero was determined by placing dishes on ice for 10 min prior to transport assay and by using ice-cold transport buffer that contain ^{3}H-nucleoside. The cells were solubilized in 5% (v/v) Triton X-100 and combined with EcoLite scintillant for radioactivity measurement. Uptake rates calculated from the time courses are presented in Table 3.1.

At the time when assays were conducted, there were 2 x 10^6 cells per 60-mm dish. Each value represents the mean ± SD of three dishes. Error bars are not shown where SD values were smaller than the data symbols.

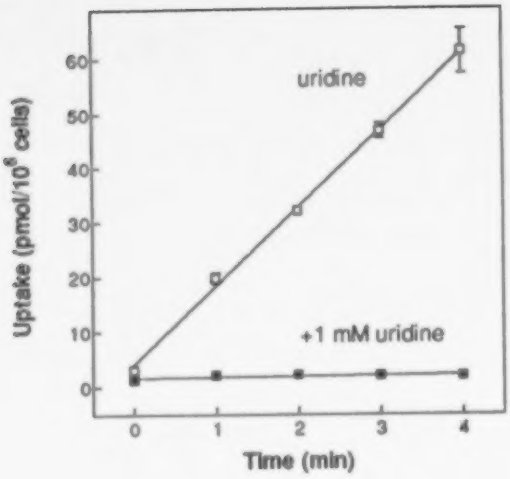
uridine
+1 mM uridine
Uptake (pmol/10^6 cells)
0
10
20
30
40
50
60
0
1
2
3
4
Time (min)

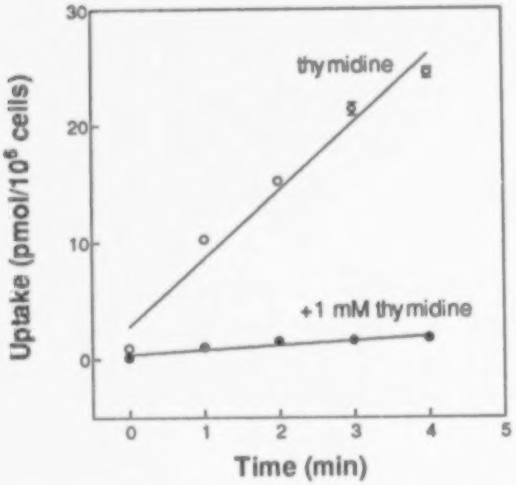
thymidine
+1 mM thymidine
Uptake (pmol/10^6 cells)
0
10
20
30
0
1
2
3
4
5
Time (min)

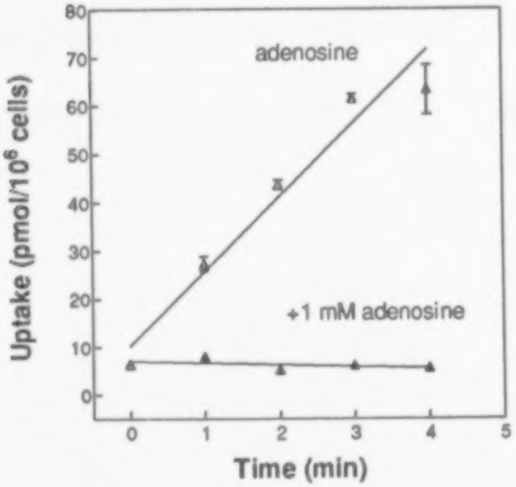
adenosine
+1 mM adenosine
Uptake (pmol/10^6 cells)
0
10
20
30
40
50
60
70
80
0
1
2
3
4
5
Time (min)

Figure 3.2 The effect of NBMPR on initial rates of uptake of uridine and thymidine by COS-1 cells

Uptake of 10 μM ^{3}H-uridine or ^{3}H-thymidine by COS-1 cells was measured in the absence (□, ○) or in the presence (■, ●) of 10 nM NBMPR as described in the legend of Figure 3.1, except that the cultures (■, ●) were preincubated for 30 min in the presence of 10 nM NBMPR before the uptake started. At the time when assays were conducted, there were 1.6 x 10^6 cells per 60-mm dish. Each value represents the mean ± SD of three dishes. Error bars are not shown where SD values were smaller than the data symbols.

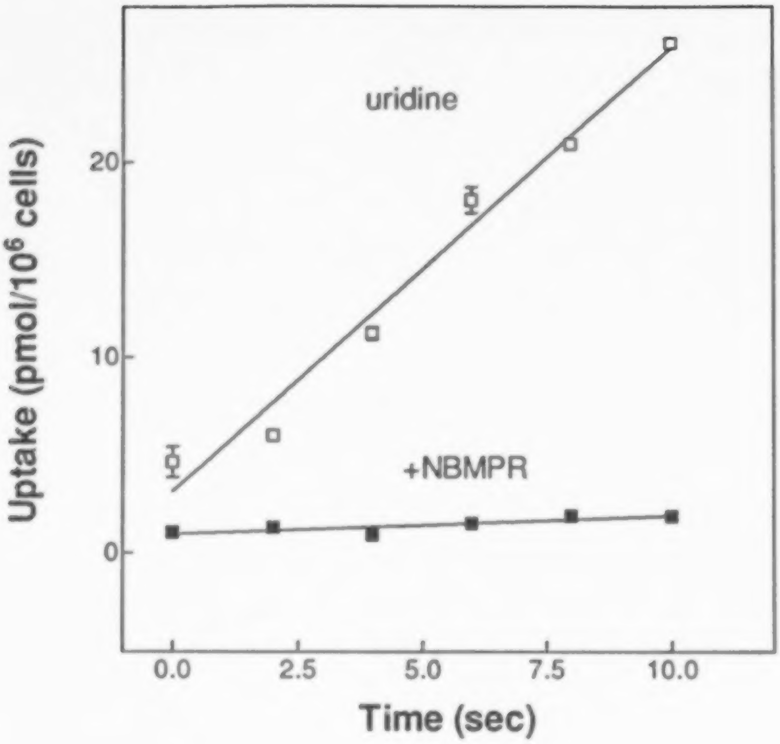
uridine
+NBMPR
Uptake (pmol/10^6 cells)
20
10
0
0.0
2.5
5.0
7.5
10.0
Time (sec)

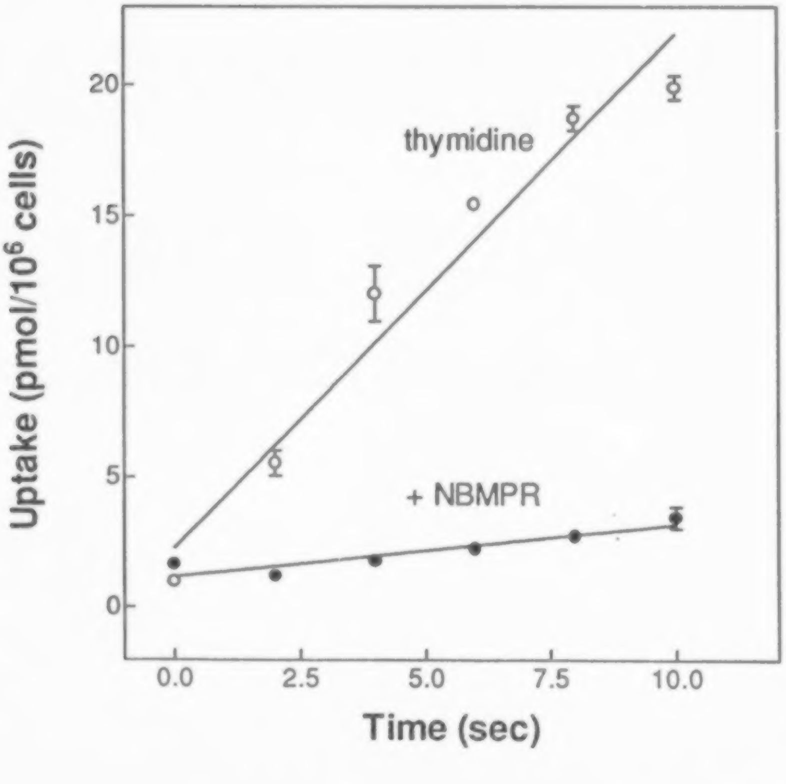
thymidine
+ NBMPR
Uptake (pmol/10^6 cells)
20
15
10
5
0
0.0
2.5
5.0
7.5
10.0
Time (sec)

Figure 3.3 Effects of NBMPR, dilazep and dipyridamole on uridine and thymidine uptake in COS-1 cells

Initial rates of uptake of 100 μM ^{3}H-uridine or ^{3}H-thymidine by COS-1 cells was measured in the absence of NT inhibitors or in the presence of graded concentrations of NBMPR (■), dilazep (▲) or dipyridamole (●) as described in the legend of Figure 3.2. The initial rates were determined from 10 sec time course. The rates measured in the absence of NT inhibitors served as a control (100%) and rates measured in the presence of various concentrations of inhibitors were calculated as percentages of the control values. Each value represents the mean ± SD of three dishes. Error bars are not shown in the figure because SD values were smaller than the data symbols. Each concentration-effect relationship was determined with a separate preparation of cells; at the times when assays were conducted there were about 1.5 x 10^6 to 2 x10^6 cells per 60-mm dish.

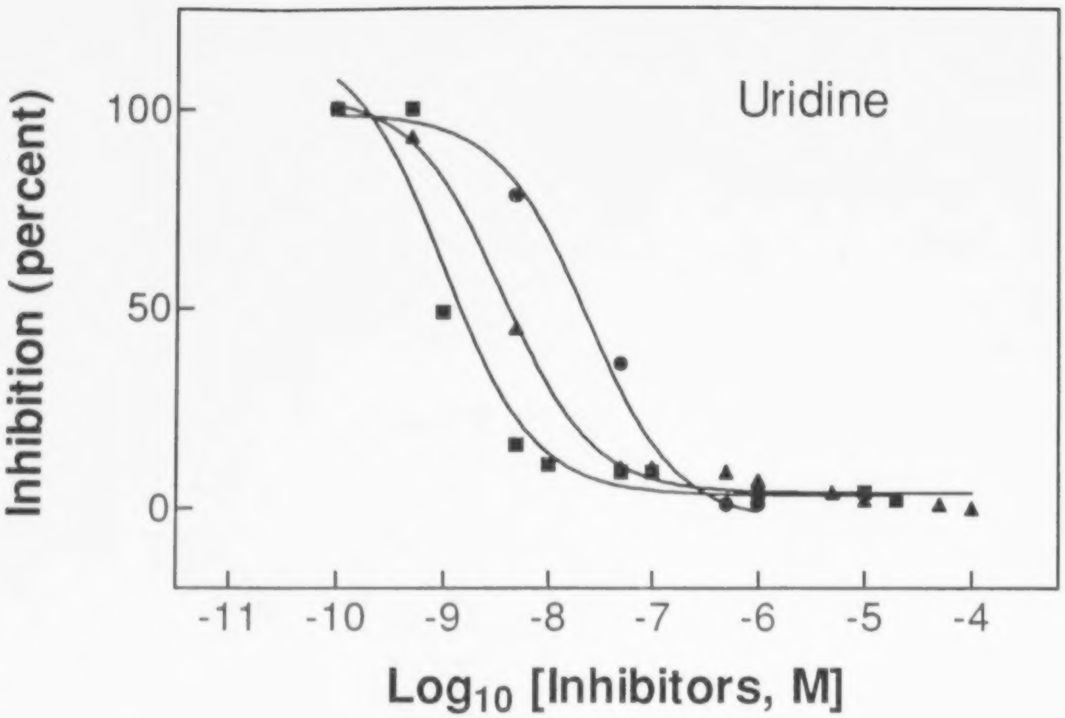
Uridine
Inhibition (percent)
100
50
0
-11
-10
-9
-8
-7
-6
-5
-4
Log10 [Inhibitors, M]

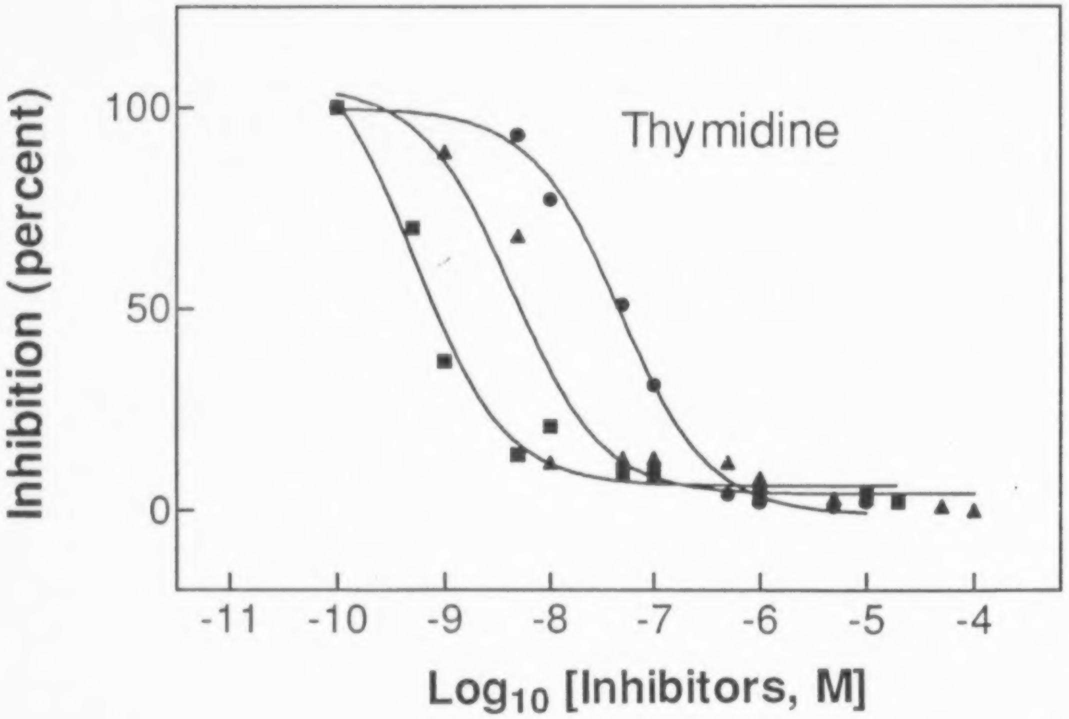
Thymidine
Inhibition (percent)
100
50
0
-11
-10
-9
-8
-7
-6
-5
-4
Log10 [Inhibitors, M]

Figure 3.4 Scatchard analysis of NBMPR binding by COS-1 cells

NBMPR binding by COS-1 cells was determined under equilibrium conditions. Cells were preincubated in sodium buffer in the presence or absence of 10 μM nonradioactive NBMPR at RT for 15 min. A portion of binding medium (sodium buffer that contained one of several graded concentrations of ^{3}H-NBMPR) was then added. Cultures were incubated at RT for 30 min and the binding assays were ended by aspiration of the binding medium. The cells were air dried and solubilized with 5% Triton X-100. Cell-associated radioactivities were determined by liquid scintillation counting. Free NBMPR concentrations were determined from the radioactive content of the binding medium at the end of the assay. Specific NBMPR binding was defined as the difference between cell-associated radioactivity in the presence and the absence of 10 μM nonradioactive NBMPR. Each value represents the mean ± SD of three dishes. Error bars are not shown where SD values were smaller than the data symbols. K_d and B_{max} values were 0.8 nM and 1.2 pmol/10^6 cells, respectively.

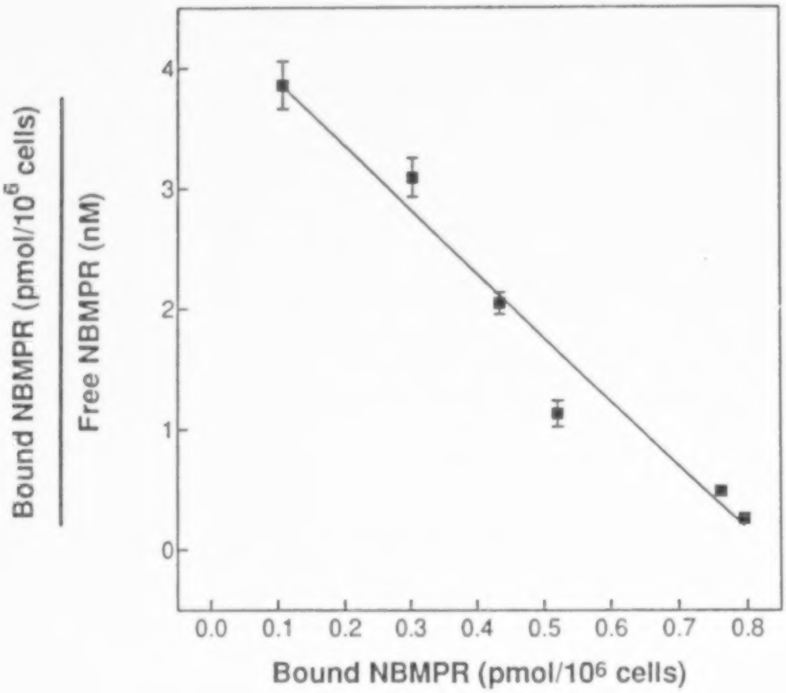
Bound NBMPR (pmol/10^6 cells) / Free NBMPR (nM)
4
3
2
1
0
0.0
0.1
0.2
0.3
0.4
0.5
0.6
0.7
0.8
Bound NBMPR (pmol/10^6 cells)

Figure 3.5 Transport of nucleoside by COS-1 cells in sodium-containing or sodium-free buffer

Uptake of 1 μM ^{3}H-uridine, ^{3}H-thymidine or ^{3}H-adenosine by COS-1 cells was measured in sodium-free buffer (□, ○, △) or in sodium-containing buffer (■, ●, ▲) as described in the legend of Figure 3.1. At the time when assays were conducted, there was 1.8 x 10^6 cells per 60-mm dish. Uptake rates (pmol/10^6 cells/sec) calculated from the time courses are presented in Table 3.3

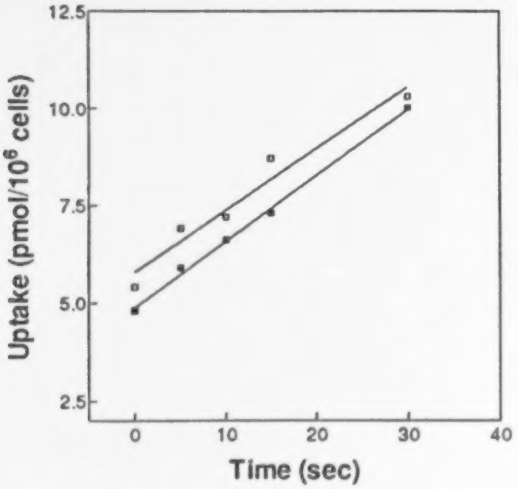
Uptake (pmol/10^6 cells)
12.5
10.0
7.5
5.0
2.5
0
10
20
30
40
Time (sec)

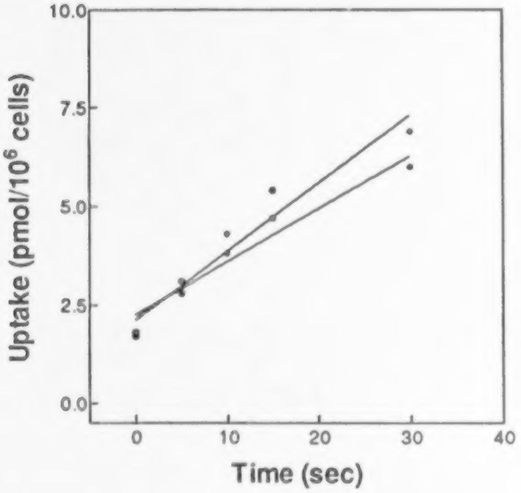
Uptake (pmol/10^6 cells)
10.0
7.5
5.0
2.5
0.0
0
10
20
30
40
Time (sec)

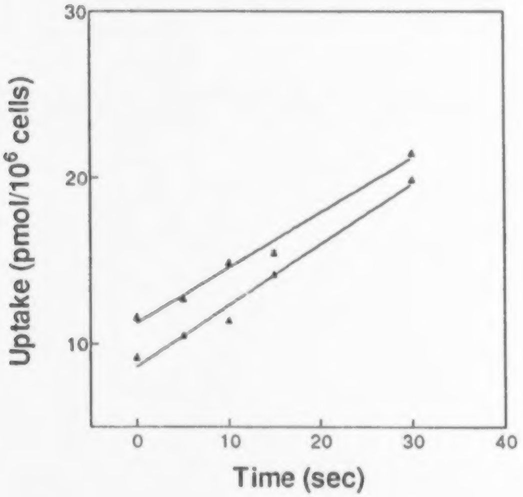
Uptake (pmol/10^6 cells)
30
20
10
0
10
20
30
40
Time (sec)

Figure 3.6 Uridine uptake kinetics in COS-1 cells

Initial rates of uptake of ^{3}H-uridine by COS-1 cells were determined in sodium-containing buffer as described in the legend of Figure 3.1. Velocities of transport were (i) estimated from 10 sec-time courses of different concentrations that ranged from 1-500 µM, and (ii) used to produce the plots shown in the three panels. The kinetic constants derived from these plots were:

Top Panel (Lineweaver-Burke plot): K_m, 184 µM; V_{max}, 44 pmol/sec/10^6 cells.

Middle Panel (Eadie-Hofstee plot): K_m, 164 µM; V_{max}, 41 pmol/sec/10^6 cells

Bottom Panel (Woolf plot): K_m, 179 µM; V_{max}, 43 pmol/sec/10^6 cells.

At the time when the assay was conducted, there was 0.5 x 10^6 cells per 60-mm dish.

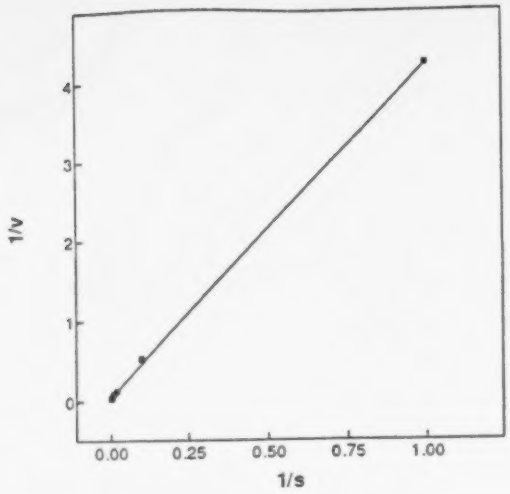
1/v
0
1
2
3
4
0.00
0.25
0.50
0.75
1.00
1/s

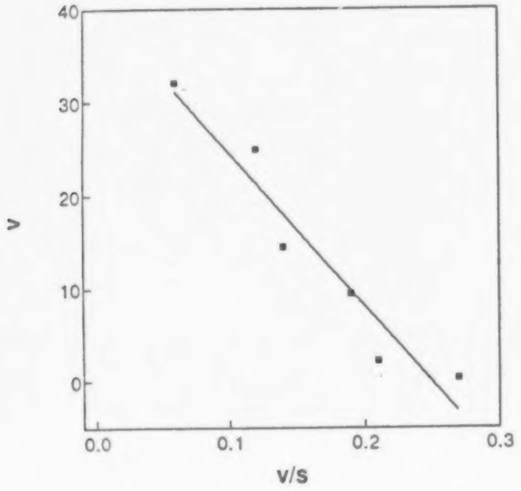
v
40
30
20
10
0
0.0
0.1
0.2
0.3
v/s

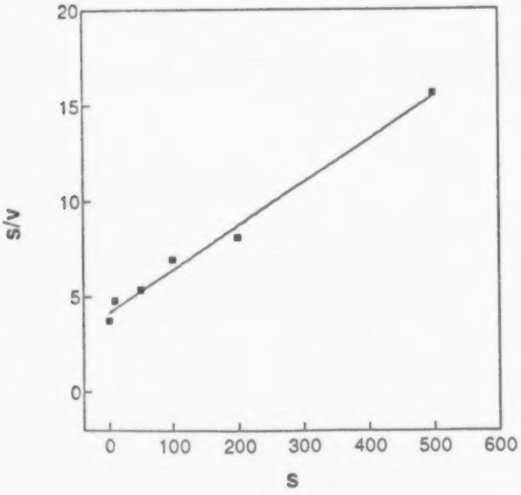
s/v
20
15
10
5
0
0
100
200
300
400
500
600
s

CHAPTER IV

TRANSIENT EXPRESSION OF cNT1$_{rat}$ IN COS-1 CELLS

4.1 Overview

Most cells naturally express multiple nucleoside transport processes. This has sometimes complicated characterization of individual nucleoside transport processes with respect to sensitivity to inhibitors, substrate selectivity and dependence on sodium cotransport. The availability of cloned NT cDNAs and transfection techniques in mammalian cells provides an approach to precisely study the various transporter subtypes.

To express a foreign gene of interest in mammalian cells, two approaches are usually used: transient transfection and stable transfection. Transient transfection often yields high levels of expression of the transfected gene and allows rapid characterization of the functional properties of the resulting recombinant protein. Stable transfection yields a permanent cell line and provides a continuing source of cells for expression studies. Transient transfection is usually the method of choice for initial expression studies before a time-consuming attempt to produce stable tranfectant is started. This chapter describes results of studies in which transient transfection was used to express the $cNT1_{rat}$ cDNA.

The cell line to be used as the recipient for transfection of $cNT1_{rat}$ cDNA should be NT deficient either genetically or by use of NT inhibitors. Three nucleoside-transport defective cell lines have been reported. They are murine lymphoma AE1 cells (150), mouse leukemia L1210 cells (22) and pig kidney PK-15 cells (151). Among them, only AE1 cells were available and they were previously shown to be untransfectable (152). Attempts to isolate nucleoside-transport defective variants of COS-1 cell in our laboratory, using selection protocols previously used to obtain NT-defective L1210 cells (5, 153), were unsuccessful [1]. However, COS-1 cells have only the *es* transporter, which can be inhibited by nanomolar concentrations of NT inhibitors (see Chapter 3). Previous studies (9) have shown that $cNT1_{ratr}$ encodes a transporter with N2/*cit* activity, which is not sensitive to NBMPR. Thus, the endogenous NT activity of COS-1 cells could be almost completely eliminated with nucleoside transport inhibitors, making it feasible to use this readily transfectable cell line for expression of a single inhibitor-insensitive nucleoside transporter.

---

[1] unpublished results from Riegel, T, Mowles, D and Cass, C.E.

N2/*cit* NT activity has been observed in freshly isolated enterocytes, in renal brush border vesicles from non-human species and in *Xenopus* oocytes injected with rat and rabbit intestinal mRNA (84, 89-93). However, the characterization of this NT subtype was limited because the various preparations exhibit more than one nucleoside transport process. This chapter describes the functional characterization of recombinant $cNT1_{rat}$ in experiments conducted in COS-1 cells, which only exhibited $cNT1_{rat}$ activity in the presence of NT inhibitors. The characterization utilized direct measurement of uptake of radioactive nucleosides by transiently transfected COS-1 cells to demonstrate the sodium dependence of NT activity, the kinetic parameters of various substrates, and the potential transportabilities of some physiologic nucleosides and nucleoside drugs.

4.2 Construction of pCDNAI/Amp-$cNT1_{rat}$

For expression in mammalian cells, $cNT1_{rat}$ was subcloned into the mammalian expression vector, pCDNAI/Amp (Figure 4.1(a)). This vector has an ampicillin-resistance gene, which permits selection of bacteria that have the recombinant plasmids, and unique restriction sites for subcloning of DNA inserts. It also has the following elements for eukaryotic expression: (i) enhancer-promoter sequences from the human cytomegalovirus (CMV) for high-level expression, (ii) transcription termination and RNA processing signals from SV40 to enhance mRNA stability, and (iii) SV40 and polyoma origins of replication for episomal replication in cells expressing the SV40 large T antigen or that are latently infected with polyoma virus. This vector has been used to successfully express different proteins in various cell lines, including COS-1 cells (154, 155, 157).

cNT1$_{rat}$ was originally isolated from a rat intestinal cDNA library that had been constructed in the pGEM3Z vector (84). The cloning sites for the library were EcoR I (5'-end) and Xba I (3'-end). However, because the cNT1$_{rat}$ coding region also contained an EcoR I site, the subcloning of cNT1$_{rat}$ into the mammalian expression vector pCDNAI/Amp used a different pair of restriction enzymes, Afl III and Xba I (Figure 4.1(b)). The Afl III site was 46 bp upstream of the start codon in the cNT$_{rat}$ insert. Since there was no compatible site in pCDNAI/Amp for Afl III, the 5'-overhang produced in the insert by Afl III was blunt-ended with the Klenow fragment and ligated into pCDNAI/Amp at the EcoR V site. The 3'-end of cNT1$_{rat}$ was ligated into the vector at the Xba I site.

The expression construct, named pCDNAI/Amp-cNT1$_{rat}$, is shown in Figure 4.1(c). It included a 5' untranslated region (reduced from 156 bp in length to 46 bp), the complete cNT1$_{rat}$ coding region and the 3' untranslated region. For efficient eukaryotic translation, it is usually recommended that the 5' untranslated region be kept to 50-100 bp in length to minimize the formation of secondary structure that might interfere with ribosome binding (156). Therefore, the 5' untranslated region of cNT1$_{rat}$ in the expression construct met this recommendation.

The structure of pCDNAI/Amp-cNT1$_{rat}$ was confirmed by restriction mapping with either Xba I + BamH I, Hind III + Xba I and EcoR I (Figure 4.1(d)). Three fragments (5.0 + 1.8 + 0.5 Kb or 5.0 + 2.0 + 0.3 Kb) were expected when pCDNAI/Amp-cNT1$_{rat}$ was digested with Xba I + BamH I or Hind III + Xba I, respectively. Two fragments (7.2 + 0.1 Kb) were expected when pCDNAI/Amp-cNT1$_{rat}$ was digested with EcoR I. For each digestion, fragments of the expected sizes were observed. Thus, the structure of pCDNAI/Amp-cNT1$_{rat}$ was verified.

4.3 Transient Expression of cNT1$_{rat}$ in COS-1 Cells

The transient transfection studies were carried out using a modification of the DEAE-dextran method described previously (111). This method, which is simple and more reproducible than other transfection procedures (111), works very well in COS cells (110). Since the concentration of DEAE-dextran is a critical determinant of the transfection efficiency (111), it was carefully optimized as follows.

pCMVβGal (5 μg) was transfected into COS-1 cells using various concentrations of DEAE-dextran (Table 4.1). Transfection efficiencies were estimated 72 hr after transfection by quantitation of cells that stained with a β-galactosidase reporter system (139). With 100 μg/ml of DEAE-dextran, the transfection efficiency was about 10%, while with 200 μg/ml or 400 μg/ml of DEAE-dextran, it was about 25%. Positively staining cells were few, if any, with 10 μg/ml of DEAE-dextran. With 1000 μg/ml of DEAE-dextran, most cells did not survive, and the transfection efficiency could not be determined. In all subsequent transient transfection experiments, 200 μg/ml DEAE-dextran was used.

pCDNAI/Amp-cNT1$_{rat}$ was transiently transfected in COS-1 cells by the DEAE-dextran method modified as described above. At 24 hr after transfection, the cells were trypsinized, pooled and replated to eliminate any differences in transfection efficiency among the individual dishes. Since the peaks of plasmid replication and protein production in transfected COS cells occur respectively, at 48-72 hr and 72-96 hr posttransfection (111), pCDNAI/Amp-cNT1$_{rat}$ transfected COS-1 cells were used for uptake assays 72 hr after transfection.

The experiments described in Chaper 3 demonstrated that nucleoside transport in COS-1 cells is mediated by an NBMPR-sensitive process. Before the uptake assays were started, the transfected COS-1 cells were pre-incubated with 1 μM NBMPR at RT for 30 min to inhibit endogenous *es*-mediated NT activity. The uptake assay was started by removing the NBMPR-containing pre-incubation medium and adding permeant solution that contained the desired concentration of ^{3}H-nucleoside and the NT inhibitor. The assay was stopped by removing the permeant-containing solution and immediately washing the cells in ice-cold transport buffer.

A representative time course of ^{3}H-uridine uptake (10 μM, RT) by COS-1 cells transfected with cNT1$_{rat}$ cDNA is shown in Figure 4.2. Uptake was measured at 10-min intervals up to 30 min and in Na$^+$-containing buffer. COS-1 cells transfected with the pCDNAI/Amp vector served as controls; they were subjected to the same transfection conditions and assay procedures as cells transfected with pCDNAI/Amp-cNT1$_{rat}$. The 30-min time courses were linear. The substantial difference in uptake after 30 min between the cells transfected with cNT1$_{rat}$ and the cells transfected with vector alone suggested that expression of the cNT1$_{rat}$ cDNA had resulted in the production of a functional nucleoside transporter.

Since it had been shown previously (9) that cNT1$_{rat}$ is a sodium-dependent nucleoside transporter, ^{3}H-uridine uptake was also measured in transfected cells incubated in Na$^+$-free buffer to determine whether the uptake seen in cells transfected with the cNT1$_{rat}$ cDNA was Na$^+$-dependent (Figure 4.2). The transfection and transport assay conditions were the same as in the assays conducted in Na$^+$-containing buffer. The 30 min-time course was linear and there was a great difference over 30 min in uridine uptake in Na$^+$-containing buffer when compared to uptake in Na$^+$-free buffer. Therefore, uridine uptake in the pCDNAI/Amp-cNT1$_{rat}$ -transfected cells was Na$^+$-dependent. However, the uptake in Na^+-free buffer was consistently higher for cells transfected with pCDNAI/Amp-cNT1_{rat} than for cells transfected with pCDNAI/Amp alone (Figure 4.2), suggesting the presence of a minor component of Na^+-independent transport in the NT processes. Since this difference was not eliminated by dilazep, an inhibitor of the *ei* transporter (22), it did not seem to result from *ei* transport activity (Figure 4.2 insert). It thus may represent uncoupled transport (slippage) of uridine via the Na^+-linked process (9, 84, 158).

To confirm that the uptake observed in pCDNAI/Amp-cNT1_{rat} -transfected cells was transporter mediated, an excess of nonradioactive uridine (1 mM) was added to the solution that contained 10 μM ^{3}H-uridine (Figure 4.3). If uridine uptake was mediated by cNT1_{rat}, the tracer flux should have been reduced by a high concentration of nonradioactive uridine, which would compete for transporter sites with the radioactive uridine. As shown in Figure 4.3, uptake was greatly reduced by the addition of 1 mM nonradioactive uridine.

In the experiments described thus far, NBMPR was used to block endogenous nucleoside transport activity in COS-1 cell. In subsequent experiments, dilazep was used instead of NBMPR as the inhibitor, because dilazep is more soluble than NBMPR. However, as NBMPR is a diagnostic agent to distinguish *es* and *cs* NTs from other NT subtypes (22), the results of the preceding experiments indicated that the transport activity seen in cNT1_{rat} cDNA transfected cells was mediated by a transporter that belongs to the NBMPR-insensitive group of nucleoside transport processes.

4.4 Construction of c-*myc* tagged cNT1_{rat}

When this work was initiated, antibodies against cNT1_{rat} had not yet been developed. To analyze production of the cNT1_{rat} protein in transfected COS-1 cells, an epitope tag based on human c-*myc* (10 amino acid residues EQKLISEEDL) was fused to the C-terminus of the cNT1_{rat} transporter. Monoclonal antibody 9E10, which is commercially available, recognizes this ten-residue sequence of human c-*myc* specifically.

Thus, c-*myc* tagging allowed surveillance of $\mathrm{cNT1_{rat}}$ production by immunoblotting, even though antibodies against $\mathrm{cNT1_{rat}}$ were not available. The epitope tagging approach has been used to study a variety of proteins of interest (159-163). The amino or carboxyl terminus of the protein is typically chosen as a tagging site because the ends of proteins are more likely to be accessible to the antibody and to be susceptible to modification without affecting function (161, 164).

The construction of c-*myc* tagged $\mathrm{cNT1_{rat}}$ is summarized in Figure 4.4. The addition of the c-*myc* tag to the C-terminus of $\mathrm{cNT1_{rat}}$ was accomplished by PCR modification of the $\mathrm{cNT1_{rat}}$ cDNA. The PCR product was digested with EcoR I and Xba I and then subcloned into pBluescript $\mathrm{KS^-}$. The nucleotide sequence at the 3' end of the PCR-generated fragment (about 300 bp, including the c-*myc* tag) was confirmed by DNA sequencing. The unconfirmed 5' portion of the PCR product (about 1700 bp)was removed and replaced with the corresponding fragment of the original $\mathrm{cNT1_{rat}}$ cDNA. The EcoR V site is a polylinker site of pBluescript $\mathrm{KS^-}$ that is upstream of the 5'-end of the PCR product. The BamH I site was within the confirmed 3'end of the PCR product. The original $\mathrm{cNT1_{rat}}$ in pGEM3Z was removed by digestion with Afl III (5'-end) and BamH I (3'-end). The 5'-end was then blunt-ended with the Klenow fragment, and the resulting fragment was used to replace the corresponding 5'-portion of the PCR product. The *c-myc* tagged $\mathrm{cNT1_{rat}}$ was subcloned into pCDNAI/Amp at Xho I and Xba I for expression in mammalian cells. The expression construct was named pCDNAI/Amp-$\mathrm{cNT1_{rat}}$ -*myc*.

4.5 Functional Analysis of Recombinant c-myc Tagged $\mathrm{cNT1_{rat}}$ Proteins in COS-1 Cells

To test if the presence of the c-*myc* tag affected $\mathrm{cNT1_{rat}}$ function, pCDNAI/Amp-$\mathrm{cNT1_{rat}}$-*myc* transfected COS-1 cells were used for uptake assays 72 hr after transfection. The assays were conducted in sodium-containing buffer in the presence of 10 µM dilazep, as described above (see Section 4.2). Figure 4.5 shows the results. The uptake of 10 μM ^{3}H-uridine during 10 min for cells transfected with vector containing either the cNT1$_{rat}$-*myc* insert or the cNT1$_{rat}$ insert was much higher than that for cells transfected with vector alone. Since the presence of the epitope tag had reduced uridine uptake by about 20%, it appeared that recombinant cNT1$_{rat}$-*myc* was produced and correctly processed.

4.6 Identification of Recombinant c-*myc* tagged cNT1$_{rat}$ in COS Cells

pCDNAI/Amp-cNT1$_{rat}$-*myc* or pCDNAI/Amp (as a control) was transfected into COS-1 cells using the DEAE-dextran method exactly as in the preceding transport experiments. Crude cellular membranes were prepared 72 hr after transfection, and the proteins in SDS-solubilized membranes were resolved on a 12% SDS-PAGE gel and subjected to protein immunoblotting analysis (Figure 4.6). Immunostaining with anti-c-*myc* monoclonal antibodies revealed a band (about 45 kDa) that was present in the membrane fraction isolated from pCDNAI/Amp-cNT1$_{rat}$-*myc* transfected cells but not in the fraction from pCDNAI/Amp transfected cells. The 45 kDa band, seen only in the cells transfected with the cNT1$_{rat}$-*myc* cDNA, appeared to be the c-*myc* tagged cNT1$_{rat}$ protein, although this band migrated with an apparent molecular mass (45 kDa) that was lower than that (71 KDa) calculated (9) from the predicted amino acid sequence of cNT1$_{rat}$.

4.7 Inhibition of cNT1$_{rat}$-mediated Transport of Uridine by Physiological Nucleosides

To demonstrate the specificity profile of cNT1$_{rat}$, inhibition studies were conducted in COS-1 cells transfected with the cNT1$_{rat}$ cDNA (Figure 4.7). Various nonradioactive physiological nucleosides were added at concentrations of 1 mM to transport assay mixtures to test if they were able to inhibit cNT1$_{rat}$-mediated uptake of 10 μM ^{3}H-uridine during a 5-min incubation. The uptake of ^{3}H-uridine in the absence of nonradioactive nucleosides served as the uninhibited control (100%). All of these studies were conducted in the presence of 10 μM dilazep to block endogenous NT activity in COS-1 cells. As shown in Figure 4.7, cNT1$_{rat}$-mediated uptake of ^{3}H-uridine was reduced by the presence of nonradioactive uridine to 5% of control values. Similar reductions were seen with thymidine, cytidine, deoxycytidine and adenosine, whereas the significance of the apparent 20% reduction observed in presence of guanosine was questionable. These results were consistent with the reported substrate selectivities of N2/*cit* NTs (84, 89-93).

To confirm that guanosine was not a substrate of cNT1$_{rat}$, direct measurements of uptake of various concentrations (10-500 μM) of ^{3}H-guanosine were conducted in cells transfected with cNT1$_{rat}$ (Figure 4.8). Uptake by COS-1 cells transfected with vector alone served as a control. The uptake time courses of ^{3}H-guanosine by the two types of transfectants were similar, confirming that guanosine was not a substrate of cNT1$_{rat}$.

The inhibitory effects of cytidine and deoxycytidine on ^{3}H-uridine uptake were further investigated in the experiments of Figure 4.9, which examined the extent of inhibition of uptake under various concentration of cytidine or deoxycytidine. Both were relatively potent inhibitors, with a 50% reduction in uridine uptake seen at concentrations of about 50 μM.

4.8 Kinetic Studies

To further determine the functional characteristics of recombinant cNT1$_{rat}$ transiently in COS-1 cells, the kinetics of uptake of some physiologic nucleosides were determined. Uridine, thymidine and adenosine and cytidine were selected to be investigated for the following reasons:

(i) Uridine and adenosine are considered to be "universal" NT substrates since results of direct measurements and / or inhibition studies have suggested that they can be transported by all types of NT-mediated processes thus far identified (22).

(ii) Thymidine serves as a diagnostic substrate for pyrimidine-selective N2/*cit* or N4/*cit* nucleoside transporters and results of the inhibition studies with cells transfected with $cNT1_{rat}$ cDNA (see Section 4.7) had suggested that $cNT1_{rat}$ was pyrimidine-selective.

(iii) Adenosine is unique among the physiological nucleosides in that it is a local signaling molecule and is known to have a regulatory function in physiological and metabolic activities, including platelet aggregation, coronary vasodilation, cardiac contractility, and renal vasoconstriction (22).

(iv) There have been no direct studies of N2/*cit* or N4/*cit*-mediated transport of cytidine, which has many analogues with important anticancer or antiviral activities.

The transport assays described in this section were conducted in sodium-containing buffer and in the presence of 10 μM dilazep to block endogenous nucleoside transport processes of COS-1 cells. Transport velocities were obtained from 12-sec time courses at different concentrations of each of the four ^{3}H-nucleosides (see Figures 4.10, 4.12, 4.14 and 4.16 for representative experiments). Since preliminary studies had shown that transport velocities of uridine were reduced by more than 90% in the presence of 1 mM nonradioactive uridine, the small contribution of the diffusion to uptake rates could be ignored. The 12-sec time courses were linear and sufficiently short to allow estimation of initial rates. Apparent K_m and V_{max} values were determined by three plots: Woolf plot, Eadie-Hofstee plot and Lineweaver-Burke plot. The Lineweaver-Burke plot is the most widely recognized and used plot. The Woolf plot emphasizes data obtained at relatively high concentrations and the Eadie-Hofstee plot emphasizes the opposite. Figures 4.11, 4.13, 4.15 and 4.17 show these plots for $cNT1_{rat}$-mediated uptake of uridine, thymidine, cytidine and adenosine, respectively. For each nucleoside, the individual K_m and V_{max} values derived from the three different plots were similar.

The kinetic studies of uridine, thymidine, cytidine and adenosine showed that these four nucleosides had similar K_m values, indicating that each had a high affinity for $cNT1_{rat}$. However, the maximum velocities of transport differed (uridine > thymidine > cytidine > adenosine). The V_{max}/K_m ratios for uridine, thymidine, cytidine and adenosine were 0.65, 0.20, 0.10 and 0.009, respectively. The maximum velocity and V_{max}/K_m ratio for adenosine were dramatically lower than those for uridine, thymidine and cytidine.

To confirm that adenosine was poorly transported by $cNT1_{rat}$, a direct comparison was made between uridine and adenosine transport in the same preparation of transfected cells. Figure 4.18 shows that the initial rate of uptake of 10 μM uridine was 3.26 pmol/sec/10^6 cells, while that of 10 μM adenosine was only 0.24 pmol/sec/10^6 cells. The initial rate of uridine uptake was 13-fold higher than that of adenosine. Therefore, although adenosine and uridine exhibited almost identical K_m values, adenosine was poorly transported by $cNT1_{rat}$ compared to uridine.

Table 4.2 presents the K_m and V_{max} values obtained in this study for $cNT1_{rat}$-mediated transport of uridine, thymidine, cytidine and adenosine in COS-1 cells and those reported elsewhere (138) for $cNT1_{rat}$-mediated transport of uridine and adenosine in *Xenopus* oocytes. The absolute V_{max} values are not comparable because of the differences (e.g, cell size, amounts of recombinant protein produced) between the two expression systems. However, the K_m values, which represent a measure of transporter affinities, are directly comparable. The K_m values obtained in the two expression systems for transport of uridine were quite close, and the K_m values for adenosine were almost the same, suggesting that recombinant $cNT1_{rat}$ functioned similarly in mammalian cells and *Xenopus* oocytes.

4.9 Inhibition Studies of Nucleoside Drugs

Many nucleoside analogues are important anti-cancer and anti-AIDS drugs. Since most of these drugs are hydrophilic, functional nucleoside transport processes in the plasma membrane are required for their phamacologic actions. While many nucleoside drugs have been tested for transportability with *es* systems of various cell types, only a few have been tested with the pyrimidine-selective concentrative transporters (22). $cNT1_{rat}$ has been shown to be capable of transporting AZT and ddC (9). Therefore, several pyrimidine nucleoside analogue drugs were tested for their ability to inhibit $cNT1_{rat}$-mediated transport in COS-1 cells. They were AZT, ddC, FUdR, IUdR, araC, gemcitabine and 3TC.

In the experiment of Figure 4.19, $cNT1_{rat}$-mediated uptake of ^{3}H-uridine (10 μM, 5 min) was measured in sodium-containing buffer with 10 μM dilazep. Uptake was inhibited by the addition of nonradioactive 5 mM AZT, FudR, IUdR, gemcitabine, araC or ddC, suggesting that these drugs were either substrates or inhibitors of $cNT1_{rat}$. The extent of inhibition by 5 mM AZT, ddC and araC was about 50%, whereas that by 5 mM IUdR and FUdR was greater than 90%. Inhibition was not seen with 5 mM 3TC. The effects of IUdR and FUdR were further examined in the experiments of Figure 4.20, where uptake of 10 μM [^{3}H]uridine was measured in the presence of various concentrations of nonradioactive IUdR or FUdR. Uptake was reduced to 50% by 40-60 μM of FUdR or IUdR, indicating that both interacted with recombinant $cNT1_{rat}$ with relatively high affinity. Since nonradioactive 3TC (5 mM) was not able to block ^{3}H-uridine uptake, it was neither a substrate or an inhibitor of $cNT1_{rat}$.

4.10 Summary

This chapter describes results of experiments in which cNT1$_{rat}$ cDNA was transiently transfected into COS-1 cells, and its expression was examined by functional assay and protein immunoblotting analysis. In the functional assays, a substantial increase in uptake of uridine was observed in COS-1 cells transfected with cNT1$_{rat}$ cDNA when compared to cells transfected with vector alone, indicating high levels of functional recombinant cNT1$_{rat}$. The cNT1$_{rat}$-dependent nucleoside transport activity was sodium-dependent. A residual sodium-independent transport activity was observed when cells transfected with cNT1$_{rat}$ cDNA were assayed in sodium-free buffer.

At the time when these studies were conducted, antibodies against cNT1$_{rat}$ were not available. To demonstrate the presence of recombinant cNT1$_{rat}$ by protein immunoblotting, a *myc*-tagged cNT1$_{rat}$ cDNA was constructed and transfected into COS-1 cells. The recombinant *myc*-tagged transporter was shown to be fully functional. Recombinant cNT1$_{rat}$-*myc* migrated in SDS-PAGE with an apparent molecular mass that was lower than that predicated from its amino acid sequences. This discrepancy could have been due to one or more of the following reasons: (i) aberrant electrophoretic mobility, because of its high hydrophobicity, which has been reported for other hydrophobic proteins (110, 165-167); (ii) degradation of the recombinant protein to a smaller size, which could occur during the course of crude membrane preparation as reported for calpastatin (168); or (iii) a shorter actual amino acid sequence than predicted.

The inhibition studies with physiological nucleosides showed the potential transportabilities of uridine, thymidine, cytidine, deoxycytidine and adenosine by cNT1$_{rat}$, but not guanosine. The permeant selectivity profile was consistent with that for N2/*cit* from previous inhibition studies (84, 89-93). However, the kinetic studies showed that, although it had a high affinity to cNT1$_{rat}$, similar to that for uridine, thymidine and cytidine, its V_{max} value was very low, suggesting that adenosine was not a good substrate of cNT1$_{rat}$.

The potential transportability of several clinically important nucleoside drugs by $cNT1_{rat}$ was tested by inhibition studies. These nucleoside drugs inhibited uridine uptake by $cNT1_{rat}$ to different extents, suggesting that $cNT1_{rat}$ may be involved in the gastrointestinal absorption of some of these drugs, and that the different modifications of the drugs may be related to their different inhibition abilities. This information may be useful for drug design in the future.

Table 4.1 Optimization of the DEAE-dextran concentration used in transfection of COS-1 cells

Concentration of DEAE-dextran (μg/ml)	10	100	200	400	1000
transfection effeciency	N	10%	25%	25%	*

The same quantities (5 μg) of pCMVβGal were transfected into COS-1 cells using five different concentrations of DEAE-dextran in the protocol described in Materials and Methods (Section 2.4). Transfection efficiencies were estimated 72 hr after transfection by counting cells that stained (positives) or did not stain (negatives) with a β-galactosidase reporter system.

* The transfection efficiency could not be determined because most of the cells had detached from the culture dishes by 72 hr.

N No positive cells were detected.

Table 4.2 Kinetic parameters of uridine, cytidine,thymidine and adenosine for recombinant cNT1$_{rat}$ in COS-1 cells and *Xenopus* oocytes

		K_m (µM)	V_{max}*	V_{max} / K_m
uridine	COS cells	**(1) 18.9 ± 1.8**	**12.3 ± 0.6**	**0.65 ± 0.03**
		(2) 23.0 ± 10	10.2 ± 5.0	0.43 ± 0.16
	oocytes	37.2	20.8	0.56
thymidine	COS cells	**(1) 13.9 ± 0.6**	**2.72 ± 0.12**	**0.20 ± 0.003**
		(2) 8.6 ± 2.3	2.97 ± 0.45	0.35 ± 0.05
cytidine	COS cells	**4.04 ± 0.05**	**0.3 ± 0.006**	**0.097 ± 0.0025**
adenosine	COS cells	**(1) 18.7 ± 2.9**	**0.17 ± 0.04**	**0.009 ± 0.0002**
		(2) 11.3 ± 0.1	0.08 ± 0.01	0.007 ± 0.005
	oocytes	20.7	0.053	0.003

The kinetic parameters of cNT1$_{rat}$-mediated transport of uridine, thymidine, cytidine and adenosine in COS cells are the means (± SD) of values that were derived from Woolf, Eadie-Hofstee and Lineweaver-Burke plots. Values in bold letters are derived from Figures 4.11, 4.13, 4.15 and 4.17; the other values were from experiments conducted under the same conditions. The kinetic parameters of cNT1$_{rat}$-mediated transport of uridine and adenosine in *Xenopus* oocytes are the work of Sylvia Yao (138).

* The unit of V_{max} in COS cells is pmol/sec/10^6 cells and in oocytes is pmol/min/oocyte.

Figure 4.1(a) Structure of pCDNAI/Amp vector

SV40: SV40 origin of replication for episomal replication in cells that express the SV40 large T antigen

ColE 1: ColE 1 origin for growth in *E. coli*

M13 ori: M13 origin for single-strand rescue of the antisense strand for mutagenesis and sequencing

Amp: ampicillin-resistance gene to permit selection of bacteria that have the recombinant plasmids

pCMV: enhancer-promoter sequences from the immediate early gene of the human cytomegalovirus (CMV) for high-level expression

SV40 SS/pA: transcription termination and RNA processing signals from SV40 to enhance mRNA stability

Polyoma ori: polyoma origin of replication for episomal replication in cells expressing latently infected with polyoma virus

Hind III → Xba I: polylinker sites for subcloning

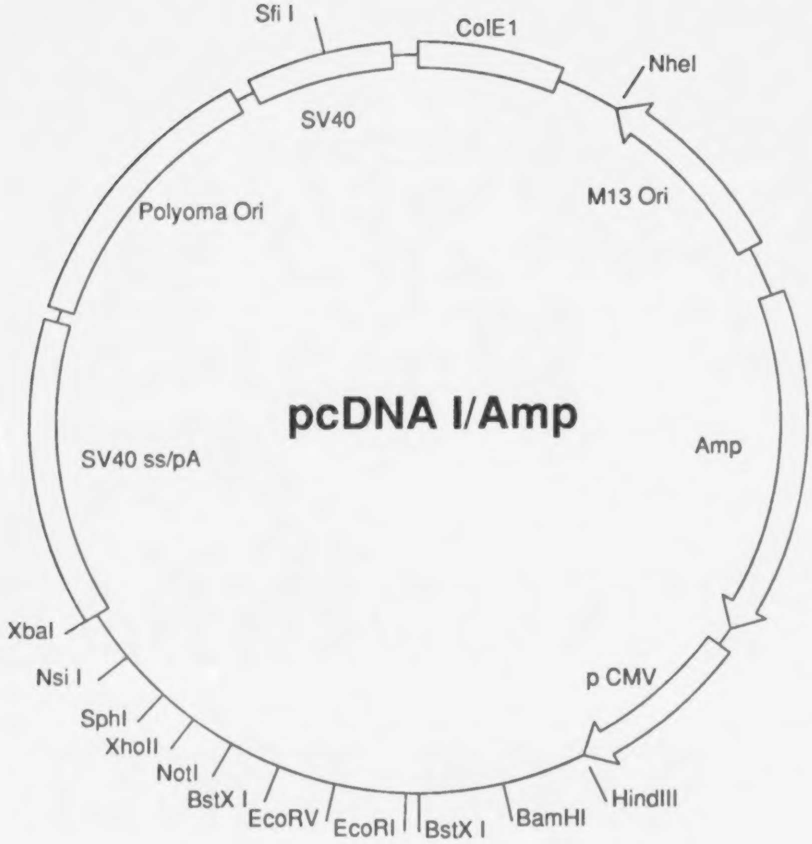
Sfi I
ColE1
NheI
SV40
M13 Ori
Polyoma Ori
pcDNA I/Amp
Amp
SV40 ss/pA
XbaI
p CMV
Nsi I
SphI
XhoII
NotI
BstX I
EcoRV
EcoRI
BstX I
BamHI
HindIII

Figure 4.1(b) Construction of pCDNAI/Amp-$cNT1_{rat}$

$cNT1_{rat}$ was originally isolated as a cDNA fragment that had been cloned in pGEM3Z at the EcoR I and XbaI I sites. $cNT1_{rat}$ was removed from pGEM3Z by cutting at the unique restriction sites, Afl III and Xba I. The 5'-end was blunted with Klenow and ligated into pCDNAI/Amp at EcoR V. The 3' end of $cNT1_{rat}$ was ligated into pCDNAI/Amp at Xba I. The expression construct was named "pCDNAI/Amp-$cNT1_{rat}$".

□ polylinker sites of pCDNAI/Amp

■ coding region of $cNT1_{rat}$

▥ 5' and 3' noncoding regions of $cNT1_{rat}$

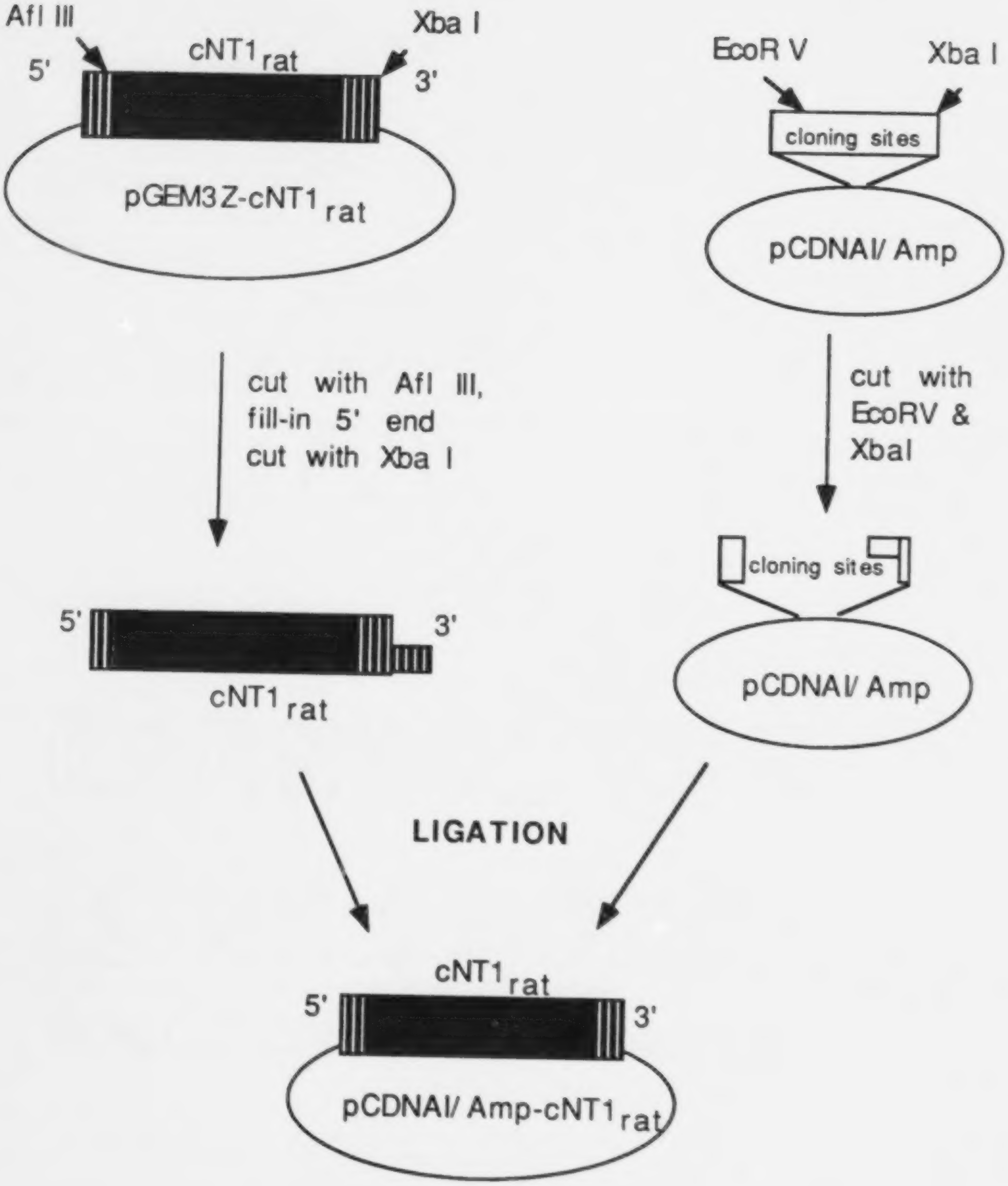
Afl III
cNT1$_{rat}$
Xba I
5'
3'
pGEM3Z-cNT1$_{rat}$
EcoR V
Xba I
cloning sites
pCDNAI/ Amp
cut with Afl III,
fill-in 5' end
cut with Xba I
cut with EcoRV & XbaI
5'
3'
cNT1$_{rat}$
cloning sites
pCDNAI/ Amp
LIGATION
cNT1$_{rat}$
5'
3'
pCDNAI/ Amp-cNT1$_{rat}$

Figure 4.1(c) pCDNAI/Amp-cNT1$_{rat}$ expression construct

pCDNAI/Amp-cNT1$_{rat}$ contained the cNT1$_{rat}$ cDNA insert. For the cNT1$_{rat}$ insert, 5' and 3' designate the 5'- and 3'-ends, respectively.

▨ represents the 5' untranslated region

■ represents the 3' untranslated region

■ represents the coding region

The positions of some restriction endonucleases sites (used for restriction mapping, Figure 4.1(d)) are shown on the map. The map is not to scale.

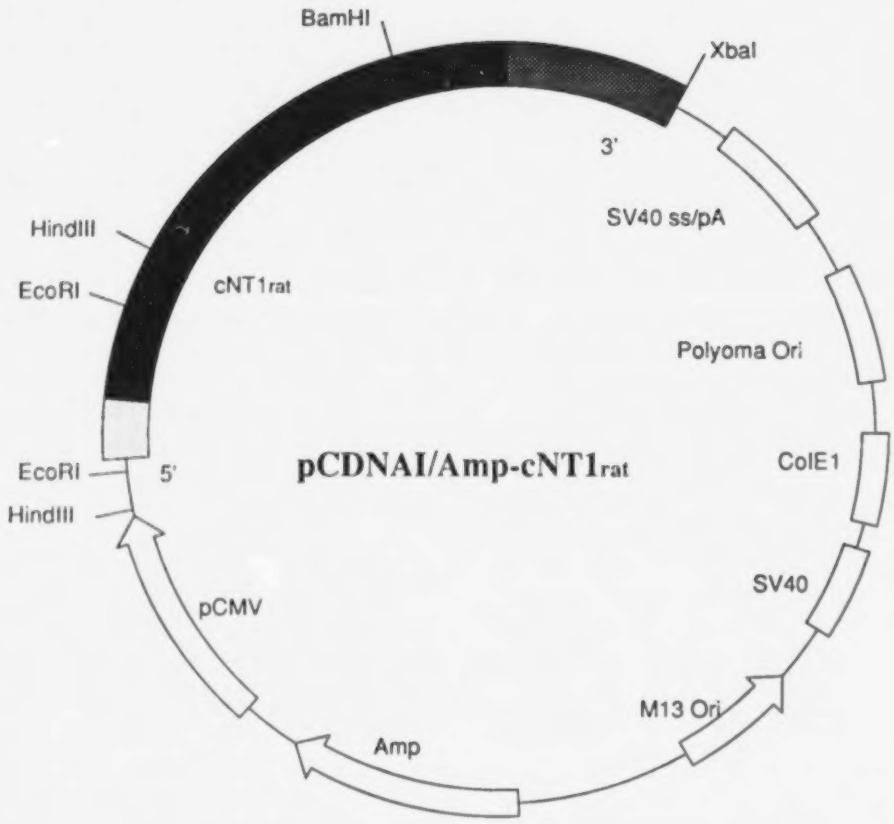
BamHI
XbaI
3'
SV40 ss/pA
HindIII
EcoRI
cNT1rat
Polyoma Ori
pCDNAI/Amp-cNT1rat
EcoRI
5'
ColE1
HindIII
SV40
pCMV
M13 Ori
Amp

Figure 4.1(d) Restriction mapping of pCDNAI/Amp-cNT1$_{rat}$

The structure of pCDNAI/Amp-cNT1$_{rat}$ was verified by restriction mapping. pCDNAI/Amp-cNT1$_{rat}$ was digested with Xba I + BamH I (lane 1), EcoR I (lane 2) or Xba I + Hind III (lane 3). Undigested pCDNAI/Amp-cNT1$_{rat}$ was on lane 4. λ DNA/Hind III marker (23, 9.4, 6.6, 4.4, 2.3, 2.0 Kb; from the top to the bottom) was on lane M. The resulting fragments were analyzed by electrophoresis on a 0.8% agarose gel and visualized with a UV light box. Where DNA sizes were less than 500 bp, the bands were faintly visible on the original gel photograph.

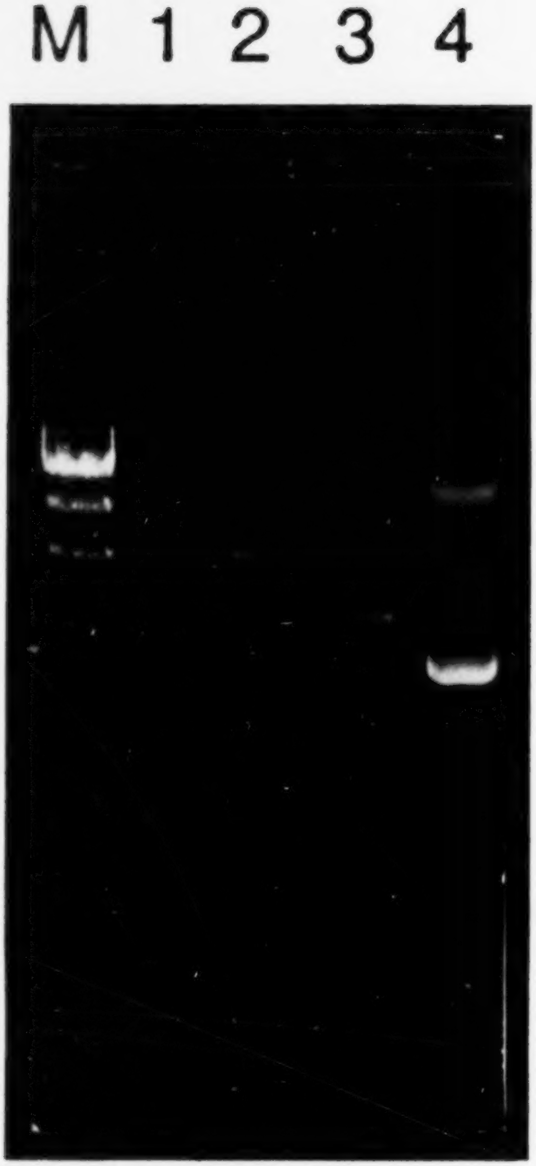
M
1
2
3
4

Figure 4.2 Uridine uptake by COS-1 cells transfected with $cNT1_{rat}$ cDNA.

Actively proliferating cells were transfected with pCDNAI/Amp-$cNT1_{rat}$ (▲, ●) or pCDNAI/Amp (control, △, ○) by the DEAE-dextran method (see Materials and Methods, Section 2.4). Uptake measurements were conducted in cells 72 hours after transfection. In this representative experiment, there were 1.1×10^6 cells per 60-mm dish, and the transfection efficiency, which was determined in parallel cultures that had been transfected with pCMVβ, was about 25%.

Transfected cells were incubated with 1 μM NBMPR at RT for 30 min before the uptake assay. Uptake measurements were conducted in the presence of 1 μM NBMPR in either sodium-containing transport buffer (△, ▲) or sodium-free transport buffer (○, ●). Uptake assays were started by adding 1.5 ml of transport buffer containing 10 μM ^{3}H-uridine and 1 μM NBMPR, ended by aspirating the solution and immediately washing the dishes by immersion in 1.5 liter of ice-cold transport buffer. Uptake at time zero was determined by placing dishes on ice for 10 min prior to transport assay and by using ice-cold transport buffer containing 10 μM ^{3}H-uridine and 1 μM NBMPR. The cells were solubilized in 5% (v/v) Triton X-100 and combined with EcoLite scintillint for radioactivity measurement. Each value represents the mean ± SD of three dishes. Error bars are not shown where SD values were smaller than the data symbols.

The insert shows the uptake of 10 μM ^{3}H-uridine in sodium-free buffer at 5 min by pCDNAI/Amp-$cNT1_{rat}$ transfected cells and pCDNAI/Amp-transfected cells in an experiment in which 10 μM dilazep was substituted for 1 μM NBMPR.

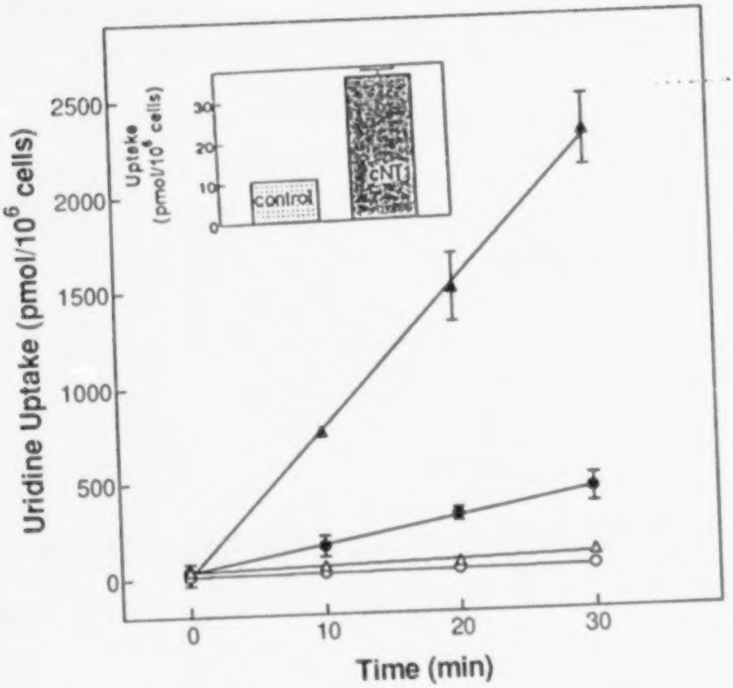
Uridine Uptake (pmol/10^6 cells)
2500
2000
1500
1000
500
0
0
10
20
30
Time (min)
Upteke (pmol/10^6 cells)
30
20
10
0
control
cNT1

Figure 4.3 ^{3}H-Uridine uptake by cNT1$_{rat}$ cDNA-transfected COS-1 cells in the presence of 1 mM nonradioactive uridine

Uptake of 10 μM ^{3}H-uridine in sodium-containing transport buffer with 1 μM NBMPR by pCDNAI/Amp-cNT1$_{rat}$-transfected cells was determined in the absence (■) or presence (●) of 1 mM nonradioactive uridine. Uptake of ^{3}H-uridine by cells transfected with pCDNAI/Amp in the absence of 1 mM nonradioactive uridine served as control (▲). Each value represents the mean ± SD of three dishes. Error bars are not shown where SD values were smaller than the data symbols.

The transfection and transport assay conditions were the same as described for Figure 4.2. There were 1.1 x 10^6 cells per 60-mm dish and the transfection efficiency which was determined in parallel cultures by transfection with pCMVβ, was about 20%.

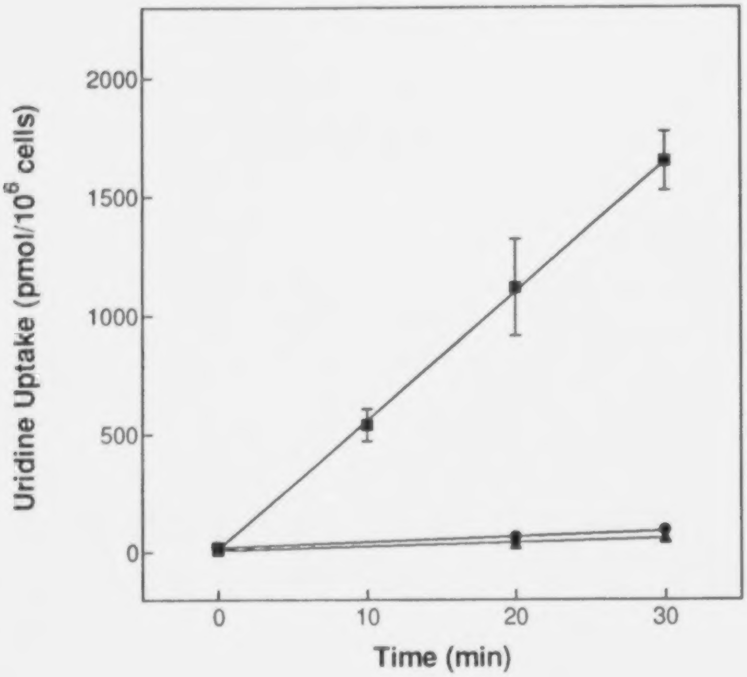
Uridine Uptake (pmol/10^6 cells)
2000
1500
1000
500
0
0
10
20
30
Time (min)

Figure 4.4 Construction of *c-myc* tagged cNT1$_{rat}$

The c-*myc* epitope tag (10 amino acids) was inserted at the C-terminus of cNT1$_{rat}$ by PCR. The 5'-and 3'-primers were 5'-GTA ATA CGA CTC ACT ATA GGG C and GCT CTA GAG CTA CAA GTC TTC TTC AGA AAT AAG CTT TTG TTC **TGT GCA GAC TGT GTG GTT GTA**-3', respectively. The bold and underlined sequences correspond to cNT1$_{rat}$ and the c-*myc* tag, respectively. The nucleotide sequence at the 3' end of the PCR-generated fragment (about 300 bp, including the *c-myc* tag) was confirmed by DNA sequencing. The unconfirmed 5' portion of the PCR product (about 1700 bp) was replaced with cNT1$_{rat}$ from the original cDNA insert. The c-*myc* tagged cNT1$_{rat}$ was then subcloned into pCDNAI/Amp at Xho I and Xba I for expression in mammalian cells. The expression construct was named pCDNAI/Amp-cNT1$_{rat}$-*myc*.

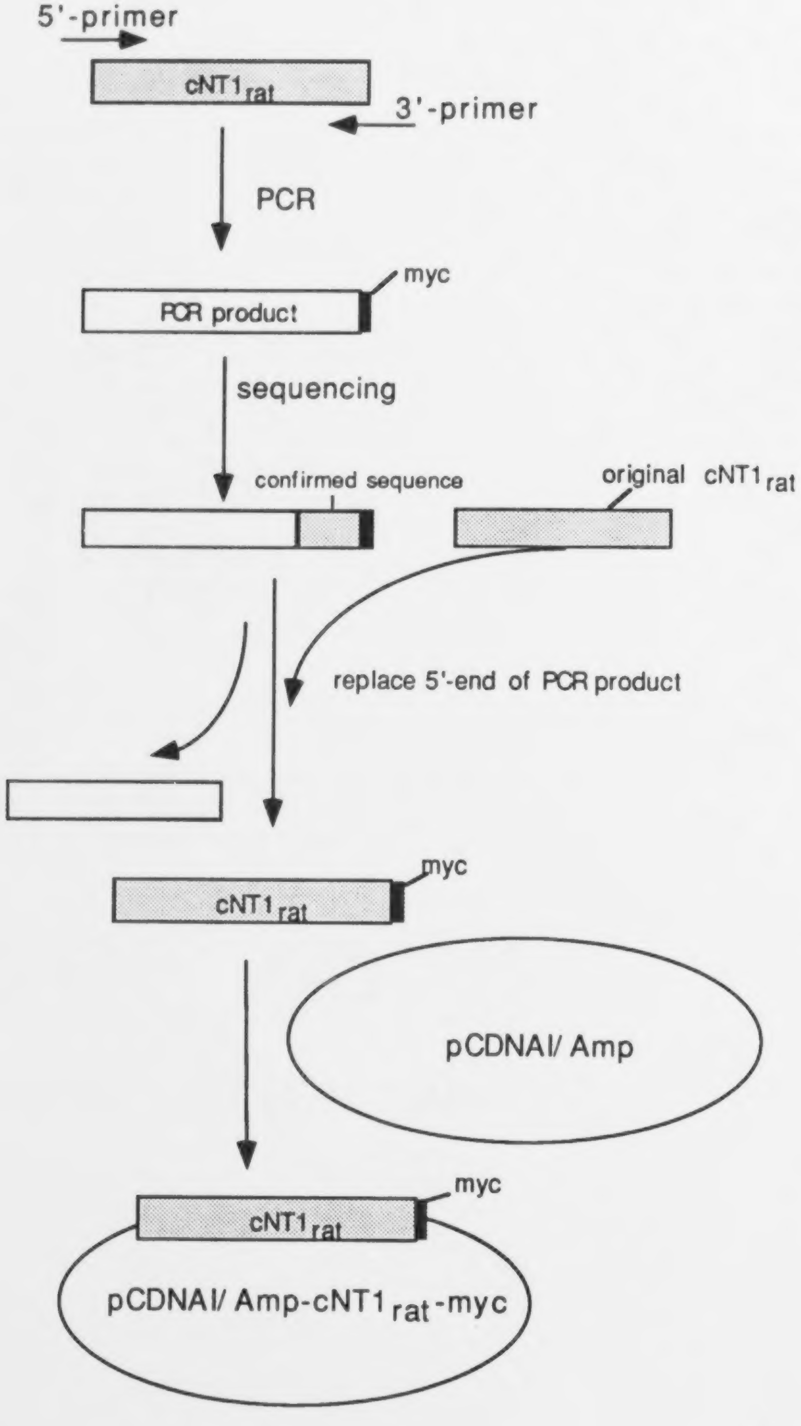
5'-primer
cNT1rat
3'-primer
PCR
myc
PCR product
sequencing
confirmed sequence
original cNT1rat
replace 5'-end of PCR product
myc
cNT1rat
pCDNAI/ Amp
myc
cNT1rat
pCDNAI/ Amp-cNT1rat-myc

Figure 4.5 Uridine uptake by recombinant cNT1$_{rat}$ and c-*myc* tagged cNT1$_{rat}$

COS-1 cells were transfected with pCDNAI/Amp, pCDNAI/Amp-cNT1$_{rat}$ or pCDNAI/Amp-cNT1$_{rat}$-*myc*. After 72 hr, uptake of 10 μM ^{3}H-uridine by transfected COS-1 cells (each dish contained 0.8 x 10^6 cells) was measured in sodium-containing transport buffer in the presence of 10 μM dilazep during a 10-min interval. Each value represents the mean ± SD of three dishes. Error bars are not shown where SD values were smaller than the data symbols.

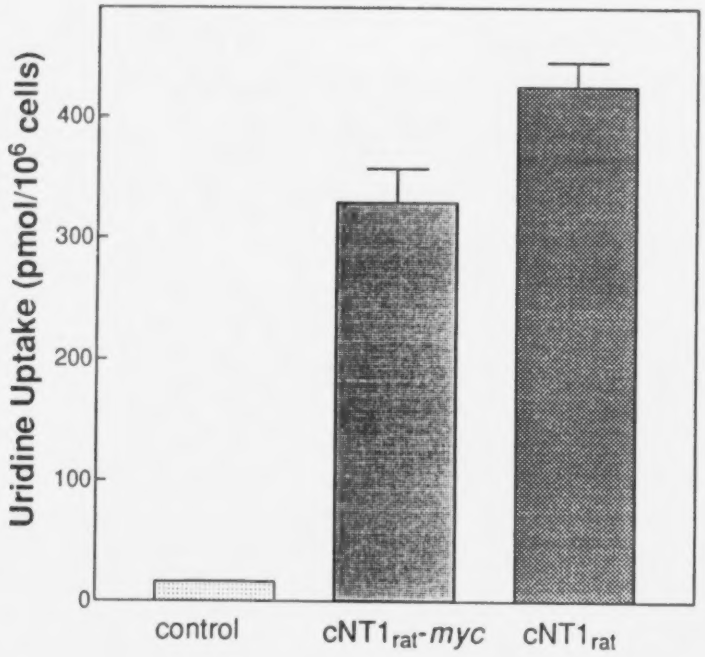
Uridine Uptake (pmol/10^6 cells)
400
300
200
100
0
control
cNT1rat-myc
cNT1rat

Figure 4.6 Western blotting of c-*myc* tagged cNT1$_{rat}$

Membrane fractions that were prepared from COS-1 cells transfected 72 hr earlier with either pCDNAI/Amp-cNT1$_{rat}$-*myc* (lane 1) or pCDNAI/Amp vector (lane 2) were solubilized and subjected to SDS-PAGE electrophoresis (12% gel, 25 µg protein per lane). The proteins were transferred to a PVDF membrane which was analyzed by immunostaining with anti-c-*myc* antibodies and goat anti-mouse horseradish peroxidase conjugate as described in Materials and Methods (Section 2.10).

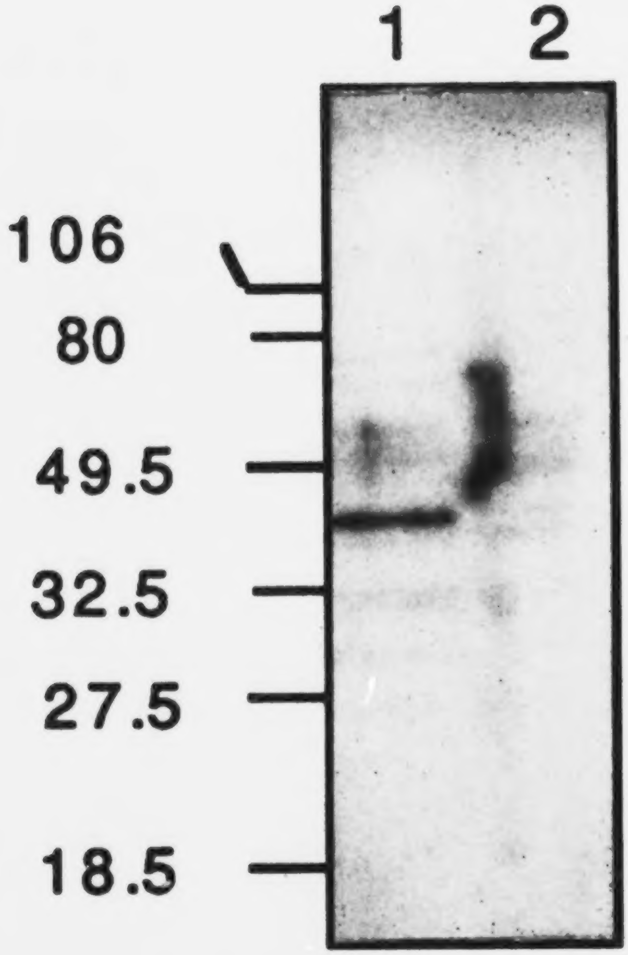
1
2
106
80
49.5
32.5
27.5
18.5

Figure 4.7 Inhibition of uridine uptake by physiological nucleosides in cNT1$_{rat}$ cDNA transfected COS-1 cells

Uptakes assays were started by adding 1.5 ml of transport buffer containing ^{3}H-uridine with or without nonradioactive nucleosides. They were ended by aspirating the permeant and washing the dishes in 1.5 liter of ice-cold transport buffer. The cells were solubilized in 5% (v/v) Triton X-100 and combined with EcoLite scintillint for radioactivity measurement.

Uptake of 10 μM ^{3}H-uridine was determined in sodium-containing transport buffer in the presence of 10 μM dilazep without (control) or with competing nonradioactive physiological nucleosides (1 mM of either uridine, thymidine, cytidine, deoxycytidine, adenosine or guanosine) over 5 min. Each value represents the mean ± SD of three dishes. Error bars are not shown where SD values were smaller than the data symbols.

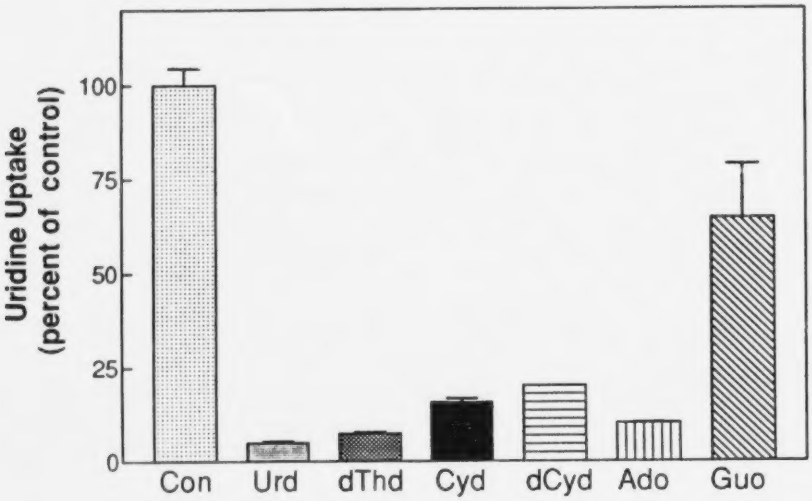
Uridine Uptake
(percent of control)
100
75
50
25
0
Con
Urd
dThd
Cyd
dCyd
Ado
Guo

Figure 4.8 Uptake ^{3}H-guanosine in cNT1$_{rat}$ cDNA-transfected COS-1 cells

Uptake of various concentrations of ^{3}H-guanosine was measured in sodium-containing transport buffer in the presence of 10 μM dilazep by cNT1$_{rat}$ cDNA-transfected (●, ▼, ■) or vector alone-transfected COS-1 cells (control, ○, ▽, □). Each value represents the mean ± SD of three dishes. Error bars are not shown where SD values were smaller than the data symbols. The transfection and transport assay conditions were the same as described for Figure 4.2. There were 1.05 x 10^6 cells per 60-mm dish and the transfection efficiency, which was determined in parallel cultures by transfection with pCMVβ, was about 25%.

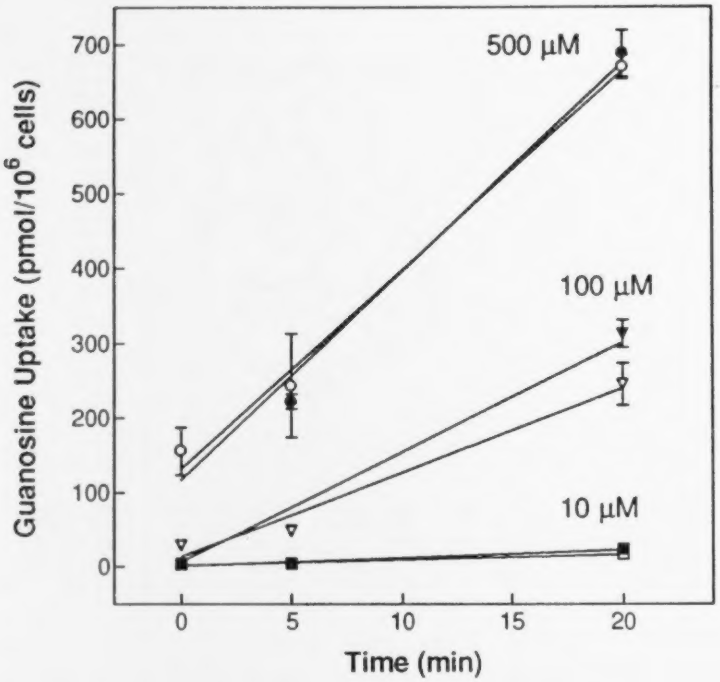

500 μM
100 μM
10 μM
Guanosine Uptake (pmol/10^6 cells)
0
100
200
300
400
500
600
700
0
5
10
15
20
Time (min)

Figure 4.9. Concentration-effect relationships for inhibition by cytidine and deoxycytidine of recombinant $cNT1_{rat}$-mediated uridine transport.

Cells were transfected with pCDNAI/Amp-$cNT1_{rat}$ and processed as described for Figure 4.2, except that dilazep (10 μM) was substituted for NBMPR. Uptake of 10 μM ^3H uridine during a 5-min incubation was determined in Na^+-containing buffer either without additives (control, 100%) or with various concentrations of cytidine (■) or deoxycytidine (▲). Values are presented as a percentage of control values. Each value represents the mean ± SD of three dishes, and error bars are not shown where SD values were smaller than the data symbols.

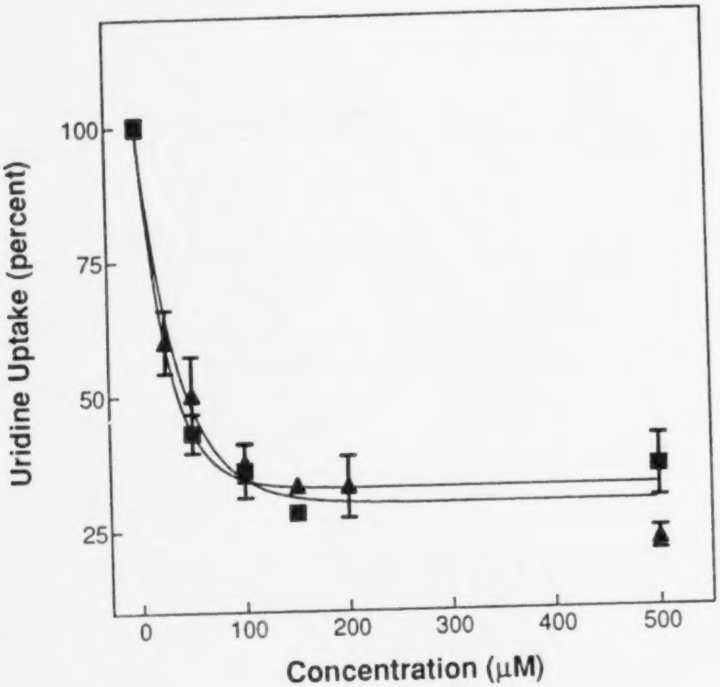

Uridine Uptake (percent)
100
75
50
25
0
100
200
300
400
500
Concentration (μM)

Figure 4.10 Time-courses of uridine uptake in cNT1$_{rat}$ cDNA transfected COS-1 cells.

Cells were transfected with pCDNAI/Amp-cNT1$_{rat}$ and processed as described for Figure 4.2, except that dilazep (10 μM) was substituted for NBMPR. Uptake intervals (0, 6, 12 sec) were timed by metronome signals. Initial rates of uptake were determined at the concentrations of ^{3}H-uridine indicated. All assays were in sodium-containing transport buffer in the presence of 10 μM dilazep. Each value represents the mean ± SD of three dishes. Error bars are not shown where SD values were smaller than the data symbols. In this experiment, at the time when the transport assay was conducted, there were 1.0 x 10^{6} cells per 60-mm dish and the transfection efficiency, which was determined in parallel cultures by transfection with pCMVβ, was 30%.

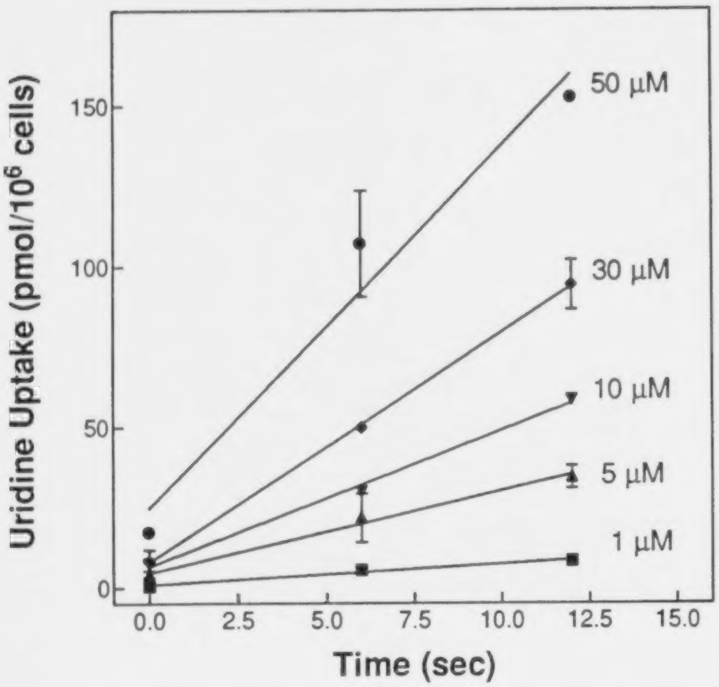
Uridine Uptake (pmol/10^6 cells)
150
100
50
0
0.0
2.5
5.0
7.5
10.0
12.5
15.0
Time (sec)
50 µM
30 µM
10 µM
5 µM
1 µM

Figure 4.11 Kinetics of uridine uptake in cNT1$_{rat}$ cDNA transfected COS-1 cells

Data from the experiment of Figure 4.10 are presented in each of three linear forms: concentration/velocity versus concentration (Top Panel); velocity versus velocity/concentration (Middle Panel); and 1/velocity versus 1/concentration (Bottom Panel). The kinetic constants derived from these plots were:

Top Panel (Woolf plot): K_m, 21.0 μM; V_{max}, 13 pmol/sec/10^6 cells.

Middle Panel (Eadie-Hofstee plot): K_m, 18.0 μM; V_{max}, 12 pmol/sec/10^6 cells.

Bottom Panel (Lineweaver-Burke plot): K_m, 17.9 μM; V_{max}, 12 pmol/sec/10^6 cells.

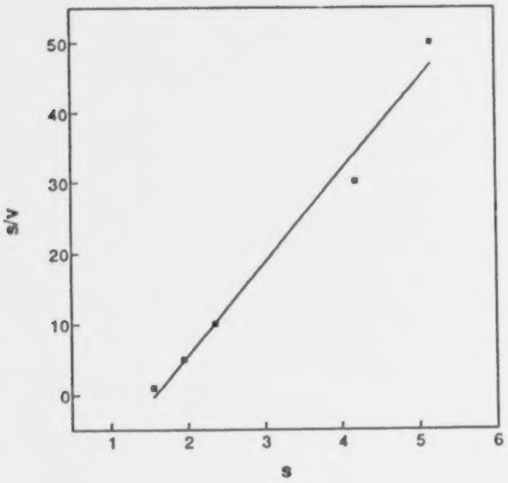
s/v
0
10
20
30
40
50
s
1
2
3
4
5
6

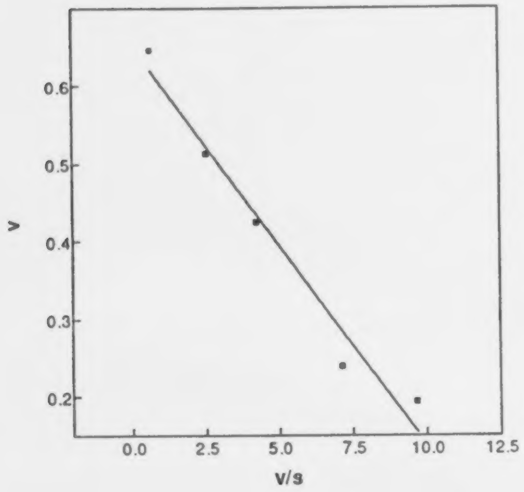
v
0.2
0.3
0.4
0.5
0.6
v/s
0.0
2.5
5.0
7.5
10.0
12.5

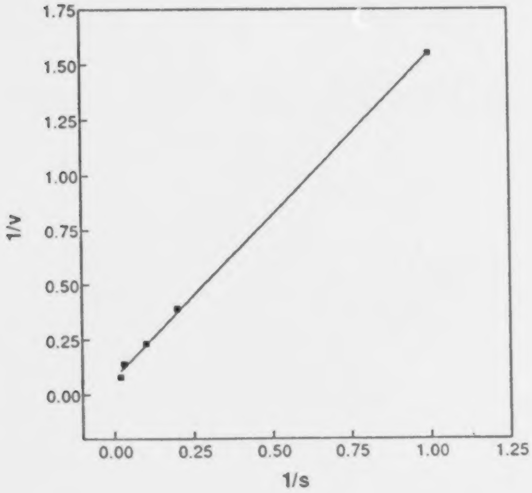
1/v
0.00
0.25
0.50
0.75
1.00
1.25
1.50
1.75
1/s
0.00
0.25
0.50
0.75
1.00
1.25

Figure 4.12 Time-course of thymidine uptake in cNT1$_{rat}$ cDNA transfected COS-1 cells.

Cells were transfected with pCDNAI/Amp-cNT1$_{rat}$ and processed as described for Figure 4.2, except that dilazep (10 μM) was substituted for NBMPR. Uptake intervals (0, 6, 12 sec) were timed by metronome signals. Initial rates of uptake were determined at the concentrations of ^{3}H-thymidine indicated. All assays were in sodium-containing transport buffer in the presence of 10 μM dilazep. Each value represents the mean ± SD of three dishes. Error bars are not shown where SD values were smaller than the data symbols. In this experiment, at the time when the transport assay was conducted, there were 1.16 x 10^6 cells per 60-mm dish and the transfection efficiency, which was determined in parallel cultures by transfection with pCMVβ, was 20%.

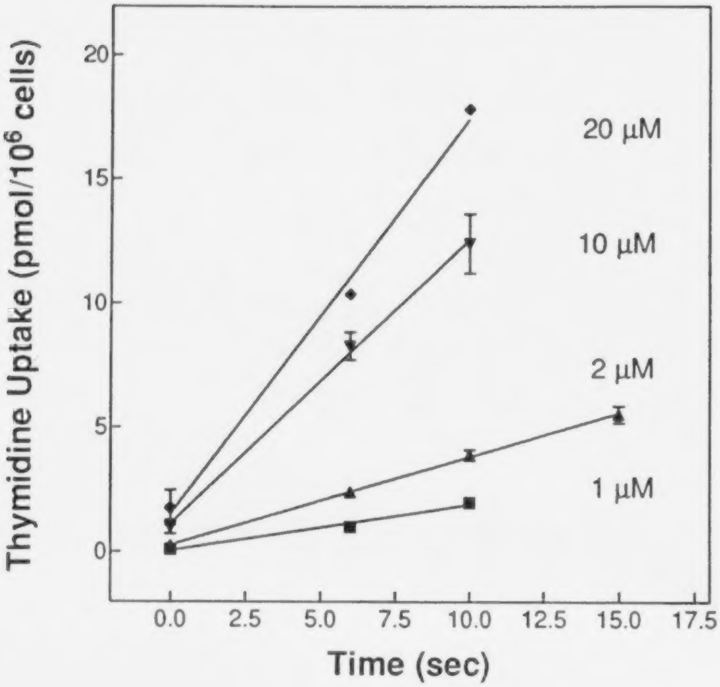
Thymidine Uptake (pmol/10⁶ cells)
20
15
10
5
0
20 μM
10 μM
2 μM
1 μM
0.0
2.5
5.0
7.5
10.0
12.5
15.0
17.5
Time (sec)

Figure 4.13 Kinetics of thymidine uptake in $cNT1_{rat}$ cDNA transfected COS-1 cells

Data from the experiment of Figure 4.12 are presented in each of three linear forms concentration/velocity versus concentration (Top Panel); velocity versus velocity/concentration (Middle Panel); and 1/velocity versus 1/concentration (Bottom Panel). The kinetic constants derived from these plots were:

Top Panel (Woolf plot): K_m, 13.6 μM; V_{max}, 2.64 pmol/sec/10^6 cells.

Middle Panel (Eadie-Hofstee plot): K_m, 13.4 μM; V_{max}, 2.66 pmol/sec/10^6 cells

Bottom Panel (Lineweaver-Burke plot): K_m, 14.6 μM; V_{max}, 2.86 pmol/sec/10^6 cells.

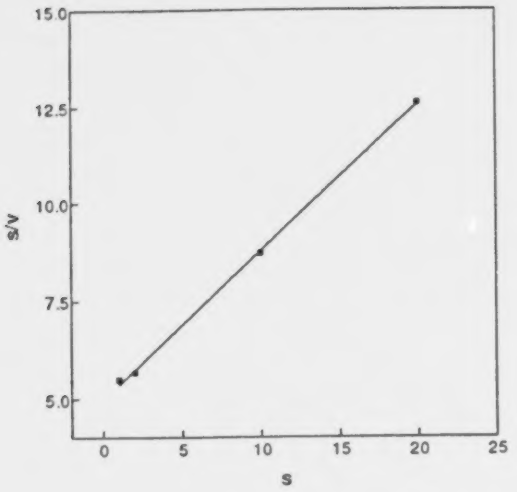

15.0
12.5
10.0
7.5
5.0
s/v
0
5
10
15
20
25
s

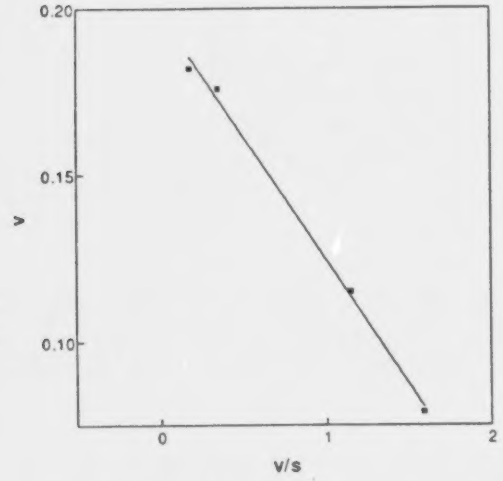

0.20
0.15
0.10
v
0
1
2
v/s

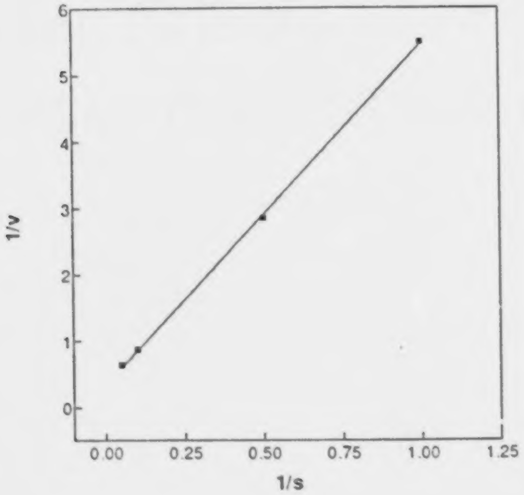

6
5
4
3
2
1
0
1/v
0.00
0.25
0.50
0.75
1.00
1.25
1/s

Figure 4.14 Time-course of cytidine uptake in cNT1$_{rat}$ cDNA-transfected COS-1 cells.

Cells were transfected with pCDNAI/Amp-cNT1$_{rat}$ and processed as described for Figure 4.2, except that dilazep (10 μM) was substituted for NBMPR. Uptake intervals (0, 6, 12 sec) were timed by metronome signals. Initial rate of uptake were determined at the concentration of ^{3}H-cytidine indicated. All assays were in sodium-containing transport buffer in the presence of 10 μM dilazep. Each value represents the mean ± SD of three dishes. Error bars are not shown where SD values were smaller than the data symbols. In this experiment, at the time when the transport assay was conducted, there were 0.5 x 10^6 cells per 60-mm dish and the transfection efficiency, which was determined in parallel cultures by transfection with pCMVβ, was 20%.

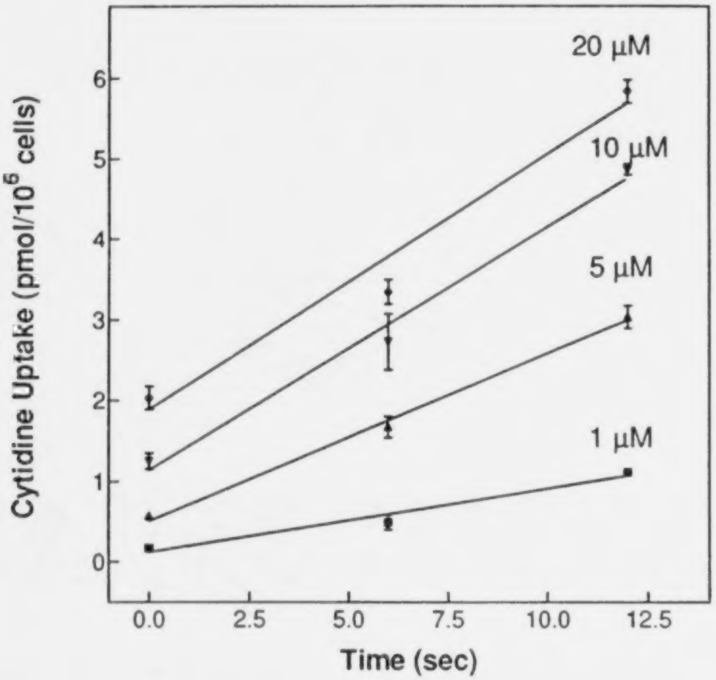
20 µM
10 µM
5 µM
1 µM
Cytidine Uptake (pmol/10^6 cells)
0
1
2
3
4
5
6
0.0
2.5
5.0
7.5
10.0
12.5
Time (sec)

Figure 4.15 Kinetics of cytidine uptake in cNT1$_{rat}$ cDNA-transfected COS-1 cells

Data from the experiment of Figure 4.14 are presented in each of three linear forms concentration/velocity versus concentration (Top Panel); velocity versus velocity/concentration (Middle Panel); and 1/velocity versus 1/concentration (Bottom Panel). The kinetic constants derived from these plots were:

Top Panel (Lineweaver-Burke plot): K_m, 4.02 µM; V_{max}, 0.39 pmol/sec/10^6 cells

Middle Panel (Eadie-Hofstee plot): K_m, 4.1 µM; V_{max}, 0.39 pmol/sec/10^6 cells

Bottom Panel (Woolf plot): K_m, 4.0 µM; V_{max}, 0.4 pmol/sec/10^6 cells.

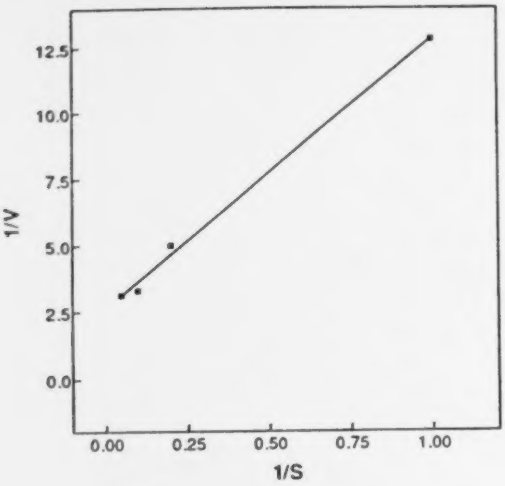
12.5
10.0
7.5
5.0
2.5
0.0
1/V
0.00
0.25
0.50
0.75
1.00
1/S

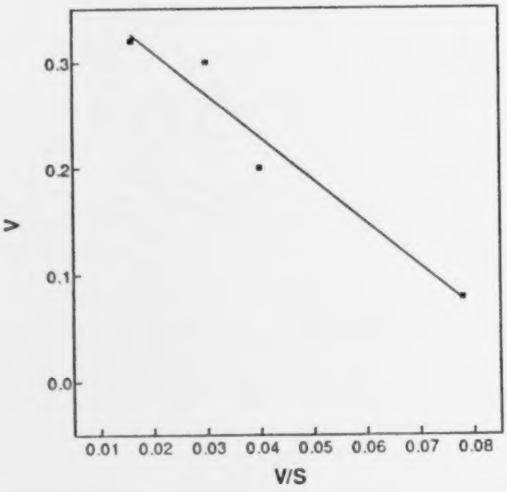
0.3
0.2
0.1
0.0
V
0.01
0.02
0.03
0.04
0.05
0.06
0.07
0.08
V/S

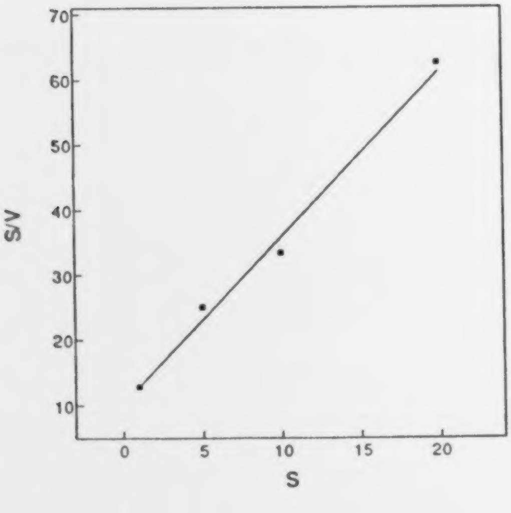
70
60
50
40
30
20
10
S/V
0
5
10
15
20
S

Figure 4.16 Time-course of adenosine uptake in cNT1$_{rat}$ cDNA-transfected COS-1 cells.

Cells were transfected with pCDNAI/Amp-cNT1$_{rat}$ and processed as described for Figure 4.2, except that dilazep (10 μM) was substituted for NBMPR. Uptake intervals (0, 6, 12 sec) were timed by metronome signals. Initial rates of uptake were determined at the concentrations of ^{3}H-adenosine indicated. All assays were in sodium-containing transport buffer in the presence of 10 μM dilazep. Each value represents the mean ± SD of three dishes. Error bars are not shown where SD values were smaller than the data symbols. In this experiment, at the time when the transport assay was conducted, there were 1.2 x 10^6 cells per 60-mm dish and the transfection efficiency, which was determined in parallel cultures by transfection with pCMVβ, was 20%.

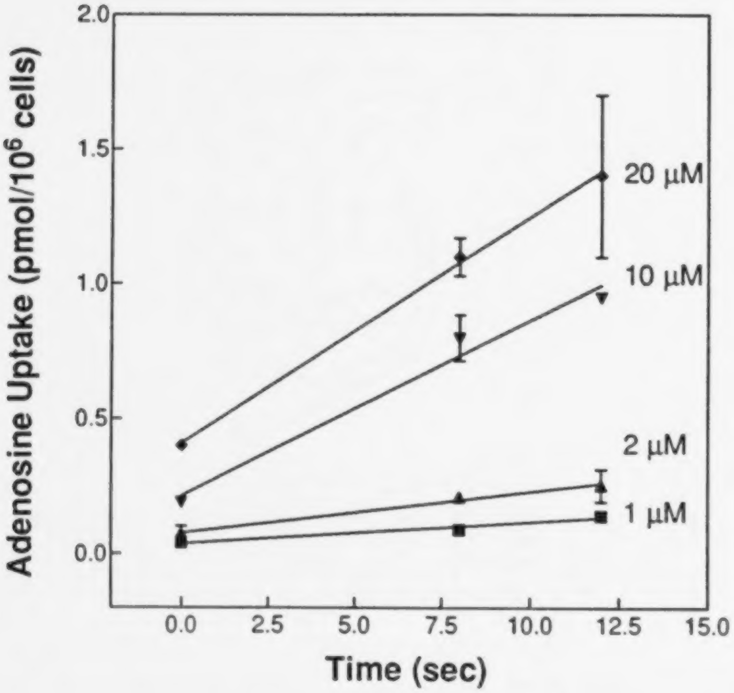
Adenosine Uptake (pmol/10^6 cells)
2.0
1.5
1.0
0.5
0.0
0.0
2.5
5.0
7.5
10.0
12.5
15.0
Time (sec)
20 µM
10 µM
2 µM
1 µM

Figure 4.17 Kinetics of adenosine uptake in cNT1$_{rat}$ cDNA transfected COS-1 cells

Data from the experiment of 4.16 are presented in each of three linear forms concentration/velocity versus concentration (Top Panel); velocity versus velocity/concentration (Middle Panel); and 1/velocity versus 1/concentration (Bottom Panel). The kinetic constants derived from these plots were:

Top Panel (Woolf plot): K_m, 16.0 μM; V_{max}, 0.15 pmol/sec/10^6 cells.

Middle Panel (Eadie-Hofstee plot): K_m, 15.0 μM; V_{max}, 0.14 pmol/sec/10^6 cells

Bottom Panel (Lineweaver-Burke plot): K_m, 25.0 μM; V_{max}, 0.21 pmol/sec/10^6 cells.

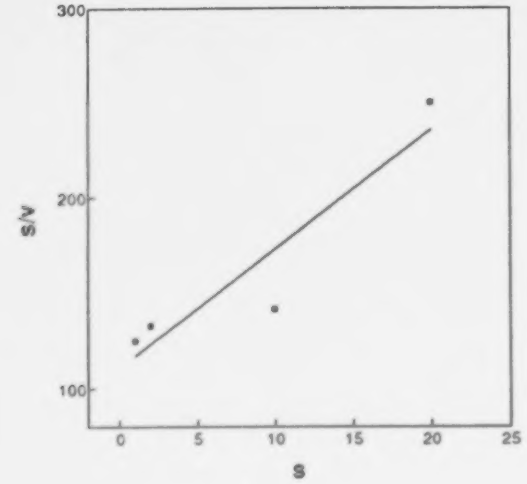
300
200
100
s/v
0
5
10
15
20
25
s

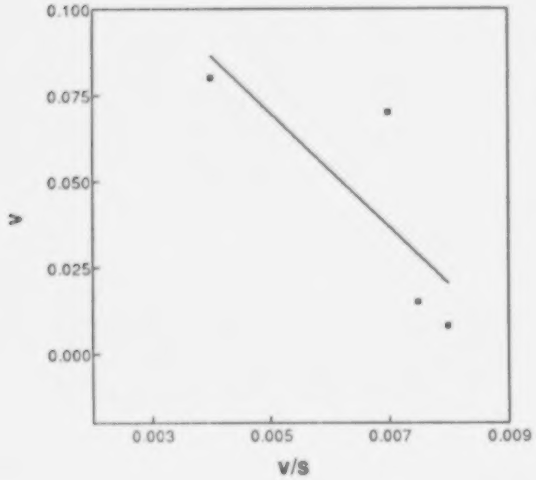
0.100
0.075
0.050
0.025
0.000
v
0.003
0.005
0.007
0.009
v/s

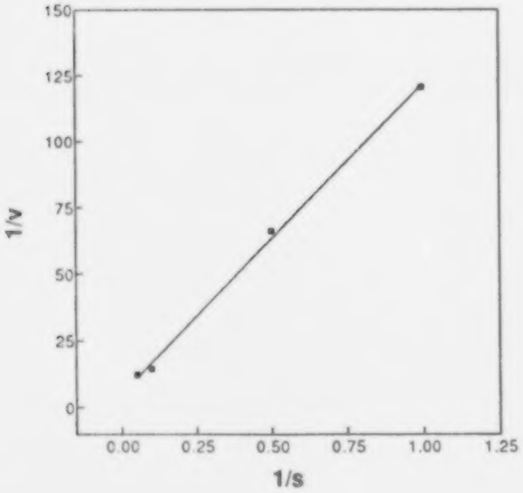
150
125
100
75
50
25
0
1/v
0.00
0.25
0.50
0.75
1.00
1.25
1/s

Figure 4.18 Comparison of ^{3}H-adenosine and ^{3}H-uridine uptake in cNT1$_{rat}$ cDNA transfected COS-1 cells

Cells were transfected with pCDNAI/Amp-cNT1$_{rat}$ and processed as described for Figure 4.2, except that dilazep (10 μM) was substituted for NBMPR. Uptake intervals (0, 6, 12 sec) were timed by metronome signals. Uptake of 10 μM ^{3}H-uridine (■) or ^{3}H-adenosine (▲) by pCDNAI/Amp-cNT1$_{rat}$-transfected COS-1 cells was determined in sodium-containing transport buffer in the presence of 10 μM dilazep. Uptake of ^{3}H-adenosine by pCDNAI/Amp (Δ) served as a control. Each value represents the mean ± SD of three dishes. Error bars are not shown where SD values were smaller than the data symbols.

In this experiment, at the time when transport assay was conducted, there were 1.07 x 10^6 cells per 60-mm dish and the transfection efficiency which was determined in parallel cultures by transfection with pCMVβ, was about 25%.

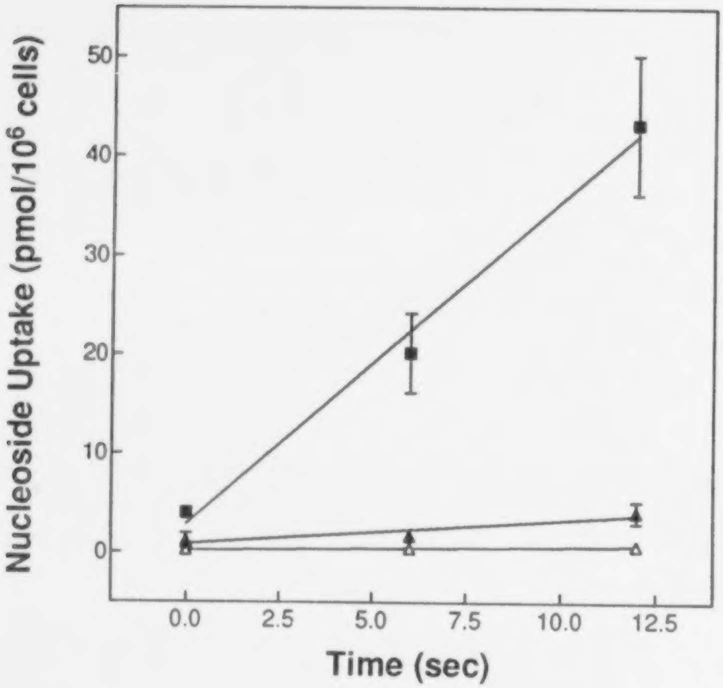
Nucleoside Uptake (pmol/10^6 cells)
50
40
30
20
10
0
0.0
2.5
5.0
7.5
10.0
12.5
Time (sec)

Figure 4.19 Inhibition of cNT1$_{rat}$-mediated uridine uptake in COS-1 cells by nucleoside drugs

Uptake assays were conducted as described in Figure 4.7. Uptake of 10 µM ^{3}H-uridine was determined in sodium-containing transport buffer in the presence of 10 µM dilazep without (control) or with competing nonradioactive nucleoside analogues (5 mM of AZT, ddC, IUdR, FUdR, araC, gemcitabine and 3TC). Each value represents the mean ± SD of three dishes. Error bars are not shown where SD values were very small.

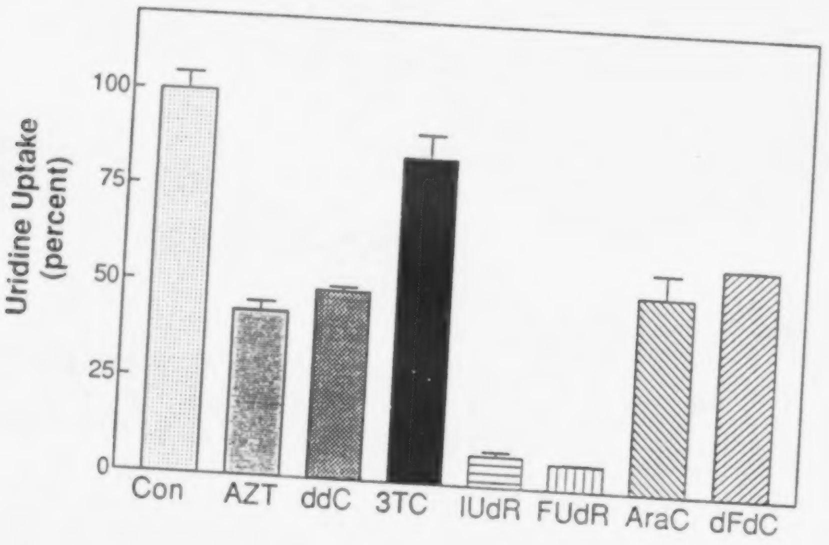
Uridine Uptake
(percent)
100
75
50
25
0
Con
AZT
ddC
3TC
IUdR
FUdR
AraC
dFdC

Figure 4.20. Concentration-effect relationships for inhibition by IUdR and FUdR of recombinant cNT1$_{rat}$-mediated uridine transport.

Cells were transfected with pCDNAI/Amp-cNT1$_{rat}$ and processed as described for Figure 4.2, except that dilazep (10 µM) was substituted for NBMPR. Uptake of 10 µM ^{3}H uridine during a 5-min incubation was determined in Na$^+$-containing buffer either without additives (control, 100%) or with various concentrations of FUdR (■) or IUdR (▲). Values are presented as a percentage of control values. Each value represents the mean ± SD of three dishes. Error bars are not shown where SD values were smaller than the data symbols.

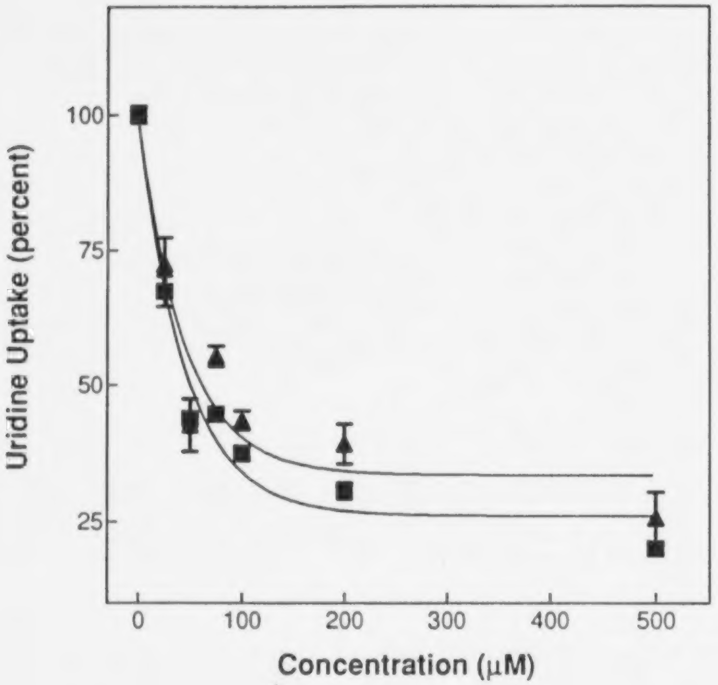
Uridine Uptake (percent)
100
75
50
25
0
100
200
300
400
500
Concentration (μM)

CHAPTER V

DISCUSSION

5.1 Discussion

Previously, the knowledge of the N2/*cit* nucleoside transport process was based on functional studies that were conducted with freshly isolated mouse intestinal epithelial cells, brush kidney border membrane vesicles of rat, rabbit and bovine kidney, and *Xenopus* oocytes microinjected with intestinal mRNA (84, 89-93). However, it has been difficult to precisely determine the functional characteristics of N2/*cit* processes, because most preparations contained more than one NT-mediated process. With the recent cloning and functional expression of $cNT1_{rat}$ cDNA in *Xenopus* oocytes (9), it became feasible to establish a mammalian expression system that exhibits only the N2/*cit* subtype for further molecular and functional analysis.

The aims of my work were to express DNA encoding $cNT1_{rat}$ in mammalian cells for use in the functional characterization of recombinant $cNT1_{rat}$ in a mammalian genetic and physiologic environment. The approach used was transient transfection of cloned $cNT1_{rat}$ cDNA into a mammalian cell line, followed by analysis of fluxes of ^{3}H-nucleosides in the transfected cells.

For transient transfection, COS-1 cells were used as the host cell line, because they are readily transfectable and usually express transfected DNAs at high levels (110). Studies conducted with nontransfected cells revealed that nucleoside transport in COS-1 cells was mediated in large part, if not completely, by an equilibrative NBMPR-sensitive (*es*) transporter. The transport of several different nucleosides was almost completely eliminated by nanomolar concentration of NBMPR, a characteristic that is diagnostic of *es*-mediated nucleoside transport. Other NT inhibitors, like dilazep and dipyridamole, also blocked nucleoside transport in COS-1 cells. Thus, COS-1 cells appeared to be suitable for expression of the $cNT1_{rat}$ cDNA since the recombinant transporter has been shown to be NBMPR-insensitive in *Xenopus* oocytes (9).

The substantial differences in ^{3}H-uridine uptake observed between COS-1 cells transfected with the cNT1$_{rat}$-containing vector and cells transfected with vector alone indicated high levels of the functional recombinant transporter. Uptake in cNT1$_{rat}$ cDNA transfected cells was transporter mediated because it was reduced to basal levels in the presence of a high concentration (1 mM) of non-radioactive uridine. The nucleoside transport activity of recombinant cNT1$_{rat}$ was shown to be sodium-dependent, since substitution of NMDG for sodium greatly reduced transport rates in cells transfected with the cNT1$_{rat}$-containing vector.

Uptake in sodium-free buffer was consistently higher for cells transfected with the cNT1$_{rat}$ vector than for cells transfected with vector alone. The residual sodium-independent transport was not eliminated by treatment of cells with high concentrations of dilazep, a compound that inhibits both *es* and *ei* NTs (22), suggesting that it had not resulted from *ei* activity; the latter is sodium-independent but sensitive to dilazep. The residual sodium-independent NT activity may have been due to uncoupled transport, or "slippage," of permeant (uridine) and the co-transported cation (sodium), as has been reported previously (9, 84, 158).

The presence of recombinant transporter protein in COS-1 cell membranes was demonstrated by western analysis of cells transfected with a cDNA construct that encoded complete cNT1$_{rat}$ with a c-*myc* epitope tag at the C-terminus. Epitope tagging to the amino or carboxyl terminus of protein has been widely used to study many recombinant proteins for which antibodies are not available. The c-*myc* epitope-tagged cNT1$_{rat}$ -containing vector was transfected into COS-1 cells and the function of epitope tagged recombinant cNT1$_{rat}$ was tested and compared with that of non-epitope tagged cNT1$_{rat}$. No substantial differences in function were detected, indicating apparently normal synthesis, processing and functioning of c-*myc*-tagged recombinant protein.

When crude membrane protein from cNT1$_{rat}$-*myc* cDNA transfected cells was subjected to 12% SDS-PAGE and protein immunoblotting, it migrated much faster than was expected, giving an apparent molecular mass (45 kDa) that was lower than that (71 kDa) predicted from the amino acid sequence of cNT1$_{rat}$. This discrepancy in the observed and predicted electrophoretic mobilities may have resulted from the high hydrophobicity of the recombinant protein, since hydropathy analysis predicted 14 transmembrane segments (9). A similar phenomenon has also been found with other membrane proteins. For example, lactose permease is a bacterial transporter protein that has a molecular mass of 46.5 kDa according to amino acid sequence and a molecular mass of 30 kDa determined by 10% SDS/PAGE (166); and the bacterial nucleoside transporter NUPG showed a molecular mass of 33 kDa on 12.5% SDS/PAGE, while its predicted molecular mass was 45 kDa (110). It is also possible that recombinant cNT1$_{rat}$-*myc* protein was partially degraded, although the proteinase inhibitor PMSF (phenylmethylsulfonyl fluoride) was present during the isolation of membrane fractions. Finally, the initiating codon of the cNT1$_{rat}$ cDNA may be further downstream than originally predicted (9).

Recombinant cNT1$_{rat}$ has been functionally produced in oocytes of *Xenopus laevis* and shown to transport a variety of pyrimidine nucleosides, including uridine thymidine and cytidine, and to be inhibited by adenosine, but not by guanosine (9, 138). The direct measurements of uptake of ^{3}H-guanosine in this study confirmed that guanosine was not a substrate of cNT1$_{rat}$. The substrate selectivity of N2/*cit*-mediated nucleoside transport processes was defined in functional studies with freshly isolated mouse intestinal epithelial cells, *Xenopus* oocytes injected with rabbit and rat intestinal mRNA and brush border membrane vesicles from renal epithelial cells of a few non-human species (84, 89-93). In these studies, uptake of ^{3}H-thymidine was strongly inhibited by cytidine, deoxycytidine, uridine, deoxyuridine, thymidine, adenosine, deoxyadenosine, but not by guanosine or inosine, leading to the conclusion that the process accepted pyrimidine nucleosides and adenosine but not other purine nucleosides. Thymidine was concluded to be a diagnostic substrate for identification of N2/*cit*-mediated processes (22). The selectivity of recombinant cNT1_{rat} when produced in COS-1 cells was consistent with that previously described for N2/cit mediated processes.

K_m values for inward transport of uridine and thymidine have been previously reported for N2/*cit* processes in rat intestinal (84), bovine, rat and rabbit renal vesicles (90-92) and human kidney brush-border membrane vesicles (96). These values are similar to the K_m values obtained in this study with cNT1_{rat} cDNA transfected COS-1 cells, indicating that recombinant cNT1_{rat} behaved like the native N2/*cit* transporter.

The kinetic studies with uridine and adenosine yielded similar K_m values but markedly different V_{max} values (uridine > adenosine) from recombinant cNT1_{rat} in COS-1 cells. The order of V_{max} values for the four nucleosides was uridine > thymidine > cytidine > adenosine, even though all four nucleosides had similar K_m values. The adenosine V_{max}/K_m ratio was only 0.008 compared with 0.65 for uridine. Therefore, it appeared that although adenosine bound with high affinity to cNT1_{rat}, it was not actually transported very well. This conclusion was confirmed in an experiment in which uptake of uridine and adenosine were measured under identical conditions in the same preparation of transfectants. Uridine fluxes were much greater than adenosine fluxes, indicating clearly that adenosine was not as good a substrate as uridine, although it was found to be a "high affinity" inhibitor of uridine transport. Permeants with similar K_m values but different V_{max} values have been observed for other transport systems (169-171). For example, the amino acid transporter from rat kidney transports L-alanine and L-methionine with similar K_m values (50 μM and 71 μM, respectively), but exhibits a V_{max} for transport of L-methionine (151 pmol per oocyte per 5 min) that is 2.7-fold higher than that of L-alanine (56 pmol per oocyte per 5 min) (169).

Direct measurements of ^{3}H-adenosine transport have been reported for N1/*cif* and N3/*cib*-mediated processes of murine leukemia L1210 cells (86, 88), rat renal brush-border membrane vesicles (172), rat hepatocytes (85) and rabbit intestinal brush-border membrane vesicles (173). However, the transport of ^{3}H-adenosine by the N2/*cit* transporter has not been measured directly in mammalian cells. The ability to block uptake does not necessarily establish that a substance is a substrate, as is evidently the case for adenosine, which exhibited inhibitory activity similar to that of uridine and thymidine in the experiments of Figure 4.18 yet was transported with a relatively low V_{max} value. A similar situation was reported (89) for tubercidin, which inhibited Na^+-dependent thymidine transport in mouse intestinal cells, but was not itself transported.

Kinetic parameters for $cNT1_{rat}$-mediated transport of uridine and adenosine have recently also been determined in *Xenopus* oocytes (138) (Table 4.2). While the absolute V_{max} values obtained for recombinant $cNT1_{rat}$ in oocytes and COS-1 cells can not be directly compared because of differences in cell size and amounts of recombinant protein, the K_m values, which represent a measure of transporter affinity, are directly comparable. The K_m values obtained in the two expression systems differed by only 2-fold for uridine and were essentially the same for adenosine, suggesting that recombinant $cNT1_{rat}$ functioned similarly in mammalian and amphibian cells. Agreements of kinetic values in *Xenopus* oocytes and in mammalian cells were also observed when the γ-aminobutyric acid transporter (89) and human glucose transporters (174) were studied in these two expression systems.

Although inhibition studies have the limitations illustrated by the contradictory results obtained with adenosine (this study) and tubercidin (89), they can be efficiently used to provide an indication of the (i) permeant selectivity of a particular transporter, and (ii) potential transportability of non-radioactive test compounds. I examined the ability of a group of clinically important nucleoside analogues to inhibit $cNT1_{rat}$-mediated uridine uptake by COS-1 cells. The most potent inhibitors were FUdR and IUdR, which are used, respectively, in the treatment of cancer and viral infections. FUdR and IUdR most closely resemble thymidine with substituents at the 5-position of the pyrimidine ring. Other nucleoside drugs (araC, gemcitabine, AZT, ddC, 3TC) were shown to be less potent inhibitors. Particularly, 3TC, which has more diverse modifications than any of the other compounds tested, exhibited little, if any, inhibition of $\mathrm{cNT1_{rat}}$-mediated nucleoside uptake.

The rank order of transportability of pyrimidine nucleosides was uridine > thymidine > cytidine, which was consistent with the strong inhibitory ability of FUdR and IUdR. Although AZT is a thymidine analogue as well, it showed less inhibitory ability, which was probably due to its sugar modifications. These possible relationships between nucleoside analogue structures and their potential transportabilities may have implications in further structure/activity studies and new drug design. It may also help develop anti-cancer and anti-viral therapeutic strategies that maximize the selective penetration of nucleoside drugs into diseased cells.

In summary, the successful production of $\mathrm{cNT1_{rat}}$ in transiently transfected COS-1 cells is the first example of expression of a cDNA encoding an NT protein in mammalian cells at levels sufficient to allow detailed kinetic analyses of tracer fluxes. It also indicated that it would be feasible to develop $\mathrm{cNT1_{rat}}$ stable transfectants in mammalian cells.

5.2 Future Work

Using the $\mathrm{cNT1_{rat}}$ expression system developed in this study, some further analysis of $\mathrm{cNT1_{rat}}$ could be done.

Cellular localization. By immunostaining $\mathrm{cNT1_{rat}}$ cDNA transfected mammalian cells with anti-$\mathrm{cNT1_{rat}}$ antibodies, the cellular and subcellular localizations of the recombinant protein could be determined. While NTs are clearly present in plasma membranes, it would be interesting to see if $\mathrm{cNT1_{rat}}$ is in any subcellular organelles. For example, many nucleoside analogue drugs have been found to have mitochondrial toxicity. Immunostaining of cDNA-transfected cells has been widely used to identify the cellular location of an expressed protein. For example, when expressed in CHO cells, the glucose transporter isoform GLUT3 is detected on cell surface by immunostaining (122).

Topology. Using antibodies directed against epitopes present at either the N-or C-terminus of $cNT1_{rat}$, the orientation of the N- or C-terminus could be determined. They are predicted to be located in the cytoplasm (9, 138). If so, reactivity of antibodies with cells transfected with $cNT1_{rat}$ cDNA would be observed only after permeabilization, for example by treatment with the detergent. Additionally, more detailed transmembrane topology of $cNT1_{rat}$ could be determined by introducing an epitope tag into each of the predicted linker regions. The cDNA constructs could be expressed transiently in COS-1 cells, and the location of epitopes could be demonstrated by immunocytochemical staining. This strategy was successfully used to determine the topology of rhodopsin by insertion of a 12-amino acid c-*myc* epitope into various regions of the protein (175).

Residues involved in substrate selectivity. $cNT1_{rat}$ and SPNT are both sodium/nucleoside cotransporters, and , although they are 64% identical in amino acid sequences, they have different substrate specificities. A number of amino acid stretches in the transmembrane regions differ between the two proteins and thus, may be responsible for different substrate specificities. Several regions of $cNT1_{rat}$ share significant identity with SPNT and NUPC. These conserved regions may be responsible for nucleoside transport function, which is the common characteristic shared by the three proteins. These hypothetical predictions could be examined by constructing various functional chimeras between the different portions of the three proteins and or by site mutagenesis of some critical amino acid residues. Since COS-1 cells were shown to be able to rapidly and successfully express "native" recombinant $cNT1_{rat}$ in this study, they could be employed to express chimeras and mutants. Functional characterization could be readily conducted in transiently transfected cells. All such studies should include protein immunoblotting analysis of membrane fractions to establish the presence or absence of recombinant protein.

Regulation of cNT1$_{rat}$ activity: Using the cNT1$_{rat}$-transfectant as a model, the effects of two kinds of pharmacologic agents could be assessed. Reagents that activate or inhibit regulatory pathways could be used to determine if protein kinases and phosphatases are involved in regulation of cNT1$_{rat}$ activity. The predicted amino acid sequence of cNT1$_{rat}$ has several consensus protein kinase C phosphorylation sites, suggesting that cNT1$_{rat}$ activity may be regulated by protein kinase C. It has been reported that *in vivo* the sensitivity to inhibition by ethanol of adenosine uptake of the *es* NT can be altered by activation of cAMP-dependent kinase (176).

Cytotoxicities and transportabilities of some nucleoside drugs. Studies in this thesis showed that some important anticancer and antiviral nucleoside drugs were able to inhibit ^{3}H-uridine uptake by cNT1$_{rat}$. To confirm their transportabilities, uptake can be directly measured in cNT1$_{rat}$ cDNA transfected cells when these drugs are radiolabeled, and their kinetic values can be characterized. In addition, the cytotoxicities of these drugs can be assessed in cNT1$_{rat}$ cDNA transfected cells. Ideally, stable transfectants should be used due to the requirement of long-time treatment.

APPENDIX

STABLE EXPRESSION OF cNT1$_{rat}$ IN CHO-K1 CELLS

A.1 Overview

The studies described in chapter 4 demonstrated that it was feasible to produce functional recombinant cNT1_{rat} in transiently transfected mammalian cells. The objective of the work described in this chapter was to establish a stably transfected cell line that produced cNT1_{rat}. The approach to establish such a cell line was stable transfection of cloned transporter cDNA into NT defective cells or into cells whose endogenous nucleoside transport activity could be eliminated with transport inhibitors. Although COS-1 cells met the latter condition, they were not suitable for stable transfection, because they have the SV40 large T antigen. pCDNAI/Amp-cNT1_{rat}, which contains the SV40 origin of replication, would replicate episomally, eventually killing the host cells.

CHO-K1 cells are commonly used as recipients for stable transfection (110). Previous studies (97) showed that the uptake of a purine nucleoside (formycin B) by CHO-K1 cells was the same in sodium-containing and sodium-free buffer, and that uptake was inhibited almost completely by 10 μM dipyridamole. The results suggested that nucleoside transport in CHO-K1 cells is mediated by a sodium-independent, dipyridamole-sensitive process of either the *es*- or *ei* subtype. Thus, CHO-K1 cells seemed to be suitable to express NBMPR-insensitive NTs, like cNT1_{rat}, because the endogenous nucleoside transport activity could be eliminated by NT inhibitors.

The strategy to select cNT1_{rat} transfectants was based on geneticin, an antibiotic drug, which is toxic to mammalian cells (110). Integration of a geneticin resistance gene into the host cells' genome, if also functionally expressed, can confer resistance to geneticin, allowing selection of stable transfectants (110). The vector (pCDNAI/Amp) which contained cNT1_{rat} cDNA did not itself have a geneticin resistance gene. However, since cotransfection of a resistance plasmid with a plasmid of interest will frequently produce cells stably tranfected with both plasmids (111), cotransfection was used. The cNT1_{rat} plasmid was cotransfected with a plasmid with a geneticin resistance gene at a molar ratio of about 20:1. Thus, cells that survived prolonged exposures to the geneticin selection medium should have integrated the geneticin resistant gene, as well as cNT1$_{rat}$ cDNA, into their genome. The functional expression of cNT1$_{rat}$ cDNA in these cells was then examined by nucleoside uptake assays.

Using this strategy, a stable transfectant of cNT1$_{rat}$ was isolated, and its nucleoside transport actvity was investigated in sodium-containing and sodium-free buffer, with nontransfected CHO-K1 cells as a control.

A.2 Isolation of Stable Transfectants Producing cNT1$_{rat}$

In the experiment of Figure A.1, 10 μM ^{3}H-uridine uptake by CHO cells was used as a control (100%). Addition of 1 mM nonradioactive uridine to the uptake assay reduced uptake rate of ^{3}H-uridine to 3% of the control value, whereas addition of either 10 μM NBMPR or dilazep reduced uptake to 8% or 6% of control value, respectively. These results indicated, since the endogenous nucleoside transport activity could be reduced to near basal levels by inhibitors of both *es* and *ei*-mediated transport, that uridine transport in CHO-K1 cells was mostly *es*-mediated. Since the residual nucleoside transport activity in the presence of the inhibitors was small and probably could be ignored, CHO-K1 cells were chosen as recipients for stable transfection with the cNT1$_{rat}$ construct. Dilazep was used to inhibit endogenous nucleoside transport activity in CHO-K1 cells during uptake assays.

pCDNAI/Amp-cNT1$_{rat}$ (containing cNT1$_{rat}$ sequence) and pSV2neo (containing the geneticin resistant gene) were cotransfected at a molar ratio of about 20:1 into CHO-K1 cells by the calcium-phosphate method. Forty-eight hours after the transfection, geneticin (400 μg/ml) was added to the growth medium to select stable transfectants. Cells selected for expression of the geneticin-resistant gene (pSV2neo) were expected to also have incorporated pCDNAI/Amp-cNT1$_{rat}$ into their genomes. Seven colonies were isolated randomly from the 25 colonies that had survived in the geneticin-containing medium. The seven colonies were then expanded and screened for expression of the $cNT1_{rat}$ cDNA by a functional assay that compared uptake of ^{3}H-uridine by transfectants with that of nontransfected cell.

In the experiment of Figure A.2, uptake of 10 µM ^{3}H-uridine by nontransfected CHO-K1 cells (control) was 9.3 pmol/10^6 cells. The uptake values of the seven transfected clones varied between 8.65 pmol/10^6 cells and 23.2 pmol/10^6 cells. Three clones (A, E, G) of the seven appeared to be transfectants that expressed the $cNT1_{rat}$ cDNA. Because Clone A showed the highest uptake level, it was selected for further sutdy.

In order to demonstrate the integration of the $cNT1_{rat}$ cDNA into the host cell genome, DNA was isolated from clone A (hereafter designated CHO-K1/$cNT1_{rat}$) cells or nontransfected CHO-K1 cells. PCR amplification was performed using the genomic DNA as a template and a pair of primers. They were 5'-ATG GCA GAC AAC ACA CAG-3' (5'-primer) and 5'-GAA CAC ACA GAT CCC TGC-3' (3'-primer), which corresponded to nucleotides 157-174 and 2097-2122 of $cNT1_{rat}$ cDNA. If the $cNT1_{rat}$ cDNA was integrated into the host cell genome, a 2 Kb PCR product should be detected. As shown in Figure A.3, the expected PCR product were amplified from the genomic DNA of CHO-K1/$cNT1_{rat}$ in lane S, but not in the sample from the nontransfected CHO-K1 cells in lane C. These results indicated integration of the $cNT1_{rat}$ cDNA in the genome of the stable transfectant. There were two extra bands in lane S, which might have been due to non-specific priming.

To further characterize the transport characteristics of CHO-K1/$cNT1_{rat}$ cells, uptake of 10 µM ^{3}H-uridine was measured in sodium-containing or sodium-free buffer to determine if the transfectants had acquired a sodium-dependent process (Figure A.4). Dilazep was used to inhibit endogenous NT activity of CHO-K1 cells. The 30-min time courses were linear, and the ratio of uptake in sodium-containing buffer to that in sodium free buffer was 2.6 to 1. Therefore, the $cNT1_{rat}$ stable transfectant exhibited sodium-dependent uptake of uridine, indicating the presence of functional recombinant $cNT1_{rat}$ in the transfectant cells. Uptake of uridine in the sodium-free buffer by CHO-K1/$cNT1_{rat}$ cells was higher than uptake by CHO-K1 cells. This small difference, which was also observed in $cNT1_{rat}$-transfected COS-1 cells (Chapter 4, Section 4.3), may represent slippage by the sodium-linked system.

The results of Figure A.4 also suggested that CHO-K1 cells possessed low levels of endogenous sodium-dependent nucleoside transport activity. When the uptake of 10 μM ^{3}H-uridine by nontransfected cells was measured in the presence of 10 μM dilazep, it was consistently lower in sodium-free buffer than in sodium-containing buffer. This endogenous activity gave a small but significant background when CHO-K1 cells served as controls in $cNT1_{rat}$ stable expression experiments.

A.3 Summary

In this chapter, $cNT1_{rat}$ cDNA was stably transfected into CHO-K1 cells. One clone, which showed the highest ^{3}H-uridine uptake activity, was chosen for further characterization. PCR amplification of genomic DNA of this clone indicated chromosomal integration of $cNT1_{rat}$. The nucleoside transport activity of the clone was sodium-dependent, as had been observed in transiently transfected COS-1 cells and *Xenopus* oocytes. However, the $cNT1_{rat}$ activity observed in the stable CHO-K1 transfectants was much lower than that observed in the transient COS-1 transfectants. The ^{3}H-uridine uptake rate in transient COS-1 cells was 50-fold higher than that in CHO-K1 stable transfectants. A lower expression level in stable transfectants than in transient COS-1 transfectants has been observed for other recombinant proteins (177, 178). The most likely explanation was that the $cNT1_{rat}$ containing plasmid could not replicate episomally in CHO-K1 cells, which lack the large T antigen, required for episomal replication. It is also possible that the expression level was influenced by the chromosomal elements that surrounded the integrated cDNA.

Because of the relatively low expression level in the stable transfectants, it was important to completely eliminate the endogenous nucleoside transport activity of recipients. Results of previous studies of CHO cells (97) indicated an absence of sodium-dependent, concentrative nucleoside transport. However, the results of the experiment of Figure A.1 demonstrated that dilazep inhibited 94% of ^{3}H-uridine uptake, whereas 1 mM nonradioactive uridine inhibited 97% of ^{3}H-uridine uptake. Thus, even in the presence of 10 μM dilazep, the nucleoside transport activity was consistently higher than the basal level. This tiny difference may indicate the presence in CHO-K1 cells of a small component of endogenous concentrative NT activity, since nanomolar concentrations of dilazep completely inhibit equilibrative NT activity (*es* and *ei*) (22). The difference observed in the uptake of uridine in CHO-K1 cells in sodium-containing or sodium-free buffer was consistent with this conclusion. In CHO-K1 cells, the uptake level was reduced in sodium-free buffer when compared to that in sodium-containing buffer, suggesting that there might be a small component sodium-dependent NT activity. This NT inhibitor-insensitive activity would be expected to give a small but significant background level of transport when CHO-K1 cells were used as recipients for cNT1$_{rat}$ cDNA stable expression.

Previous studies (97) showed that the uptake of formycin B by CHO-K1 cells was about the same in sodium-containing and sodium-free buffer. This observation led to the conclusion that no significant sodium-dependent, concentrative nucleoside transport was detectable in CHO-K1 cells. However, formycin B is a diagnostic substrate of N1/*cif* processes and is not a substrate of N2/*cit* processes (22). Therefore, if sodium-dependent N2/*cit* activity is present in CHO-K1 cells, it could not have been detected in experiments that used formycin B as the tracer nucleoside.

Further studies need to be carried out to confirm the presence of sodium-dependent NT activity in CHO-K1 cells and to determine to which NT subtype it belongs. When the NT processes in CHO-K1 cells are well characterized, isolation of NT-deficient mutant of CHO-K1 cells could be attempted. Cells would be treated with a frameshift mutagen, and selected by exposure to cytotoxic nucleoside analogues whose uptake is largely dependent on the NT (5, 153). By this strategy, NT-deficient mutant could be isolated because only cells lacking NTs could survive in the selection medium. The resulting NT-deficient cell line would be useful for stable expression of other members of cNT family in the future. Recently, a stable transfectant of cNT1rat has been successfully obtained in NT-deficient mouse leukemia L1210 cells in the laboratory of Dr. J.A. Belt (St. Jude Children"s Research Hospital, Memphis, TN). Transport assays conducted with these transfectants showed that (i) they exhibited nucleoside transport activity, (ii) the transport activity was sodium-dependent and (iii) thymidine uptake was inhibited by uridine, cytidine and adenosine.[1]

---

[1] Crawford, C.R., Cass, C.E, Young, J.D. and Belt, J.A., unpublished results.

Figure A.1 Inhibition of endogenous uridine transport in CHO-K1 cells by NBMPR and dilazep

Actively proliferating CHO-K1 cells were plated and grown to about 1 x 10^6 cells/60-mm dish for assay of uridine transport as described in Materials and Methods (Section 2.12). Uptake of 10 μM ^{3}H-uridine was determined in sodium-containing transport buffer in the absence (◆) or in the presence of either 10 μM NBMPR (▼), 10 μM dilazep (■) or 1 mM nonradioactive uridine (▲). Each value represents the mean ± SD of three dishes. Error bars are not shown where SD values were smaller than the data symbols.

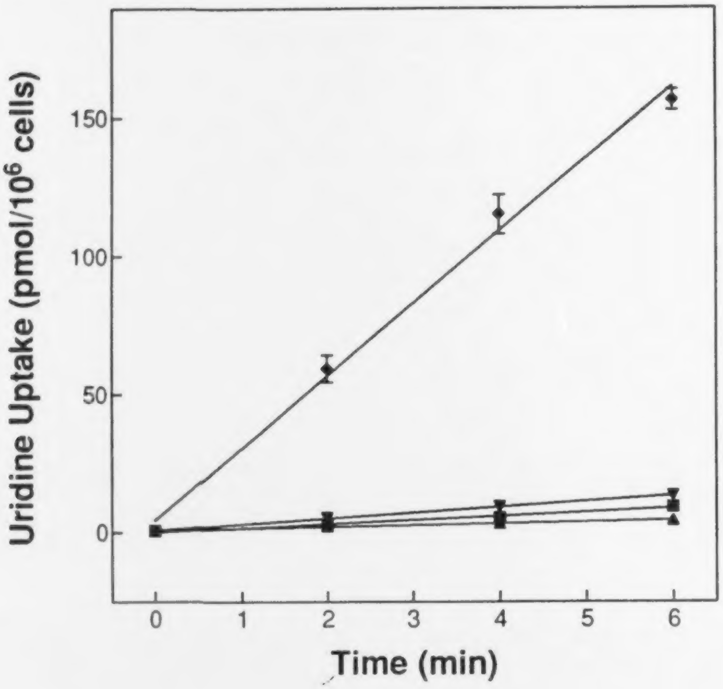
Uridine Uptake (pmol/10^6 cells)
150
100
50
0
0
1
2
3
4
5
6
Time (min)

Figure A.2 Nucleoside uptake by geneticin-resistant stable transfectants

Geneticin-resistant colonies were isolated and expanded to about 1 x 10^6 cells/60-mm dish (three dishes each colony). The uptake of 10 μM ^{3}H-uridine was determined in sodium-containing transport buffer in the presence of 10 μM dilazep over 15 min. Nontransfected CHO-K1 cells served as a control for determination of basal uptake in dilazep-inhibited transfectants (A, B, C, D, E, F, G). Each value represents the mean ± SD of three dishes.

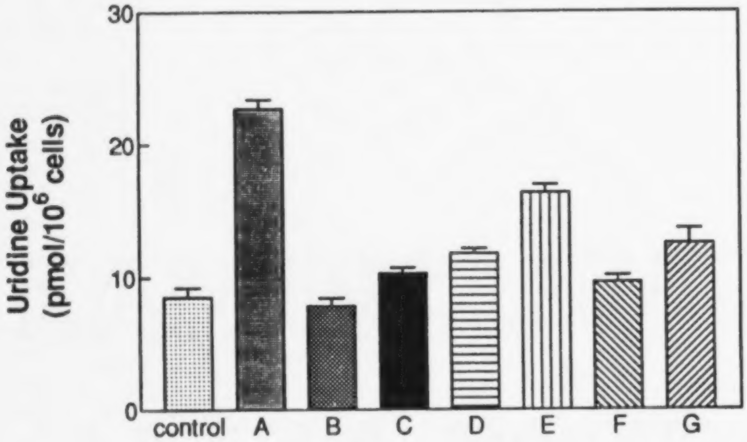

Uridine Uptake
(pmol/10^6 cells)
30
20
10
0
control
A
B
C
D
E
F
G

Figure A.3 Demonstration of integration of cNT1$_{rat}$ cDNA into genomic DNA of CHO-K1/cNT1$_{rat}$ by PCR amplification

Genomic DNA from CHO-K1/cNT1$_{rat}$ or nontransfected CHO-K1 cells was isolated as follows. Briefly, cells were trypsinized from culture dishes, subjected to centrifugation (100x g, 5 min, 4°C) and washed twice with PBS. The cell pellet was resuspended in lysis buffer (1 M Tris-Cl, pH7.8, 10% nonidet P40 (v/v), 1 M dithiothreitol). The DNA was amplified by PCR, using a pair of primers that corresponded to nucleotides 157-174 and 2097-2122 of cNT1$_{rat}$ (5'-ATG GCA GAC AAC ACA CAG-3' (5'-primer) and 5'-GAA CAC ACA GAT CCC TGC-3' (3'-primer)). A 30 µl-portion of PCR product was then used as template and amplified by second round PCR. A 10 µl-portion of second round PCR product was analyzed on a 0.8% agarose gel by electrophoresis and visualized by a UV light box. λ DNA/Hind III marker (23, 9.4, 6.6, 4.4, 2.3, 2.0 Kb; from the top to the bottom) was on lane M. The PCR products of CHO-K1/cNT1$_{rat}$ and nontransfected CHO-K1 cells were loaded on lane S and lane C, respectively.

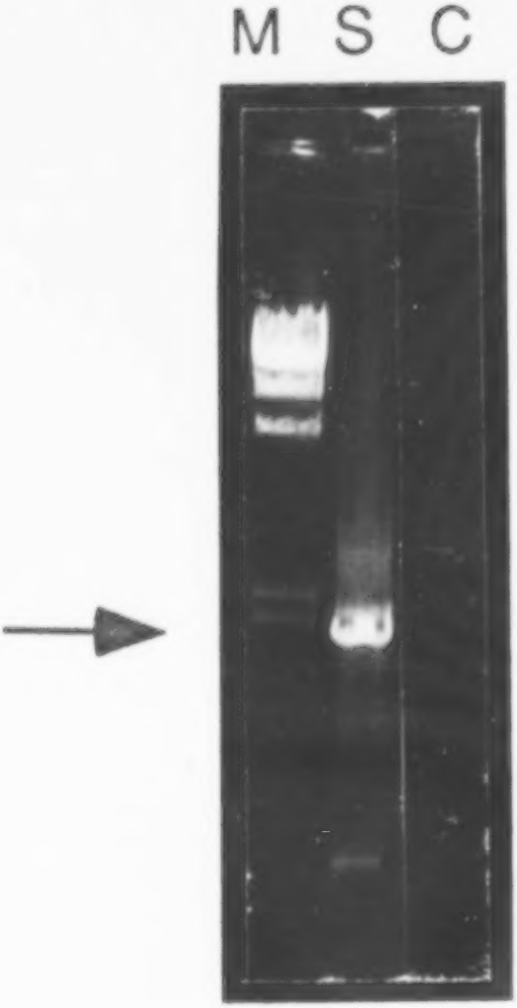
M
S
C

Figure A.4 Uridine uptake by nontransfected CHO-K1 cells and CHO-K1/cNT1$_{rat}$ cells in sodium-containing or sodium-free buffer

CHO-K1/cNT1$_{rat}$ cells (■, □) or CHO-K1 cells (▼, ▽) were grown to about 1 x 10^6 cells/60-mm dish. Uptake of 10 μM ^{3}H-uridine was measured in sodium-containing transport buffer (■, ▼) or sodium-free transport buffer (□, ▽), with 10 μM dilazep. Cells were incubated with 10 μM dilazep at RT for 30 min before the uptake assay. Uptake assays were started by adding 1.5 ml of transport buffer containing 10 μM ^{3}H-uridine and 10 μM dilazep, ended by aspirating the permeant solution and immediately washing the dishes by immersion in 1.5 liter of ice-cold transport buffer. Uptake at time zero was determined by placing dishes on ice for 10 min prior to transport assay and by using ice-cold permeant solution. The cells were solubilized in 5% (v/v) Triton X-100 and combined with EcoLite scintillint for radioactivity measurement. Each value represents the mean ± SD of three dishes. Error bars are not shown where SD values were small.

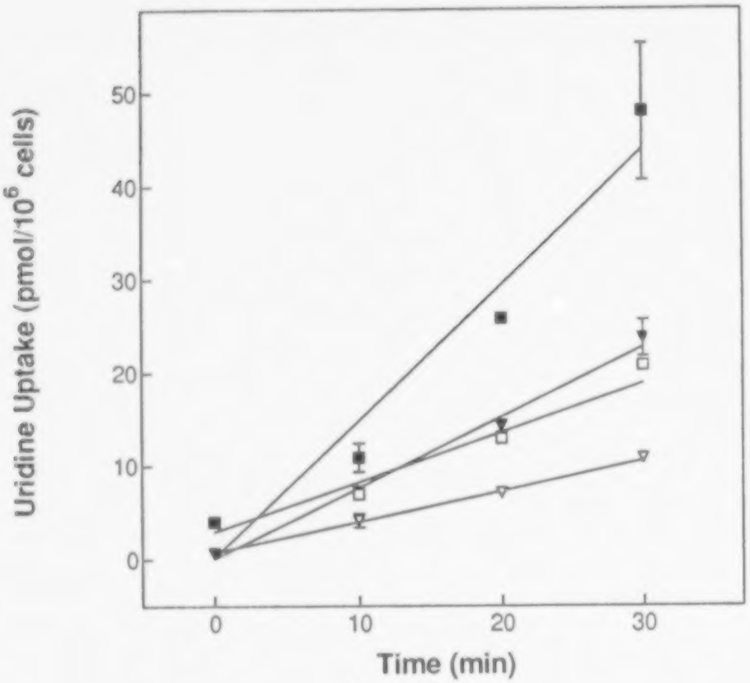
Uridine Uptake (pmol/10^6 cells)
50
40
30
20
10
0
0
10
20
30
Time (min)

BIBLIOGRAPHY

1. Cohen, A., Ullman, B. and Martin, D.W. (1979). Characterization of a mutant mouse lymphoma cell with deficient transport of purine and pyrimidine nucleosides. *J. Biol. Chem.* **254**, 112-116
2. Cass, C.E., Kolassa N, and Uehara, Y., *et al* (1981). Absence of binding sites for the transport inhibitor nitrobenzylthioinosine on nucleoside transport deficient mouse lymphoma cells. *Biochim. Biophys. Acta.* **649**, 769-777
3. Cohen, A., Leung, C. and Thompson, E. (1985). Characterization of mouse lymphoma cells with altered nucleoside transport. *J. Cell. Physiol.* **123**, 431-434
4. Sobrero, A.R., Moir, R.D., Bertino, J.R., *et al.* (1985). Defective facilitated diffusion of nucleosides, a primary mechanism of resistance to 5-fluoro-2'-deoxyuridine in the HCT-8 human carcinoma line. *Cancer. Res.* **45**, 3155-360
5. Vijayalakshmi, D., Dagnino, L., Belt, J.A., *et al.* (1992). L210/B23.1 Cells express equilibrative inhibitor-tensitive nucleoside transport activity and lack two parental nucleoside transport activities. *J. Biol. Chem.* **267**, 16951-16956
6. Warnick, C.T., Muzik, H. and Paterson, A.R.P. (1972). Interference with nucleoside transport in mouse lymphoma cells proliferating in culture. *Cancer Res.* **32**, 2017-2022
7. Paterson, A.R.P., Yang, S., Lau, E.Y. and Cass, C.E. (1979). Low specificity of the nucleoside transport mechanism of RPMI 6410 cells. *Mol. Pharmacol.* **16**, 900-908
8. Cass, C.E., King K.M., Montano, J.T., *et al.* (1992). A comparison of the abilities of nitrobenzylthioinosine, dilazep, and dipyridamole to protect human hematopoietic cells from 7-deazaadenosine (tubercidin). *Cancer Res.* **52**, 5879-5886

9. Huang, Q.Q., Yao, S.Y.M., Ritzel, M.W.L., Paterson, A.R.P., Cass, C.E. and Young, J.D. (1994) Cloning and functional expression of a complementary DNA encoding a mammalian nucleoside transport protein. *J. Biol. Chem.* **269,** 17757-17760

10. Boss, G. R. and Seegmiller, J.E. (1982). Genetic defects in human purine and pyrimidine metabolism. *Annu. Rev. Genet.* **16**, 297-382

11. Bhalla, K., Nayak, R. and Grant, S. (1984). Isolation and characterization of a deoxycytidine kinase-deficient human promyelocytic leukemic cell line highly resistant to 1-β-D-arabinofuranosylcytosine. *Cancer Res.* **44**, 5029-5037

12. Barlow, S.D. and Ord, M.G. (1975). Thymidine transport in phytohaemagglutinin-stimulated pig lymphocytes. *Biochem. J.* **148,** 295-302

13. Ullman, B. (1989). Adenosine, deoxyadenosine, and deoxyguanosine. In: *Drug resistance in mammalian cells*. (ed Gupta RS) Boca Raton, Fl: CRC Press. pp.69-88

14. Olah, M.E. and Stiles, G.L. (1995). Adenosine receptor subtypes: characterization and therapeutic regulation. *Annu. Rev. Pharmacol. Toxicol.* **35**, 581-606

15. Newby, A.C. (1984). Adenosine and the concept of "retaliatory metabolites". *Trends. Biochem. Sci.* **9**, 42-44

16. Morris, N.R., Reichard, P. and Fischer, G.A. (1963). Studies concerning the inhibition of cellular reproduction by deoxyribonucleotides. Inhibition of the synthesis of dexycytidine by thymidine, deoxyadenosine and deoxyguanosine. *Biochim. Biophys. Acta.* **68,** 93-99

17. Maley, F., and Maley, G.F. (1962). On the mature of a sparing effect by thymine on the utilization of deoxycytidine. *Biochemistry* **1,** 847-851

18. Peterson, A.R., Landolph, J.R., Peterson, H. and Heidelberger, C. (1978). Mutagenesis of Chinese hamster cells facilitated by thymidine and deoxycytidine. *Nature (Lond.)* **276**, 508-510

19. Neuth, M. (1981). Role of deoxynucleoside triphosphate pools in the cytotoxic and mutagenic effects of DNA alkylating agents. *Somat. Cell Genet.* **7**, 89-102

20. Bradley, M.O. and Sharkey, N.A. (1978). Mutagenicity of thymidine to cultured Chinese hamster cells. *Nature (Lond.)* **274,** 607-608

21. O'Dwyer, P.F., King, S.A., Hoth, D.F. and Leyland-Jones, B. (1987). Role of thymidine in biochemical modulation: A review. *Cancer Res.* **47**, 3911-3919

22. Cass, C.E. (1994). Nucleoside transport. In *Drug transport in antimicrobial and anticancer chemotherapy.* (ed Georgopapadakou, N.H.), Marcel Dekker Inc. pp.403-452

23. Perigaud, C., Gosselin, G. and Imbach, J.L. (1992). Nucleoside analogues as chemotherapeutic agents: A review. *Nucleosides and Nucleotides.* **11**, 903-945

24. Clumeck, N. (1993). Current use of anti-HIV drugs in AIDS. *J. Antimicrob. Chemother.* **32**, suppl. A. 133-138

25. Mitsuya, H., Weinhold, K.J., Furman, P.A., St. Clair, M.H., Nusinoff-Lehrman, S., Gallo, R.C., Bolognesi, D., Barry, D.W., and Broder, S. (1985). 3'-Azido-3'deoxythymidine: an antiviral agent that inhibits the infectivity and cytopathic effect of human T-lymphotropic virus type III/lymphadenopathy-associated virus in vitro. *Proc. Natl. Acad. Sci. USA.* **82**, 7096-7100

26. Herdewijn, P. and De Clercq, E. (1990). in *Design of anti-AIDS drugs.* (ed De Clercq, E.) Elsevier: Amsterdam. Vol, 14, pp.141-174

27. Sarin, P.S. (1988). Molecular pharmacologic approaches to the treatment of AIDS. *Ann. Rev. Pharmacol.* **28**, 411-428

28. Broder, S. (1988). in *Human Retrovirus, cancer and AIDS: Approaches to prevention and therapy.* (ed Bolognes, D.) Liss, A.R.: New York Vol. 71, pp. 365-380

29. De Clercq, E. (1987). Perspectives for the chemotherapy of AIDS *Anticancer. Res.* **7**, 1023-1038

30. Richman, D.D. (1990). Susceptibility to nucleoside analogues of zidovudine-resistant isolates of human immunodeficiency virus. *Am. J. Med.* **88**, 8S-10S

31. Larder, B.A., Darby, G. and Richman, D.D. (1989). HIV with reduced sensitivity to zidovudine (AZT) isolated during prolonged therapy. *Science* **243**, 1731-1734

32. Shelton, M.J., O'Donnell, A.M. and Morse, G.D. (1993). Zalcitabine. Annals of Pharmacotherapy. **27**, 480-489

33. Schinazei, R.F., McMillan, A., Cannon, D., Mathis, R., Lloyd, R.M., Peck, A., Sommadossi, J.P., St. Clair, M., Wilson, J., Furman, P.A., Painter, G., Choi, W.B. and Liotta, D.C. (1992). Pharmacokinetics and metabolism of racemic 2', 3'-dieoxy-5-fluoro-3'-thiacytidine in rhesus monkeys. *Antimicrob. Agen Chemother.***36**, 2432-2438

34. Coates, J.A., Cammack, N., Jenkinson, H.J., Mutton, I.M., Pearson, B.A., Storer, R., Cameron, J.M. and Penn, C.R. (1992). The separated enantiomers of 2'-deoxy-3'-thiacytidine (BCH 189) both inhibit human immunodeficiency virus replication *in vitro. Antimicrob. Agents. Chemother.* **36**, 202-20

35. Chang, C.N., Skalski, V., Zhou, J.H. and Cheng, Y.C. (1993). Biochemical pharmacology of (+)- and (-)-2', 3'-dideoxy-3'-thiacytidine as anti-hepatitis B virus agents. *J. Biol. Chem.* **267,** 22414-22420

36. Tisdale, M., Kemp, S.D., Parry, N.R. and Larder, B.A. (1993). Rapid in vitro selection of human immunodeficiency virus type 1 resistant to 3'-thiacytidine

inhibitors due to a mutation in the YMDD region of reverse transcriptase. *Proc. Natl. Acad. Sci. USA*. **90**, 5653-5656

37. Shannon, W.M. (1984). in *Antiviral agents and viral diseases of man*. (ed Galasso, G.J.) Raven Press: New York pp.55-121

38. Robins, R.K. and Revenkar, G.R. (1987). in *Antiviral drug development. A multidisciplinary approach* (ed De Clercq, E. and Walker, R.T.) Nato advanced institutes series, series A: Life Sciences Plenum Press: New York Vol. 143 pp. 11-36

39. Black, D.J. and Livingston, R.B. (1990). Antineoplastic drugs in 1990. *Drugs*. **39**, 489-501

40. Schrecker, A.W. (1970). Metabolism of 1-β-D-arabinofuranosylcytosine in leukemia L1210: nucleoside and nucleotide kinases in cell-free extracts. *Cancer Res*. **30**, 632-641

41. Cheng, Y.C. and Capizzi, R.L. (1982). Enzymology of cytosine arabinoside. *Med. Pediatr. Oncol*., Suppl. **1**, 27-31

42. Furth, J.J. and Cohen, S.S. (1968). Inhibition of mammalian DNA polymerase by the 5'-triphosphate of 1-β-D-arabinofuranosylcytosine and 5'-triphosphate of 1-β-D-arabinofuranosylcytosine. *Cancer Res*. **28**, 2061-2067

43. Graham, F.L. and Whitmore, G.P. (1970). Studies in mouse L-cells on the incorporation of 1-β-D-arabinofuranosylcytosine into DNA and on inhibition of DNA polymerase by 1-β-D-arabinofuranosylcytosine 5'-triphosphate. *Cancer Res*. **30**, 2636-2644

44. Zahn, R., Muller, W., Foster, W., Maidhof, A. and Beyer, R. (1972). Action of 1-β-D-arabinofuranosylcytosine on mammalian tumor cells: incorporation into DNA. *Eur. J. Cancer* **8**, 391-396

45. Plagemann, P.G.W., Marz, R. and Wohlhueter, R.M. (1978). Transport and metabolism of deoxycytidine and 1-β-D-arabinofuranosylcytosine into cultured Novikoff rat hepatoma cells, relationship to phosphorylation, and regulation of triphosphate synthesis. *Cancer Res.* **38**, 978-989

46. Harris, A.W., Reynolds, E.C. and Finch, L.R. (1979). Effect of thymidine on the sensitivity of cultured mouse tumor cells to 1-β-D-arabinofuranosylcytosine. *Cancer Res.* **39**, 538-541

47. Kinahan, J.J., Kowal, E.P. and Grindey, G.B. (1981). Biochemical and antitumor effects of the combination of thymidine and 1-β-D-arabinofuranosylcytosine against leukemia L1210. *Cancer Res.* **41**, 445-451

48. Haperen, V.W.T.R., Veerman, G., Eriksson, S., Boven, E., Stegmann, A.P.A., Hermsen, M., Vermorken, J.B., Pinedo, H.M. and Peters, G.J. (1994). Development and molecular characterization of a 2', 2'-difluorodeoxycytidine-resistant variant of the human ovarian carcinoma cell line A2780. *Cancer. Res.* **54**, 4138-4143

49. Lund, S., Kristjansen, P.E.G. and Hansen, H.H. (1993) Clinical and preclinical activity of 2', 2'-difluorodeoxycytidine (gemcitabine) *Cancer Treat. Rev.* **19**, 45-55

50. Heidelberger, C., Danenberg, P.V. and Moran, R.G. (1983). in *Advances in Enzym and related areas of molecular biology.* (ed Meister, A.) Wiley, J.:New York. Vol. 54, pp. 57-119

51. Belt, J.A., Marina, N.M., Phelps, D.A., *et al.* (1993). Nucleoside transport in normal and neoplastic cells. *Adv. Enzyme. Regul.* **33**, 235-252

52. Paterson, A.R.P., Clanachan, A.S., Craik, J.D., Gati, W.P., Jakobs, E.S., Wiley, J.S., and Cass, C.E. (1991). in *Role of adenosine and adenine nucleotides in biological systems* (Imai, S., and Nakazawa, M., eds) Elsevier Science

Publishers BV, Amsterdam pp. 133-148,

53. Kwong, F.Y.P., Fincham, H.E., Davies, A. Beaumont, N., Henderson, P.J.F., Young, J.D., and Baldwin, S.A. (1992). Mammalian nitrobenzylthioinosine-sensitive nucleoside transport proteins. Immunological evidence that transporters differing in size and inhibitor specificity share sequence homology. *J.Biol.Chem.* **267**, 21954-21960

54. Kwong, F.Y.P., Wu, J.S.R., Shi, M.M., Fincham, H.E., Davies, A., Henderson, P.J.F., Baldwin, S.A. and Young, J.D. (1993). Enzymic cleavage as a probe of the molecular structures of mammalian equilibrative nucleoside transporters. *J.Biol.Chem.* **268,** 22127-22134

55. Dahlig-Harley, E., Y. Eilam, Paterson, A.R.P. and Cass, C.E. (1981). Binding of nitrobenzylthioinosine to high-affinity sites on the nucleoside transprot mechanism of HeLa cells. *Biochem. J.* **200,** 295-305

56. Belt, J.A. (1983). Heterogeneity of nucleoside transprot in mammalian cells. Two types of transport activity in L1210 and other cultured neoplastic cells. *Mol. Pharmacol.* **24,** 479-484

57. Belt, J.A. (1983). Nitrobenzylthioinosine-insensitive uridine transport in human lymphoblastoid and murine leukemia cells. *Biochem. Biophys. Res. Commun.* **110**, 417-423

58. Belt, J.A. and L.D. Noel. (1985). Nucleoside transport in Walker 256 rat carcinosarcoma and S49 mouse lymphoma cells. *Biochem. J.* **232**, 681-688

59. Plagemann, P.G.W. and R.M. Wohlhueter. (1985). Nitrobenzylthioinosine-sensitive and -resistant nucleoside transport in normal and trasformed rat cells. *Biochim. Biophys. Acta.* **816,** 387-395

60. Jarvis, S.M. and J.D. Young. (1986). Nucleoside transport in rat erythrocytes: two components with differences in sensitivity to inhibition by

nitrobenzylthioinosine and p-chloromercuriphenyl sulfonate. *J. Membr. Biol.* **93**, 1-10

61. Crawford, C.R., Ng, C.Y.C., Noel, D., Belt, J.A. (1990). Nucleoside transport in L1210 murine leukemia cells. *J. Biol. Chem.* **256**, 9732-9736

62. Wu, J.R., Jarvis, S.M. and Young, J.D. (1983). The human erythrocyte nucleoside and glucose transporters are both band 4.5 membrane polypeptides. *Biochem. J.* **214**, 995-997

63. Harley, E.R., Cass, C.E. and Paterson, A.R.P. (1982). Initial rate kinetics of the transport of adenosine and 4-amino-7-(β-D-ribofuranosyl)pyrrolo-[2,3-d]pyrimidine (tubercidin) in cultured cells. *Cancer Res.* **42**, 1289-1295

64. Kwong, F.Y.P., Baldwin, S.A., Scudder, P.R., *et al.* (1986). Erythrocyte nucleoside and sugar transport. *Biochem. J.* **240**, 349-356

65. Woffendin, C. and Plagemann, P.G. (1987). Nucleoside transporter of pig erythrocytes. Kinetic properties, isolation and reaction with nitrobenzylthioinosine and dipyridamole. *Biochim. Biophys. Acta.* **903**, 18-30

66. Dagnino, L. and Paterson, A.R.P. (1990). Sodium-dependent and equilibrative nucleoside transport systems in L1210 mouse leukemia cells: Effect of inhibitors of equilibrative systems on the content and retention of nucleosides. *Cancer Res.* **50**, 6549-6553

67. Plagemann, P.G. and Wohlhueter, R.M. (1984). Nucleoside transport in cultured mammalian cells. Multiple forms with different sensitivity to inhibition by nitrobenzylthioinosine or hypoxanthine. *Biochim. Biophys. Acta.* **773**, 39-52

68. Plagemann, P.G. and Woffendin, C. (1988). Species differences in sensitivity of nucleoside transport in erythrocytes and cultured cells to inhibition by nitrobenzylthioinosine, dipyridamole, dilazep and lidoflazine. *Biochim. Biophys. Acta.* **969**, 1-8

69. Hammond, J.R. (1991). Comparative pharmacology of the nitrobenzylthioguanosine-sensitive and -resistant nucleoside transprot mechanisms of Ehrlich ascites tumor cells. *J. Pharmacol. Exp. Ther.* **259**, 799-807

70. Jones, K.W. and Hmmond, J.R. (1992). Heterogeneity of [^{3}H]dipyridamole binding to CNS membranes: correlation with [^{3}H]nitrobenzylthioinosine binding and [^{3}H]uridine influx studies. *Neurochem.* **59**, 1363-1371

71. Cass, C.E., Gaudette, L.A. and Paterson, A.R.P. (1974). Mediated transport of nucleosides in human erythrocytes. Specific binding of the inhibitor nitrobenzylthioinosine to nucleoside transport sites in the erythrocyte membrane. *Biochim. Biophys. Acta.* **345**, 1-10

72. Jarvis, S.M. and Young, J.D. (1980). Nucleoside transport in human and sheep erythrocytes-Evidence that nitrobenzylthioinosine binds specifically to functional nucleoside transport sites. *Biochem. J.* **190**, 377-383

73. Gati, W.P. and Paterson, A.R.P. (1989). Nucleoside transport. In *Red blood cell membranes*. (Agre, P., Parker, J.C., eds.) New York: Marcel Dekker. pp. 635-661

74. Jarvis, S.M., Hammond, J.R., Paterson, A.R.P., *et al.* (1982). Species differences in nucleoside transport. A study of uridine transport and nitrobenzylthioinosine binding by mammalian erythrocytes. *Biochem. J.* **208**, 83-88

75. Cass, C.E. and Paterson, A.R.P. (1976). Nitrobenzylthioinosine binding sites in the erythrocyte membrane. *Biochim. Biophys. Acta.* **419**, 285-294

76. Smith, C.L., Pilarski, L.M., Egerton, M.L. and Wiley, J.S. (1989). Nucleoside transport and proliferative rate in human thymocytes and lymphocytes. *Blood.* **74**, 2038- 2042

77. Boumah, C.E., Hogue, D.L. and Cass, C.E. (1992). Expression of high levels of nitrobenzylthioinosine-sensitive nucleoside transport in cultured human choriocarcinoma (BeWo) cells. *Biochem. J.*, **288**, 987-996

78. Young, J.D., Jarvis, S.M., Robins M.J., *et al.* (1983). Photoaffinity labelling of the human erythrocyte nucleoside transporter by N6-(P-azidobenzyl)adenosine and nitrobenzylthioinosine. *J. Biol. Chem.* **258**, 2202-2208

79. Jarvis, S.M. and Young, J.D. (1981). Extraction and partial purification of the nucleoside-transport system from human erythrocytes based on the assay of nitrobenzylthioinosine-binding activity. *Biochem. J.* **194**, 331-339

80. Wu, JR., Kwong, F.Y.P., Jarvis, S.M., *et al.* (1983). Identification of the erythrocyte nucleoside transporter as a band 4.5 polypeptide. *J. Biol. Chem.* **258**, 13745-13751

81. Kwong, F.Y., Davies, A., Tse, C.M., *et al.* (1988). Purification of the human erythrocyte nucleoside transporter by immunoaffinity chromatography. *Biochem. J.* **255**, 243-249

82. Barros, L.F., Beaumont, N., Jarvis, S.M., et al. (1992). Immunological detection of nucleoside transporters in human placental trophoblast brush-border plasma membranes and placental capillary endothelial cells. *J. Physiol. (London)* **452,** 348P

83. Hogue, D.L., Hodgson, K.C., and Cass C.E. (1990). Effects of inhibition of N-linked glycosylation by tunicamycin on nucleoside transport polypeptides of L1210 leukemia cells. *Biochem. Cell Biol.* **68**, 199-209

84. Huang, Q.Q., Harvey, C.M., Paterson, A.R.P., Cass, C.E. and Young, J.D. (1993). Functional expression of Na$^+$-dependent nucleoside transport systems of rat intestine in isolated oocytes of *Xenopus Laevis* *J. Biol. Chem.* **268**, 20613-20619

85. Che, M., Nishida, T., Gatmaitan, Z., and Arias, I.M. (1992) A nucleoside transporter is functionally linked to ectoncleotidases in rat liver canalicular membrane. *J. Biol.Chem.* **267**, 9684-9688

86. Dagnino, L., Bennett, L.L., and Paterson, A.R.P. (1991) Substrate specificity, kinetics, and stoichiometry of sodium-dependent adenosine transport in L1210/AM mouse leukemia cells. *J. Biol. Chem.* **266**, 6312-6317

87. Jakobs, E.S., Van Os-Corby, D.J. and Paterson, A.R.P. (1990). Expression of sodium-linked nucleoside transport activity in monolayer cultures of IEC-6 intestinal epithelial cells. *J. Biol. Chem.* **265**, 22210-22216

88. Dagnino, L., Bennett, L.L. and Paterson, A.R.P. (1991). Sodium-dependent nucleoside transprot in mouse leukemia L1210 cells. *J. Biol. Chem.* **266**, 6308-6311

89. Vijayalakshmi, D. and Belt, J.A. (1988) Sodium-dependent nucleoside transport in mouse intestinal epithelial cells. Two transport systems with differing substrate specificities *J. Biol.Chem.* **263**, 19419-19423

90. Williams, T.C., and Jarvis, S.M. (1991) Multiple sodium-dependent nucleoside transport systems in bovine renal brush-border membrane vesicles *Biochem. J.* **274**, 27-33

91. Lee, C.W., Cheeseman, C.I., and Jarvis, S.M. (1990) Transport characteristics of renal brush-border Na^+-and K^+-dependent uridine carriers. *Am. J. Physiol.* **258**, F1203-1210

92. Williams, T.C., Doherty, A.J., Griffith, D.A., and Jarvis, S.M. (1989) Characterization of sodium-dependent and sodium-independent nucleoside transport system in rabbit renal brush-border and basolateral plasma-membrane vesicles from the renal outer cortex. *Biochem. J.* **264**, 223-231

93. Jarvis, S.M and Griffith, D.A. (1991). Expression of the rabbit intestinal N2 Na^+/nucleoside transporter in *Xenopus laevis* oocytes. *Biochem. J.* **278**, 605-607

94. Belt, J.A. and Harper, E., Byl, J. (1992) Na^+-dependent nucleoside transport in human myeloid leukemia cell lines and freshly isolated myeloblasts. *Cancer Res.* **33**, 20

95. Lee, C.W., Sokoloski, J.A, Sartorelli, A.C., *et al.* (1991). Induction of the differentiation of HL-60 cells by phorbol 12-myristate 13-acetate activates a Na(+)-dependent uridine-transport system. Involvement of protein kinase C. *Biochem. J.* **274**, 85-90

96. Gutierrez, M.M. and Giacomini, K.M. (1993). Substrate selectivity, potential sensitivity and stoichiometry of Na^+-nucleoside transpot in brush-border membrane vesicles from human kidney. *Biochim. Biophys. Acta.* **1149**, 202-208

97. Plagemann, P.G.W., Aran, J.M., and Woffendin, C. (1990). Na^+-dependent, active and Na^+-independent, facilitated transport of formycin B in mouse spleen lymphocytes. *Biochim. Biophys. Acta* **1022**, 93-102

98. Wu.X, Yuan.G., Brett, C.M, *et al.* (1992). Sodium-dependent nucleoside transport in choroid plexus from rabbit. Evidence for a single transporter for purine and pyrimidine nucleosides. *J. Biol. Chem.* **267**, 8813-8818

99. Paterson, A.R.P., Gati, W.P., Vijayalakshmi, D, *et al.* (1993) Inhibitor-sensitive, Na^+-linked transport of nucleoside analogs in leukemia cells from patients. *Proc Amer Assoc Cancer Res* **34**, 14

100. Che, M., Ortiz, D.F. and Arias, I.M. (1995) Primary structure and functional expression of a cDNA encoding the bile canalicular, purine-specific Na^+-nucleoside cotransporter. *J. Biol. Chem.* **270**, 13596-13599

101. Pajor, A.M. and Wright, E.M. (1992) Cloning and functional expression of a mammalian Na+/nucleoside cotransporter. *J. Biol.Chem.* **267**, 3557-3560

102. Leung, K.K. and Visser, D.W. (1977). Uridine and cytidine transport in *Escherichia coli*. *Biochim. Biophys. Acta.* **511**, 285-296

103. Roy-Burman, S. and Visser, D.W. (1975). Transport of purines and deoxyadenosine in *Escherichia coli*. *J. Biol. Chem.* **250**, 9270-9275

104. Mygind, B. and Munch-Petersen, A. (1975). Transport of pyrimidine nucleosides in cells of *Escherichia coli* K-12. *Eur. J. Biochem.* **59**, 365-372

105. Munch-Petersen, A., Mygind, B., Nicolaisen, A. and Pihl, N.J. (1979). Nucleoside transport in cells and membrane vesicles from *Escherichia coli* K-12. *J. Biol. Chem.* **254**, 3730-3737

106. Komatsu, Y. and Tanaka, K. (1972). A showdomycin-resistant mutant of *Escherichia coli* K-12 with altered nucleoside transport character. *Biochim. Biophys. Acta.* **288**, 390-403

107. Munch-Petersen, A. and Mygind, B. (1976). Nucleoside transport systems i *Escherichia coli* K-12. Specificity and regulation. *J. Cell. Physiol.* **89**, 551-560

108. Westh Hansen S.E., Jensen, N. and Munch-Petersen, A. (1987). Studies on the sequence and structure of the *Escherichia coli* K-12 *nupG* gene, encoding a nucleoside-transport system. *Eur. J. Biochem.* **168**, 385-391

109. Craig, J.E., Zhang, Y. and Gallagher, M.P. (1994). Cloning of the *nupC* gene of *Escherichia coli* encoding a nucleoside transport system, and identification of an adjacent insertion element, IS 186. *Mol. Microbiol.* **11**, 1159-1168

110. Kriegler, M. (1990). Gene transfer and expression.

111. Ausubel, F.M., Brent, R., Kingston, R.E., Moore, D.D., Seidman, J.G., Smith, J .A. and Struhl, K. (1989). Current protocols in molecular biology.

112. Southern, P.J. and Berg, P. (1982). Transformation of mammalian cells to antibiotic resistance with a bacterial gene under control of the SV40 early region promoter. *J. Mol. Appl. Gen.* **1**, 327-341

113. Gluzman, Y. (1981). SV-40 transformed simian cells support the replication of early SV40 mutants. *Cell* **23**, 175-182

114. Lusky, M. and Botchan, M. (1981). Inhibition of SV40 replication in simian cells by specific pBR322 DNA sequences. *Nature (Lond.)* **293**, 79-81

115. Rose, J.K. and Bergmann, J.E. (1982) Expression from cloned cDNA of cell-surface, secreted forms of the glycoprotein of vesicular stomatitis virus in eucaryotic cells. *Cell.* **30**, 753-762

116. Mishina, M., Kurosaki, T., Tobimatsu, T., Morimoto, Y., Noda, M., Yamamoto, T., Terao, M., Lindstrom, J., Takahashi, T., Kuno, M., and Numa, S. (1984) Expression of functional acetylcholine receptor form cloned cDNAs. *Nature (Lond.)* **307**, 604-608

117. Lsub, O. and Rutter, W.J. (1983) Expression of the human insulin gene and cDNA in a heterologous mammalian system. *J. Biol. Chem.* **258,** 6043-6050

118. Warren, T.G. and Shields, D. (1984) Expression of preprosomatostatin in heterologous cells: Biosynthesis, posttranslational processing, and secretion of mature somatostatin. *Cell* **39**, 547-555

119. Yamashita, H. Kitayama, S, Zhang, Y.X., Takahashi, T., Dohi, T. and Nakamura, S. (1995). Effect of nicotine on dopamine uptake in COS cells possessing the rat dopamine transporter and in PC12 cells. Biochemical Pharmacology. **49**, 742-745.

120. Kramer, D., Mett, H., Evans, A., Regenass, U., Diegelman, P. and Porter, C.W. (1995) Stable amplification of the S-adenosylmethionine decarboxylase gene in Chinese hamster ovary cells. *J. Biol. Chem.* **270,** 2124-2132

121. Moguilevsky, N., Varsalona, F., Noyer, M., Gillard, M., Guillaume, J.P., Garcia, L., Szpirer, C., Szpirer, J. and Bollen, A. (1995) Stable expression of human H1-histamine-receptor cDNA in Chinese hamster ovary cells. Pharmacological characterisation of the protein, tissue distribution of messenger RNA and chromosomal localization of the gene. *Eur. J. Bioche.* **224**, 489-495

123. Foecking, M.K. and Hofstetter, H. (1986) Powerful and versatile enhancer-promoter unit for mammalian expression vectors. *Gene.* **45**, 101

124. Wong, T.K. and Neumann, E. (1982). Electric field mediated gene transfer. *Biochem. Biophys. Res. Commun.* **107**, 584-587

125. Felgner, P.L., Gadek, T.R., Holm, M., Roman, R., Chan, H.W., Wenz, M, Northrop, J.P., Ringold, G.M. and Danielsen, M. (1987). Lipofection: a highly efficient, lipid-mediated DNA-transfection procedure. *Proc. Natl. Acad., Sci. USA.* **84,** 7413-7417

126. Graham, F.L. and Vander Eb, A.J. (1973). A new technique for the assay of infectivity of human adenovirus 5 DNA. *Virology* **52**, 456

127. Chen, C., and H.Okayama. (1987). Calcium phosphate-mediated gene transfer: A highly efficient transfection system for stably transforming cells with plasmid DNA. *BioTechniques* **6**, 632

128. McCutchan, J.H. and Pagano, J.S. (1968). Enhancement of the infectivity of simian virus 40 deoxyribonucleic acid with diethyl aminoethyl-dextran. *J. Natl. Cancer Inst.* **41**, 351-357

129. Warden, D. and Thorne, H.V. (1968). Infectivity of polyoma virus DNA for mouse embryo cells in presence of diethylaminoethyl-dextran. *J. Gen. Virol.* **3**, 371

130. Vaheri, A and Pagano, J.S. (1965). Infectious poliovirus RNA: A sensitive method of assay. *Virology.* **27**, 434

131. Lopata, M.A., Cleveland, D.W. and Sollner-Webb, B. (1984). High-level expression of a chloramphenicol acetyltransferase gene by DEAE-dextran-mediated DNA transfection coupled with a dimethysulfoxide or glycerol shock treatment. *Nucl. Acids Res.* 12, 5707-5717

132. Neumann, E., Schafer-Ridder, M., Wang, Y. and Hofschneider, P.H. (1982). Gene transfer into mouse lyoma cells by electroporation in high electric fields. *EMBO J* **1**, 841-845

133. Rabussay, D., Uher, L, Bates, G. and Piastuch, W. (1987). Electroporation of mammalian and plant cells. *Bethesda Res. Lab. Focus* **9**, 1

134. Patterson, M.K., Jr. (1979). Measurement of growth and viability of cells in culture. *Methods Enzymol.* **58**, 141-152

135. Chen, C. and Okayama, H. (1987). High-efficiency transformation of mammalian cells by plasmid DNA. *Mol.Cell Biol.* **7**, 2745-2752

136. Loyter, A., Scangos, G.A. and Ruddle, F.H. (1982). Mechanisms of DNA uptake by mammalian cells: fate of exogenously added DNA monitored by the use of fluorescent dyes. *Proc. Natl. Sci. USA* **79**, 422-426

137. Kawai, S. and Nishizawa, M. (1984). New procedure for DNA transfection with polycation and dimethyl sulfoxide. *Mol.Cell Biol.* **4**, 1172

138. Yao, S.Y.M. (1995) Intestinal nucleoside and amino acid transport. thesis, Department of Physiology, University of Alberta

139. Lin, W. and Culp, L.A. (1991). Selectable plasmid vectors with alternate and ultrasensitive histochemical marker genes. *BioTechniques* **11**, 344-351

140. Birnboim, H.C. and Doly, J. (1979). A rapid alkaline extraction procedure for screening recombinant plasmid DNA. *NuclAcids Res.* **7**, 1513-1523

141. Saiki, R.K., Gelfand, D.H., Stoffel, S., Scharf, S.J., Higuchi, R., Hom, G.T.,

Mullis, K.B. and Erlich, H.A. (1988). Primer-directed enzymatic amplification of DNA with a thermostable DNA polymerase. *Science*, **239**, 487-491

142. Smith, P.K., Krohn, R.I., Hermanson, G.T., Mallia, A.K., Gartner, F. H., Provenzano, M.D., Fujimoto, E.K., Goeke, N.M., Olsen, B.J., and Klenk, K.C. (1985). Measurement of Protein using bicinchoninic acid. *Anal. Biochem.* **150**, 76-85

143. Boleti, H. (1991). Nucleoside transport in K562 leukemia cells. thesis, Department of Biochemistry, University of Alberta

144. Dagnino, L. (1988). Sodium-driven nucleoside transport in mouse leukemia L1210 cells. thesis, Department of Pharmaclolgy, University of Alberta

145. Matthews, J.C. (1993) *in Fundamentals of Receptor, Enzyme, and Transport Kinetics*, pp.134, CRC Press, Florida

146. Eadie, G.S. (1952). The inhibition of cholinesterase by physostigmine and prostigmine. *J. Biol. Chem.*, **146**, 85

147. Hofstee, B.H. J. (1942). On the evaluation of the constants Vm and Km in enzyme reactions. *Science*, **116,** 329

148. Lineweaver, H. and Burk, D. (1934) The determination of enzyme dissociation constants. *J. Am. Chem. Soc.* **56**, 658

149. Jakobs, E.S. and Paterson, A.R. (1986). Sodium-dependent, concentrative nucleoside transport in cultured intestinal epithelial cells. *Biochem. Biophys. Res. Commun* **140**, 1028-1035

149. Asano, T., Katagiri, H., Takata, K., Tsukuda, K., Lin, J., Ishihara, H., Inukai, K., Hirano, H., Yazaki, Y. and Oka, Y. (1992). Characterization of GLUT3 protein expressed in Chinese hamster ovary cells. *Biochem. J.* **288**, 189-193

150. Plagemann, P.G.W. (1991) Na$^+$-dependent, active nucleoside transport in S49 mouse lymphoma cells and loss in AE1 mutant deficient in facilitated nucleoside transport. *J. Cell. Biochem.* **46,** 54-59

151. Aran, J.M. and Plagemann, P.G.W. (1992) Nucleoside transport-deficient mutants of PK-15 pig kidney cell line. *Biochim. Biophys. Acta.* **110**, 51-58

152. Hogue, D.L. (1994) Funtional and Molecular Studies of Eucaryotic Nucleoside Transporters. thesis, Department of Biochemistry, University of Alberta

153. Crawford, C.R., Ng, C.Y.C. and Belt, J.A. (1991) Isolation and characterization of an L1210 cell line retaining the sodium-dependent carrier *cif* as its sole nucleoside transport activity. *J. Biol. Chem.* **265**, 13730-13734

154. Lin, H.Y., Kaji, E.H., Winkel, G.K. and Lodish, H.F. (1991) Cloning and functional expression of a vascular smooth muscle endothelin 1 receptor. *Proc. Natl. Acad., Sci. USA.* **88**, 3135-3189

155. Reiser, H., Freeman, G.J., Razi-Wolf, Z, Gimmi, C.D., Banacerraf, B. and Nadler, L.M. (1992). Murine B7 antigen provides an efficient costimulatory signal for actvation of murine T lymphocytes via the T-cell receptor/CD3 complex. *Proc. Natl. Acad., Sci. USA* **89**, 271-275

156. Pelletier, J. and Sonenberg, N. (1985) Insertion mutagensis to increase secondary structure within the 5' noncoding region of a eukaryotic mRNA reduces translational efficiency. *Cell* **40**, 515-526

157. Adamo, H.P., Verma, A.K., Sanders, M.A., Heim, R., Salisbury, J.L., Wieben, E.D. and Penniston, J.T. (1992). Overexpression of the erythrocyte plasma membrane Ca^{2+} pump in COS-1 cells. *Biochem. J.* **285**, 791-797

158. Stein, W.D. (1986). in *Transport and Diffusion across Cell Membranes*, pp. 397-400 , Academic Press, London

159. Field, J., Nikawa, J., Broek, D., MacDonald, B., Rodgers, L., Wilson, I.A., Lerner, R. and Wigler, M. (1988). Purification of a RAS-responsive adenylyl cyclase complex from saccharomyces cerevisias by use of an epitope addition method. *Mol. Cell. Biol.* **8**, 2159-2165

160. Kolodziej, P.A. and Young, R. (1989) RNA polymerase II subunit RPB3 is an essential component of the mRNA transcription apparatus *Mol. Cell. Biol.* **9**, 5387

161. Mouillac, B., Caron, M., Bonin, H., Dennis, M. and Bouvier, M. (1992) Agonist-modulated Palmitoylation of β_2-adrenergic receptor in Sf9 cells. *J. Biol. Chem.* **267**, 21733-21737

162. Zastrav, M.V. and Kobilka, B.K. (1992) Ligand-regulated internalization and recycling of human β_2-adrenergic receptors between the plasma membrane and endosomes containing transferrin receptors. *J.Biol. Chem.* **267**, 3530-3538

163. Emrich, T., Forster, R. and Lipp, M. (1993) Topological characterization of the lymphoid-specific seven transmembrane receptor BLR1 by epitope-tagging and high level expression. *Biochem. Biophys. Res. Commun.* **197**, 214-220

164. Kolodziej, P.A. and Young, R.A. (1991) Epitope tagging and protein surveillance. *Methods Enzymol.* **194**, 508-519

165. Takano, E., Maki, M., Mori, H., Hatanaka, M., Marti, T., Titani, K., Knnagi, R., Ooi, T. and Murachi, T. (1988). Pig heart calpastatin: Identification of repetitive domain structures and anomalous behaviour in polyacrylamide gel electrophoresis. *Biochemistry.* **27**, 1964-1972

166. Beyreuther, K., Bieseler, B., Ehring, R., Griesser, H.W., Mieschendahl, M., Muller-Hill, B. and Triesch, I. (1980). Active transport in micro-organisms. *Biochem. Soc. Trans.* **8**, 675-676

167. Ito, K. (1984). Identification of the secY (prlA) gene product involved in protein export in *Escherichia coli. Mol. Gen.Genet.* **197**, 204-208

168. Nakamura, M., Inomata, M., Hayashi, M., Imahori, K. and Kawashima, S. (1985). Purification and characterization of 210,111-dalton inhibitor of calcium-activated neutral protease from rabbit skeletal muscle and its relation to 50,000-dalton inhibitor. *J. Biochem. (Tokyo).* **98**, 757-765166.

169. Tate, S.S., Yan, N. and Udenfriend, S. (1992) Expression cloning of a Na^+-independent neutral amino acid transporter from rat kidney. *Proc.Natl. Acad. Sci. USA* **89**, 1-5

170. Fincham, D.A., Mason, D.K., Paterson, J.Y., & Young, J.D. (1987). Dibasic amino acid interactions with Na+-independent transport system asc in horse erythrocytes. Kinetic evidence of functional and structural homology with Na+-dependent system ASC. *J.Physiol.* **389**, 385-409

171. Fincham, D.A., Mason, D.K., & Young, J.D. (1988). Heterogeneity of amino acid transport in horse erythrocytes: a detailed kinetic analysis of inherited transport variation. *Biochim. Biophys. Acta.* **937**, 184-194

172. Le Hir, M. (1990). Evidence for separate carriers for purine nucleosides and for pyrimidine nucleosides in the renal brush border membrane. *Renal Physiol. Biochem.* **13**, 154-161

173. Betcher, S.L., Forrest, J.N.Jr., Knichelbein, R.G. and Bobbins, J.W. (1990). Sodium-adenosine cotransport in brush-border membranes from rabbit ileum. *Am. J. Physiol.* **259**, G504-G510

174. Gould, G.W., Thomas, H.M., Jess, J. and Bell, G.I. (1991). Expression of human glucose transporters in Xenopus oocytes: kinetic characterizattion and substrate specificities of the erythrocyte, liver, and brain isoforms. *Biochemistry.* **30**, 5139-5145

175. Borjigin, J. and Nathans, J. (1994) Insertional mutagenesis as a probe of Rhodopsin's Topography, stability, and activity. *J. Biol. Chem.* **269**, 14715-14722

176. Nagy, L.E., Diamond, I. and Gordon, A.S. (1991) cAMP-dependent protein kinase regulates inhibition of adenosine transport by ethanol. *Mol. Pharmacol.* **40**, 812-817

177. Cui, Z., Vance, J.E., Chen, M.H., Voelker, D.R. and Vance, D.E. (1993) Cloning and expression of a novel phosphatidylethanolamine N-methyltransferase. *J. Biol. Chem.* **268**, 16655-16663

178. Ward, C.L., Omura, S. and Kopito, R. (1995). Degradation of CFTR by the ubiquitin-proteasome pathway. *Cell* **83**, 121-127

179. Wohlhueter, R.M., Marz, R. and Plagemann, P.G. (1978). Properties of the thymidine transport system of Chinese hamster ovary cells as probed by nitrobenzylthioinosine. *J. Membr. Biol.* **42**, 247-264

180. Wohlhueter, R.M., Marz, R. and Plagemann, P.G. (1979). Thymidine transport in cultured mammalian cells. Kinetic analysis, temperature dependence and specificity of the transport system. *Biochim. Biophys. Acta.* **553**, 261-283